

UC Irvine

UC Irvine Electronic Theses and Dissertations

Title

Rad52 competes with Ku70/Ku86 for binding to switch region DSB ends to modulate immunoglobulin class switch DNA recombination

Permalink

<https://escholarship.org/uc/item/03f400k9>

Author

Tat, Connie

Publication Date

2015

Copyright Information

This work is made available under the terms of a Creative Commons Attribution-NonCommercial-NoDerivatives License, available at <https://creativecommons.org/licenses/by-nc-nd/4.0/>

Peer reviewed|Thesis/dissertation

UNIVERSITY OF CALIFORNIA,
IRVINE

Rad52 competes with Ku70/Ku86 for binding to switch region DSB ends to modulate
immunoglobulin class switch DNA recombination

DISSERTATION

submitted in partial satisfaction of the requirements
for the degree of

DOCTOR OF PHILOSOPHY

in Biomedical Sciences

by

Connie Tat

Dissertation Committee
Professor Paolo Casali, Thesis Advisor
Professor Klemens Hertel, Co-Chair
Professor Manuela Raffatellu

2015

DEDICATION

To:

My father and mother, William and Josephine Tat
for their continuous love and support,
my sisters, Winnie and Shelly,
for their friendship and advice,
and Alvin for his unrelentless
devotion throughout my studies

TABLE OF CONTENTS

	Page
LIST OF ABBREVIATIONS	v
LIST OF FIGURES	ix
LIST OF TABLES	xi
ACKNOWLEDGEMENTS	xii
CURRICULUM VITAE	xiii
ABSTRACT OF THE DISSERTATION	xvi
CHAPTER 1 Immunoglobulin Class Switch DNA Recombination and the Antibody Response	1
1.1 Innate and adaptive immunity	2
1.2 Maturation of the immune response	6
1.3 Immunoglobulin Class Switch DNA Recombination and Somatic Hypermutation	9
1.4 Induction of CSR and SHM	14
1.5 AID mediates the generation of DSB	17
1.6 Resolution of DSB	20
1.7 References	24
CHAPTER 2 The role of Rad52 in class switch DNA recombination	
2.1 Homologous Recombination	31
2.2 The role of Rad52 in CSR	35
2.3 Rad52 deficiency increases the class switched antibody response <i>in vivo</i>	39
2.4 Rad52 deficiency increases CSR <i>in vitro</i>	43
2.5 Enforced Rad52 expression impairs CSR	48
2.6 Methods	50
2.7 Discussion	57
2.8 References	60
CHAPTER 3 Rad52 competes with Ku70/Ku86 to modulate immunoglobulin class switch DNA recombination	
3.1 Introduction	63
3.2 Rad52 deficiency is associated with a reduction in the frequency and length of microhomologies at the S-S junctions	66
3.3 Rad52 deficient B cells activated for CSR display reduced	

	<i>c-myc/IgH</i> translocations	71
3.4	Rad52 deficiency increases recruitment of Ku70/Ku86 to S region DSB	74
3.5	Rad52 competes with Ku70/Ku86 in binding to S region dsDNA ends	76
3.6	Rad52 mediated repair favors intra-S region rejoining	80
3.7	Methods	82
3.8	The potential role of Pol θ in CSR	87
3.9	Discussion	93
3.10	References	100
CHAPTER 4	Conclusions, Future Directions and Perspectives on Rad52	
4.1	Future directions	104
4.2	The significance of Rad52 mediated repair in CSR	107
4.3	Implications of Rad52 in human health and disease	108
4.4	References	111

7-AAD	7-Amino-actinomycin D
Ab	Antibody
AID	Activation induced cytidine deaminase
APCs	Antigen presenting cells
APE	Apurinic/aprimidinic endonuclease
BCR	B cell receptor
BIO-DUTP	Biotinylated dUTP
CFSE	Carboxyfluorescein succinyl diamide ester
C _H	Constant region of heavy chains
ChIP	Chromatin immunoprecipitation
C _L	Constant region of light chains
CML	Chronic Myelogenous Leukemia
C-NHEJ	Classic non-homologous end joining
CSR	Class switch DNA recombination
DC	Dendritic cell
DSB	Double strand break
ELISA	Enzyme-linked immunosorbent assay

Fab	Fragment antigen binding
Fc	Fragment crystallizable
FTK	Fusion tyrosine kinase
GC	Germinal center
GFP	Green fluorescent protein
HIGM	Hyper IgM Syndrome
HR	Homologous recombination
IFN γ	Interferon gamma
Ig	Immunoglobulin
I _H	Intervening exon
IgH	Ig heavy chain
IP	Immunoprecipitation
ISD	Internal Switch Region Deletion
LPS	Lipopolysaccharide
MAB	Monoclonal antibody
MFI	Mean fluorescence intensity
MHC II	Major histocompatibility II

NK	Natural killer cells
NP-CGG	Nitrophenyl-chicken gamma globulin
PCR	Polymerase chain reaction
PKA	Protein kinase A
PNA	Peanut agglutinin
PRR	Pattern recognition receptor
PST	Post-recombination transcript
QRT-PCR	Quantitative real-time PCR
RAG	Recombination activating gene
RPA	Replication protein A
SSB	Single strand break
SSDNA	Single strand DNA
SHM	Somatic hypermutation
TACI	Transmembrane activator and CAML interactor
TD	T-dependent
TDT	Terminal deoxynucleotidyl Transferase
T _{FH}	T follicular helper

TGF	Transforming growth factor beta
TI	T-cell independent
TLS	Translesion synthesis
V(D)J	Variable (Diversity) Joining
V _L	Variable region of light chains
V _H	Variable region of heavy chains

LIST OF FIGURES

		Page
Figure 1.1	Maturation of the immune response	8
Figure 1.2	Antibody diversification and immunoglobulin isotypes	10
Figure 1.3	AID mediates the generation of DSBs	19
Figure 1.4	AID is critical for the initiation of SHM and CSR	21
Figure 2.1	DSB Repair Process	32
Figure 2.2	Structure of Rad52 undecamer	35
Figure 2.3	DSB Repair Process in CSR	36
Figure 2.4	Disruption of the <i>MmRad52</i> gene	38
Figure 2.5	Rad52 deficiency increases the class switched antibody response <i>in vivo</i>	41
Figure 2.6	The augmented antibody response is not due to alterations in proportions of B and T cells, plasma cell differentiation, and B cell proliferation and survival	42
Figure 2.7	Rad52 deficiency increases CSR <i>in vitro</i>	44
Figure 2.8	Rad52 deficiency increases CSR without affecting B cell division or proliferation	45
Figure 2.9	Rad52 deficiency increases CSR, as well as circle I _H -C _μ and post-recombination I _μ -C _H transcription but does not alter germline I _H -C _H transcription	47
Figure 2.10	Enforced expression of Rad52 in B cells impairs CSR	49

Figure 3.1	Rad52 deficiency is associated with reduced microhomology at the S μ -S α junctions in CSR <i>in vivo</i>	67
Figure 3.2	Rad52 deficiency is associated with reduced microhomology at the S μ -S γ 1 junctions in CSR <i>in vitro</i>	68
Figure 3.3	Total microhomologies at switch recombination junctions of <i>Rad52</i> ^{+/+} and <i>Rad52</i> ^{-/-} B cells in CSR	70
Figure 3.4	Schematic of the <i>IgH</i> and <i>c-myc</i> loci with the location of the primers used for PCR amplification to detect interchromosomal <i>c-myc/IgH</i> translocations are indicated	72
Figure 3.5	<i>Rad52</i> ^{-/-} B cells activated for CSR on a p53 deficient background display reduced <i>c-Myc/IgH</i> translocations	73
Figure 3.6	Rad52 deficiency increases recruitment of Ku70/Ku86 to S region DSBs	75
Figure 3.7	Rad52 competes with Ku70/Ku86 in binding to S region dsDNA ends	77
Figure 3.8	DNA end-labeling assay to detect recruitment of Ku70/Ku86 to DSB free ends	79
Figure 3.9.	Rad52 mediated repair favors intra-S region DNA recombination	81
Figure 3.10	Pol θ deficiency does not affect CSR	90
Figure 3.11	Pol θ deficiency does not affect the frequency or length of microhomology at switch recombination junctions in CSR	92
Figure 3.12	Schematic representation to show that Rad52 competes with Ku70/Ku86 binding to S region DNA ends to modulate class switch DNA recombination	94

LIST OF TABLES

	Page
Table 1.1 Roles of the various cell types in the innate and adaptive immune system	4
Table 2.1 Oligonucleotide sequences used in qRT-PCR, ChIP Assays, analysis of S-S Junctions, <i>c-myc/IgH translocations</i>	56
Table 3.1 Antibodies in Experimental Procedures	86

ACKNOWLEDGEMENTS

I would like to express deep appreciation to my thesis advisor, Professor Paolo Casali, for his guidance and support throughout my graduate studies. His mentorship has been paramount to my development as a graduate student. The training he has provided me as a student to always be critical and precise of my work has proven to be an invaluable asset to me as a scientist and will follow me throughout life. Furthermore, Paolo has provided the purpose and direction that I needed to complete my graduate studies. I am grateful for the amount of effort and dedication he has put into me as his student.

I would next like to thank my committee members, Professor Klemens Hertel and Professor Manuela Raffatellu for always being reasonable and rational during my committee meetings, and more importantly for their continuous faith and support of me completing my dissertation studies thirteen hundred miles away. Specifically, I would like to thank Professor Hertel for his continuous optimism, trust, and career advice, which has allowed me to complete my dissertation studies at UC Irvine. I also want to thank Professor Raffatellu for her encouragement and words of wisdom to keep going and finish strong.

I owe my sincere and earnest thankfulness to all the members of the Casali lab and our collaborators for their friendship, guidance and scientific support. My work on the role of Rad52 in class switch recombination would not have been possible without the critical guidance, advice and direction of Professor Hong Zan. I would also like to thank Professor Hong Zan from which this work stemmed off of, and for his sound experimental advice for any issues that may have arisen. Moreover, I am extremely grateful to Hong for never giving up on his students. I would also like to thank Ken L. Hayama, Julia R. Taylor, Meghan A. Guzman, and Justin A. Gurrerero for their invaluable technical assistance, friendship and contributions to my projects.

I'm appreciative of the Department of Microbiology and Molecular Genetics at UCI for the tight knit community and friendships within the Department, as well as their administrative efficiency in getting paperwork through while I was *In Absentia*. I enjoyed being part of the UCI Institute for Immunology. I would also like to thank the UTHSCSA Department of Microbiology and Immunology for their administrative assistance. Collectively, I would like to thank these Departments for supporting me over the past 2 years of my graduate studies. The training I have received through their programs has formulated my development as a scientist.

CURRICULUM VITAE

Connie Tat

EDUCATION

- 2010-2015 PhD in Medicine
 Department of Microbiology and Molecular Genetics
 University of California, Irvine
- 2005-2009 Bachelor of Arts in Molecular and Cell Biology
 Emphasis in Cell and Developmental Biology
 University of California, Berkeley

PROFESSIONAL MEMBERSHIPS

- 2014, 2015 Member, American Association of Immunologists
- 2014 Member, The American Society for Cell Biology
- 2012 Member, American Medical Writers Association
- 2011 Member, American Association for the Advancement of Science
- 2009-2010 Member, The American Society for Cell Biology
- 2004 Member, Southern California Academy of Sciences Research Training
 Program

RESEARCH EXPERIENCE

- 2014 Student Associate, Department of Microbiology and Immunology,
 University of Texas Health Science Center, San Antonio, TX
- 2013 Graduate Student Researcher, Department of Microbiology and Molecular
 Genetics, Institute for Immunology, University of California, Irvine, CA
- 2010-2013 Graduate Student Researcher, Department of Biological Chemistry,
 University of California, Irvine, CA
- 2009-2010 Research Specialist, Department of Hematology/Oncology, Children's
 Hospital Los Angeles/ University of Southern California, Los Angeles,
 CA
- 2009 Staff Research Associate, Department of Neurological Surgery, Institute
 for Regenerative Medicine, University of California, San Francisco, CA

- 2008 Summer Intern, Virology Department, Roche, Palo Alto, CA
- 2007-2009 Undergraduate Research Assistant, Life Sciences Division, Lawrence Berkeley National Laboratory, Berkeley, CA
- 2006-2007 Student Research Assistant, Life Sciences Division, Lawrence Berkeley National Laboratory, Berkeley, CA

AWARDS AND HONORS

- 2015 UTHSCSA Department of Microbiology and Immunology Retreat 1st Place Poster Award
- 2014 ASCB/EMD Millipore Scholarship
- 2014 UTHSCSA Department of Microbiology and Immunology Graduate Student Travel Award
- 2014 AAI Trainee Abstract Award
- 2010-2011 NIH Predoctoral Kirschstein-NRSA Training Grant in Translational Research for Genomic Medicine
- 2004-2005 Southern California Academy of Sciences Research Training Program
- 2004 Finalist, Southern California Regional Junior Sciences & Humanities Symposium
- 2004 California Governor's Scholar Award
- 2003, 2004 Hugh Edmondson Summer Fellowship, USC/Keck School of Medicine

PUBLICATIONS

1. Zan H., **Tat, C.**, and P. Casali. 2014. MicroRNAs in lupus. *Autoimmunity*, 47: 272-85.
2. White, C.A., E.J. Pone, T.S. Lam, **C. Tat**, K.L. Hayama, G. Li, H. Zan and P. Casali. 2014. Histone Deacetylase Inhibitors Upregulate B Cell microRNAs That Silence AID and Blimp-1 Expression for Epigenetic Modulation of Antibody and Autoantibody Responses. *J Immunol.*, 193 (12):5933-50.
3. **Tat, C.**, M.A. Guzman, T. Shen, J.R. Taylor, K.L. Hayama, H. Zan and P. Casali. 2015. Rad52 competes with Ku70/Ku86 to modulate class switch DNA recombination. *Nature Immunology*, to be submitted.
4. Zan, H., **Tat, C.**, and P. Casali. 2015. Epigenetics of immunoglobulin class switch DNA recombination and somatic hypermutation. *Frontiers in Immunology*, in press.

5. **Tat, C.,** Shen, T., K.L. Hayama, H. Zan and P. Casali. 2015. Estrogen impairs histone deacetylase inhibitors mediated dampening of Ig class switch DNA recombination through Sirt1. *Manuscript in preparation.*

PRESENTATIONS AND POSTERS

1. **Tat, C.,** K.L. Hayama, H. Zan and P. Casali. 2013. Rad52 Competes with Ku70/Ku86 Binding to Switch Region Double-Strand DNA Break Free Ends in Class Switch DNA Recombination. Presented at: *11th Annual Immunology Fair, November 21-22*, UC Irvine Institute for Immunology, Irvine. Poster.
2. **Tat, C.,** K.L. Hayama, H. Zan and P. Casali. 2014. Rad52 deficiency increases immunoglobulin class switch DNA recombination. *J. Immunol.* 192: 127.15 (Abstract). Oral and poster.
3. **Tat, C.,** J.R. Taylor, K.L. Hayama, H. Zan and P. Casali. 2014. Rad52 Deficiency Increases Immunoglobulin Class Switch DNA Recombination Presented at: *6th Annual Terry M. Mikiten Graduate Research Forum, June 6*, UT Health Science Center, San Antonio, TX. Oral.
4. **Tat, C.,** J.R. Taylor, K.L. Hayama, T. Shen, H. Zan and P. Casali. 2014. B cell Rad52 deficiency enhances class switching by increasing recruitment of Ku70/Ku86 to S region double-strand DNA breaks. Presented at: *3rd Annual Vaccine Development Center of San Antonio Conference, November 13-14*, UT Health Science Center, San Antonio, TX. Poster.
5. **Tat, C.,** M.A. Guzman, T. Shen, J.R. Taylor, J.A. Gurrerro, K.D. Gonzalez, H. Zan and P. Casali. 2015. Rad52 competes with Ku70/Ku86 for binding to switch region DSB ends to modulate immunoglobulin class switch DNA recombination. Presented at: *Microbiology and Immunology/Infection, Inflammation & Immunity. Departmental Spring Retreat 2015, April 30*. UT Health Science Center, San Antonio, TX. Poster.
6. **Tat, C.,** M.A. Guzman, T. Shen, J.R. Taylor, H. Zan and P. Casali. 2015. B cell Rad52 deficiency enhances immunoglobulin class switching through increased recruitment of Ku70/Ku86 to S region double-strand DNA breaks. *J. Immunol.* 182: 10P.618 (Abstr). Poster.

ABSTRACT OF THE DISSERTATION

Rad52 competes with Ku70/Ku86 to modulate immunoglobulin class switch DNA recombination: role in alternative non-homologous end joining

By

Connie Tat

Doctor of Philosophy in Medicine

University of California, Irvine, 2015

Professor Paolo Casali, Thesis Advisor

Class switch DNA recombination (CSR) diversifies the biological effector functions of antibodies and is critical for the maturation of the antibody response. Defective or aberrant CSR can lead to diseases such as hyper-IgM syndrome, systemic or organ-specific autoimmunity, allergy, asthma and neoplastic transformation. This process is initiated by AID-mediated introduction of double-strand DNA breaks (DSBs) in the upstream and downstream switch (S) regions that will be recombined as effected by intervention of Ku70/Ku86 and the non-homologous end joining (NHEJ) DNA repair pathway. However, Ku-deficient B cells undergo CSR, albeit at a reduced rate, suggesting the involvement of other DNA repair mechanisms. We have demonstrated that B cell deficiency of Rad52, a critical component of the homologous recombination (HR) DNA repair pathway, resulted in increased CSR. Conversely, enforced Rad52

expression impaired CSR. This elevation of CSR in *Rad52*^{-/-} B cells was associated with increased recruitment of Ku70/Ku86 to S region DSB ends. Indeed, Rad52 competed with Ku70/Ku86 for binding to blunt and staggered DSB ends, as shown by in vitro competition using purified Rad52 and Ku70/Ku86 molecules, and chromatin immunoprecipitation (ChIP) assays involving anti-Rad52 antibody (Ab) and anti-Ku70/Ku86 monoclonal antibody (mAb). In *Rad52*^{-/-} B cells, the increased role of Ku70/Ku86 in S region recombination was emphasized by decreased occurrence of microhomologies in S μ -S α and S μ -S γ 1 junctions, decreased inter-chromosomal *c-Myc/IgH* translocations and reduced intra-S μ recombination. Our findings demonstrate that Rad52 binds to S region DSB ends to facilitate a Ku-independent repair pathway, which favors intra-switch (S) region re-joining and can also resolve inter-switch (S) region DSBs, possibly as part of an alternative NHEJ pathway.

CHAPTER 1

Immunoglobulin Class Switch DNA Recombination and the Antibody Response

Contents:

1.1 Innate and adaptive immunity	2
1.2 Maturation of the immune response	6
1.3 Immunoglobulin Class Switch DNA Recombination and Somatic Hypermutation	9
1.4 Induction of CSR and SHM	14
1.5 AID mediates the generation of DSBs	17
1.6 Resolution of DSBs	20
1.7 References	24

1.1 Innate and Adaptive Immunity

The immune system is comprised of an intricate network of humoral and cellular effectors whose primary function is to detect and combat infectious pathogens that compromise the health or longevity of the host organism. The immune response comprises of two major branches of immunity: the innate and adaptive responses. Together, they share signaling molecules and effector mechanisms to achieve a highly organized immune response. The innate immune response is a rapid initial and broad-spectrum defense against pathogens that is driven by the recognition of microbial patterns and repeats and uses receptors that are inherited in the germline by nonclonal distribution. In contrast, the adaptive immune system uses receptors that are rearranged during lymphocyte development, thereby endowing a single cell with unique specificity towards a specific antigen (clonal distribution) (1-4).

The innate immune response is evolutionarily conserved and found in plants, fungi, insects, and higher organisms. For example, lipopolysaccharide (LPS), lipoproteins, microbial DNA and RNA, peptidoglycan and lipoteichoic acids (LTAs) are molecules metabolically produced by bacteria, which can be recognized as microbial signatures of invaders by the innate immune system (1,2) (3,4). These conserved molecular patterns of the microbial signatures are called pathogen-associated molecular patterns (PAMPs). PAMPs are recognized by pattern-recognition receptors (PRR). PRRs comprise various membrane receptors, including Toll-like receptors (TLRs), NOD-like receptors (NLRs), and scavenger receptors. PRR evolved before the adaptive immune response to further enhance the possibility of recognizing foreign antigens (5). The engagement of PAMP-PRRs trigger macrophages and mast cells to phagocytose the pathogen, display peptide

fragments on MHC II and I receptors, and secrete pro-inflammatory cytokines and chemokines essential for the induction of the adaptive immune response. In addition, activation of immature DCs can occur by stimulation of PRRs, which in turn activates adaptive immunity (5,6).

The adaptive immune response, which is the second branch of immunity, is activated when a pathogen overcomes the first line of defenses in the innate immune system. The adaptive immune systems of vertebrates utilize efficient mechanisms of somatic diversification to generate unlimited repertoires of diverse antigen receptors that are clonally expressed on the surface of B and T lymphocytes. Although the adaptive immune response is activated in part by innate immune components, once an effective immune response is mounted against a specific antigen, B and T lymphocytes are able to differentiate into memory cells that will recognize the same antigen upon a second exposure. The adaptive immune response provides a fine-tuned response capable of forming immunologic memory for rapid recall responses. It is highly effective against disease, and has contributed to the past developments and future therapeutic designs of vaccines (7).

While the adaptive response takes longer to form than that of innate immunity, it is essential for the clearance of microbial pathogens. The adaptive immune response is mediated by key components of the innate immune system, humoral immunity (antibody responses mounted by B cells) and cell-mediated immunity by T cells, which are generated and mature in the bone marrow and thymus, respectively (3). The adaptive immune response entails the generation of lymphocytes that specifically recognize infectious agents and confers lifelong protection.

Table 1.1 Roles of various cell types in the innate and adaptive immune system.

Cell Type	Function
Macrophages	Phagocytosis of bacteria; antigen presentation
Dendritic Cells	Antigen presentation
Neutrophils	Phagocytosis
Eosinophils	Destruction of antibody-coated parasites
Basophils	Release of granules containing enzyme and toxic proteins
Mast cells	Release of granules inflammatory agents
NK cells	Release lytic granules that kill virus-infected cells
T cells	Kill, activate and regulate cells
B cells	Produce antigen specific antibodies

The adaptive immune response can be potentiated by non-specific and specific signals, for example a non-specific signal would be the recognition of PAMPS, and a specific signal, would be the recognition of antigens by B or T cells. Antigenic stimuli are processed by components of the innate and adaptive immune system to be presented to the adaptive immune system. For instance, T cells require that an antigen is first processed by antigen presenting cells (APCs), which is on the Class I and Class II Major Histocompatibility Complex, for recognition. B cells on the other hand can recognize a naïve antigen without presentation (1).

Effective antibody responses require further enhancement of antigen specificity and diversification of the antibodies effector function. The main difference between the innate and adaptive immune systems is the existence of a class of diverse but individually specific B and T cell receptors. These B and T cell receptors are diversified through a RAG-dependent DNA rearrangement event which recombines a single variable (V), joining (J) and/or diversity (D) gene segment together from each gene family during a process called V(D)J recombination, which also increase the specificity of these receptors, making them more specific than those of the innate immune system. Once this somatic rearrangement has occurred, recombination can provide a vast number of unique B cell receptors, on the order of 10^{11} different specificities. This is essential as the clonal theory of immunity holds that only B and T lymphocytes with receptors with a high enough affinity for an antigen will become activated and differentiated (8).

1.2 Maturation of the immune response

B cell precursors reside in the bone marrow, and after undergoing RAG1/2 dependent V(D)J recombination, resting naïve B cells can enter the blood as immature (IgM^+IgD^-) or mature (IgM^+IgD^+) B cells and home to secondary peripheral lymphoid organs such as the spleen and lymph nodes, where they encounter an antigen and can differentiate into plasma cells, which secrete large volumes of antibodies (9).

There is unique antigen receptor specificity on the extracellular surface of plasma membranes that include multiple (hundreds to thousands) of identical copies of their BCR or TCR, with each cell driven by the recognition of antigen by specific lymphocytes. Each individual clone will ultimately produce antibodies with specificities identical to its surface receptor (10,11).

During the antibody response, B cells can also migrate to the follicles of the peripheral lymphoid tissues (such as the spleen, lymph nodes, Peyer's patches and tonsils, to form germinal centers (GCs) (12-14). There are two distinct zones in the germinal center: the dark zone, where B cells are in a stage of differentiation known as centroblasts and undergo rapid proliferation, and the light zone where centroblasts cease proliferating and differentiate into centrocytes (15). Here, centrocytes compete for antigen displayed by DCs and T_{FH} and only those centrocytes whose BCRs have the highest affinity for the antigen, meaning they have accumulated mutations enhancing their affinity to the cognate antigen will be preferentially selected. The remaining B cells undergo apoptosis due to neglect. The selected high affinity centrocytes can then either differentiate into short lived antibody-secreting cells known as plasmablasts, which exist for a few days after

infection and mainly produce IgM antibodies or re-enter the same GC or adjacent GC to undergo further selection through rounds of proliferation, hypermutation, class-switching, and finally emerge as long-lived plasma cells or memory B cells (**Figure 1.1**) (14).

Within the GCs, B cells first migrate to the T cell rich area and are activated upon interaction with the tumor-necrosis factor (TNF)-receptor family member CD40. CD40 is expressed on the surface of B cells by its ligand, CD154, which is expressed by follicular helper T cells (T_{FH}) (12). CD154:CD40 engagement activates the CD40 signaling pathway, and the tumor necrosis factor receptor-associated factor (TRAF) adaptor molecules activate transcription factors such as nuclear factor NF κ B, resulting in B cell proliferation and differentiation (16). In addition to membrane protein receptor interactions, interleukin (IL) molecules secreted by both T and B cells can influence differentiation. These T-dependent interactions eventually give rise to effector B cells known as plasma cells, which secrete high affinity antibodies against specific antigens, and can also give rise to memory B cells, which elicit a secondary response upon re-infection (5).

The maturation of the antibody response is critical for effective vaccines and the generation of neutralizing antibodies to defend against infectious agents and tumor cells. In GCs, the generation of affinity antibodies increases dramatically due to the cellular mechanism, somatic hypermutation (SHM). During the GC reaction, the constant region of the immunoglobulin (Ig) heavy chain changes, thereby endowing the antibody with different biological effector functions. The maturation of the antibody response is driven by two B cell intrinsic processes, immunoglobulin (*Ig*) CSR and SHM, which lead to the overall production and diversification of antibody isotypes (17).

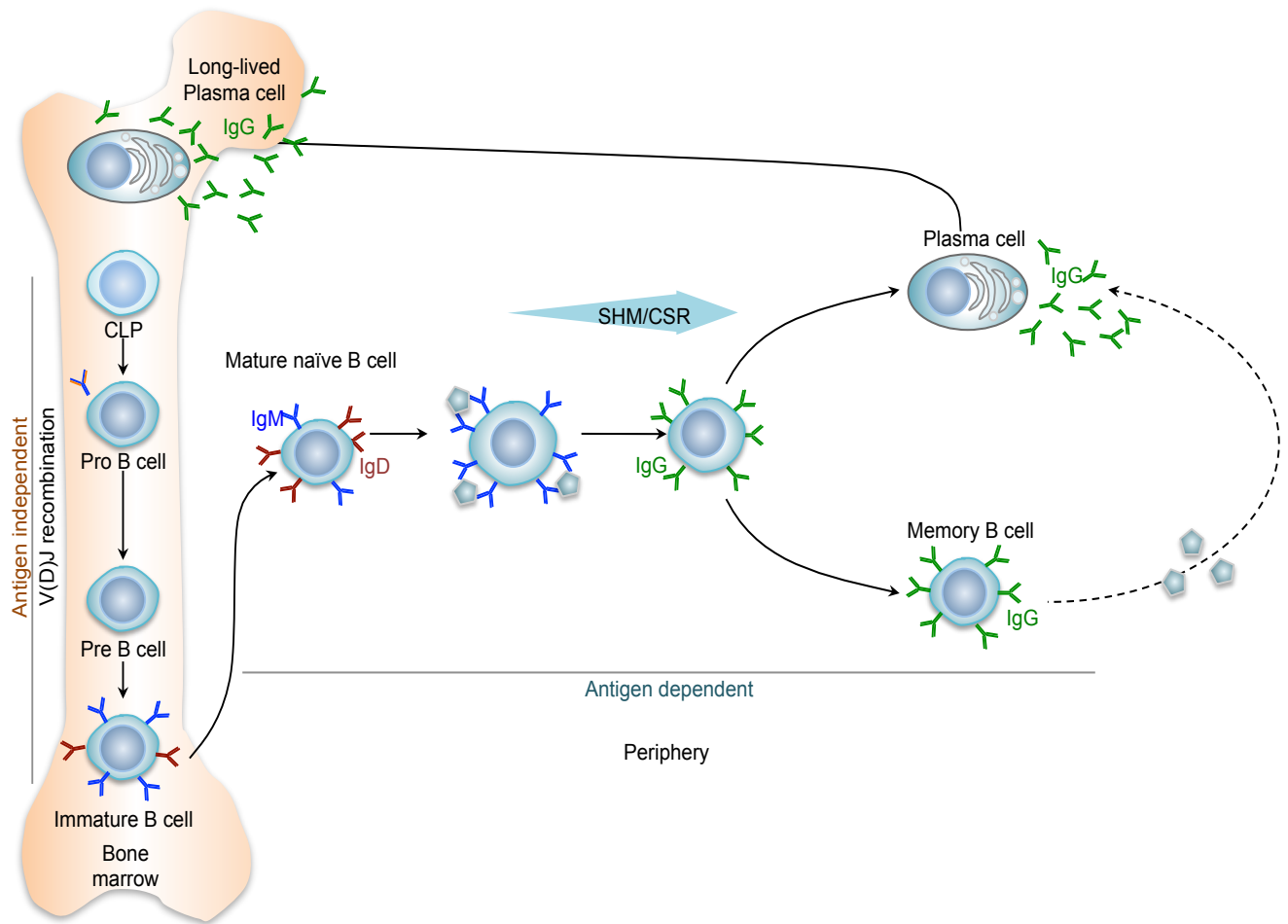


Figure 1.1. Maturation of the immune response. Upon encountering an antigen in the secondary lymphoid organs, resting naïve mature IgM^+IgD^+ B cells become activated and can proliferate and differentiate either directly into plasma cells, where large volumes of antibodies are secreted, or long-lived memory B cells, where they elicit a rapid secondary response. This response occurs mainly in the germinal centers and is driven by two critical B cell-intrinsic processes, immunoglobulin class switch DNA recombination and somatic hypermutation leading to the overall production and diversification of antibody isotypes. *Adapted from Zan et al., 2014 (18).*

1.3 Class Switch DNA Recombination and Somatic Hypermutation

B cells recognize pathogenic antigens through their BCRs and become activated to secrete antibodies to target the pathogen. The antibody is composed of two identical heavy chains and light chains (**Figure 1.2**). The secreted antibodies molecules are identical to the BCR except they lack the membrane spanning tail of the heavy chains of the BCR, which dock to the plasma membrane. Antibodies are chimeric proteins composed of a variable region, essential for the specific antigen binding site, and a constant region, which confers the specialized effector functions that determine the mode of clearing of the pathogen. The heavy chain is approximately 50kDa in size and contains a heavy chain variable region (V_H) and a heavy chain constant region (C_H). The variable region of the heavy chain is composed of different variable (V), diversity (D), and joining (J) gene segments (1-3). There are various combinations of the V(D)J genes and heavy and light chain pairings, such that they generate approximately 1.9×10^6 different antibody specificities. The introduction of random nucleotides and point mutations during DJ rearrangement can bring the total diversity to $\sim 5 \times 10^{13}$ to create the B cell repertoire, which is capable of recognizing virtually all-foreign antigens (19).

There are several distinct classes of immunoglobulin heavy chain antibodies based on the C_H region (**Figure 1.2**). The constant region has 3-4 domains: C_{H1} , C_{H2} , C_{H3} , C_{H4} . C_{H1} is the constant region of the fragment antigen binding (Fab) of the antibody, which contains the variable V_H and V_L domains, and the last 2-3 C_H form the constant fragment (Fc) of the antibody (20-22).

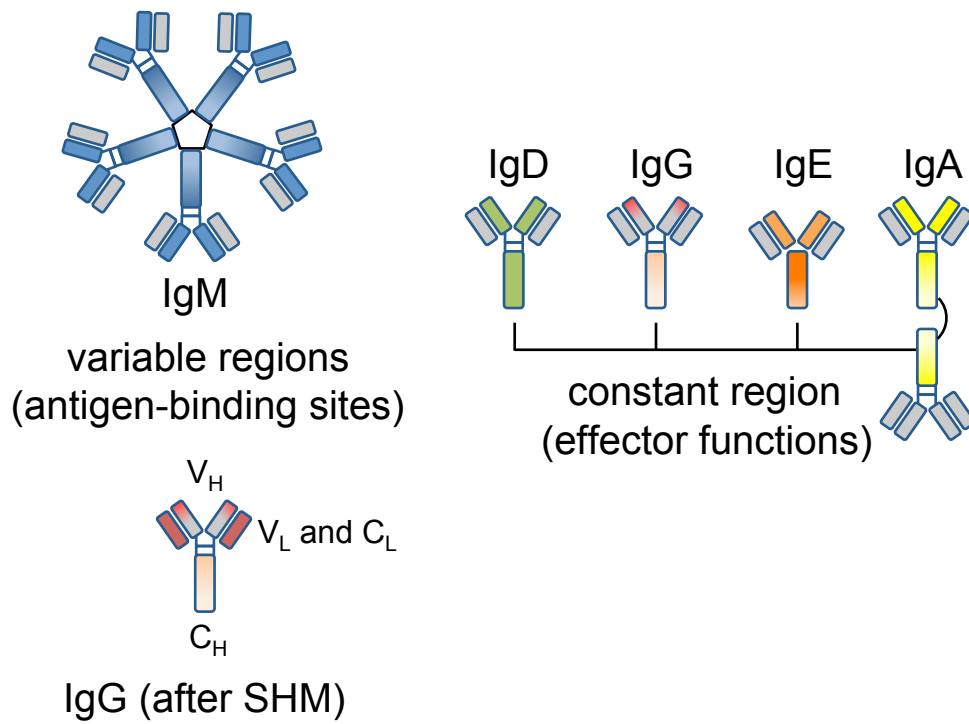


Figure 1.2 Antibody diversification and immunoglobulin isotypes. The antibody is composed of two identical heavy and light chains. Each heavy chain possesses a variable region (V_H), which binds the antigen and several constant regions (C_H) that are unique to each class or isotype. The antigen binding regions are formed from the pairing of one variable light (V_L) chain and one constant light chain (C_L). Class-switch DNA recombination (CSR) changes the constant region of the antibody heavy chain, thereby endowing the antibody with new biological effector functions. Somatic hypermutation (SHM) introduces point mutations in the immunoglobulin variable (V) region, thereby altering the antigen affinity for the antibody. *Modified from Janeway, 2005 (1).*

For example, naïve B cells exclusively express the C μ and C δ genes to produce IgM and IgD respectively. All B cells initially express IgM/IgD Igs. During the immune response, B cells receive signals to undergo CSR and eventually replace expression of C μ and C δ with a different C $_H$ gene. The five main classes of antibodies include IgM, IgD, IgG, IgE, and IgA. In humans, IgG can be further subdivided into four subclasses (i.e., IgG1, IgG2, IgG3 or IgG4) named in the order of abundance found in the serum.

The Fab varies according to each antibody based on the generated diversity during B cell activation. The Fc is constant for antibodies of the same class, which in the mouse are IgM/IgD, IgG1, IgG2a, IgG2b, IgG3, IgE, and IgA. Each Fc or antibody class is conferred with differential ability to interact with its specific Fc receptor (FcR) to neutralize antigens, activate complement, opsonize pathogens and bind macrophages, dendritic cells (DCs), phagocytes, mast cells, eosinophils, basophils, or natural killer (NK) cells and therefore directs the appropriate effector mechanisms to clear the pathogen bound by the antigen-specific Fab parts (1). For example, IgE Fc interacts with its high-affinity FcRs on eosinophils and basophils, leading to their degranulation to kill the parasite that IgE has bound. IgM and IgG2a/b antibodies have Fc that bind C1q and activate complement. IgG2a and IgG2b antibodies are responsible for clearing viral infections, and are induced by IFN γ and TGF- β . IgM and IgG3 are effective at activating complement and are secreted upon B cell activation by TLR ligands such as lipopolysaccharide LPS (20-22).

IgM is pentameric and therefore has a high avidity for antigens with repetitive motifs (microbial pathogens). However, the large size of the pentameric IgM limits its distribution to the blood and prevents it from moving efficiently across epithelia and

binding to pathogen systemically. All other antibody isotypes diffuse efficiently to extravascular sites and therefore, IgM must class switch into a monomeric or dimeric isotype such as monomeric IgG, monomeric IgE, and dimeric IgA which are distributed systemically throughout different tissues. When B cells cannot switch the constant region from IgM to one of the other isotypes, the organism cannot mount an efficient antibody response during infection, leading to hyper-IgM (HIGM syndrome in humans) (23). Individuals with defective or aberrant CSR display a variety of disease including hyper-IgM (HIGM) syndrome, which is characterized by low/undetectable levels of IgG, IgA, and IgE and high susceptibility to infections. In addition, defective or aberrant CSR can lead to diseases such as systemic or organ-specific autoimmunity, allergy, asthma and neoplastic transformation. While the antigen affinity of the antibody variable region remains unaltered, upon switching to downstream isotypes, antibodies gain new functions and unique tissue distribution (24,25).

These five antibody isotypes are distributed systemically and selectively throughout the body. For example, IgM antibodies predominate in the blood serum and heart and activate the complement system in the early stages of the B cell response before there is sufficient IgG. IgD and IgG antibodies predominate in the extracellular fluid or blood serum; IgD mainly functions as an antigen receptor on B cells (mature Ig δ Igu double positive B cells) that have not been exposed to antigens. IgG antibodies mainly neutralize and opsonize pathogens. IgA antibodies predominate in the mucosa (or the linings of mostly endodermal origin, covered in epithelium, which are involved in absorption and secretion) and function to neutralize pathogens. IgE antibodies predominate beneath the epithelial surfaces (such as the respiratory and gastrointestinal tract and skin) and are responsible for eliciting a response to an allergic reaction (1-2).

Immunoglobulin CSR and SHM are central to the maturation of the antibody response (26-28). CSR endows antibodies with new biological effector functions by exchanging the gene encoding the constant region (C_H) of the immunoglobulin heavy chain with a downstream C_H region. SHM provides the structural substrate for antigen-mediated selection of higher-affinity antibody mutants by introducing mainly point mutations in the Ig V(D)J sequence (26-29). In addition, aberrant CSR can lead to pathogenic autoantibodies in systemic autoimmune diseases such as systemic lupus erythematosus, or organ specific autoimmunity, such as type I diabetes mellitus. Furthermore, antibodies mediating allergic reactions such as asthma often are associated with atopic IgE (30). CSR and SHM are highly regulated and require the intervention of activation induced cytidine deaminase (AID), which is expressed at high levels in activated B cells in germinal centers (GCs) of peripheral lymphoid organs (31).

1.4 Induction of CSR and SHM

Both primary and secondary stimuli are required to induce CSR. Primary stimuli efficiently induce AID expression; they are comprised of T-dependent and T-independent molecules such as CD154 and TLR ligands, respectively. In response to T-dependent (CD40 engagement) and T-independent (dual TLR-BCR, transmembrane activator and CAML interactor (TACI)-BCR or TLR-TACI engagement)) stimulation, AID is highly induced by HoxC4, which has 3 estrogen response elements on its promoter and NFK β , through canonical and non-canonical NFK β signaling. *In vitro* studies performed in our laboratory have characterized the specific contribution of these stimuli to AID induction and CSR (32). Secondary stimuli, namely interleukin-4 (IL-4), transforming growth-factor beta (TGF- β) and interferon gamma (IFN γ), can enhance AID induction when combined with primary CSR-inducing stimuli by binding to immunoglobulin heavy chain intervening region (I_H) promoters to initiate germline I_H-S_H-C_H transcription for selecting S regions that are to undergo recombination to IgG, IgA, or IgE (33-37).

In the presence of IL-4, CD40 induces high levels of CSR to IgG1 and IgE and moderate to low levels of CSR to IgG2a and IgA in the presence of IFN γ and TGF- β , respectively (38-40). Deficiency in the expression of CD154 or CD40 signaling causes HIGM syndrome in humans and greatly impaired IgG, IgE, and IgA levels in mice, indicating the importance of CD154 and CD40 in the antibody response. Nevertheless, specific IgG and IgA antibodies can emerge at early stages of an infection before specific T_H cells are activated, suggesting that T-independent and CD40-independent CSR has a role in the generation of these antibodies (41).

T-independent antibody responses entail the activation of B cells from engagement of TLRs and TACI by microbial patterns (42-45). Lipopolysaccharide (LPS) is the only known microbial component that can induce CSR and engage TLR-4 through its Lipid A moiety and crosslink the BCR through its polysaccharide moiety in mice (32). The need for dual TLR and BCR engagement suggests a necessity for recognition of MAMPS and repetitive polysaccharide moieties for the induction of CSR during the adaptive immune response.

Although primary stimuli enable CSR by activating transcription factors that regulate AID transcription, they require secondary stimuli to activate transcription factors that bind to different I_H promoters to initiate germline I_H -S- C_H transcription, thereby specifying the acceptor S region for recombination. Germline transcription provides an open chromatin state allowing for access of CSR factors to the targeted S regions(46,47). In this manner, secondary stimuli instruct antibody specific effector functions, which is mediated by induction of the germline transcription at specific I_H -S- C_H regions during CSR. Each I_H -S- C_H cluster is activated by cytokine specific transcription factors that bind to conserved motifs in the I_H promoters (31). For example, IL-4 activates signal transducer and activator of transcription 6 (Stat6), which binds the $I_{\gamma 1}$ and I_{ϵ} promoters to initiate germline transcription that proceeds through $S_{\gamma 1}$ and S_{ϵ} , enabling class-switching to IgG1 and IgE, respectively (48). TGF- β activates SMAD3, SMAD4 and/or RUNX proteins to promote transcription proceeding through $S_{\gamma 2b}$ and S_{α} for class switching to IgG2b and IgA, respectively (49,50). IFN- γ activates T-bet, STAT1 and/or STAT2 for the initiation of germline transcription that proceeds through $S_{\gamma 2a}$ for class switching to IgG2a (51-53). In addition, competition between different I_H promoters for

the transcription machinery enhances isotype selection. For example, Ikaros mediates suppression of germline $I\gamma 2a-S\gamma 2a-C\gamma 2a$ and $I\gamma 2b-S\gamma 2b-C\gamma 2b$ transcription, thereby downregulating class-switching to IgG2a and IgG2b, and promoting CSR to IgG1 and IgG3 (54). Although secondary stimuli activate a distinct set of transcription factors critical for germline transcription, full induction of germline transcription requires the interplay between primary stimuli, secondary stimuli, and activated transcription factors.

1.5 AID mediates the generation of double strand breaks (DSBs)

CSR is initiated by AID, which is recruited to the core of the switch (S) regions, which contain many 5'-AGCT-3' repeats by 14-3-3 adaptor proteins (55). Germline transcription ensures that these 14-3-3 adaptor proteins are selectively recruited to the upstream and downstream switch (S) regions that are set to undergo S-S DNA recombination, necessary for CSR. 14-3-3 adaptor proteins act as scaffold proteins that nucleate the assembly of CSR factors by binding 5'-AGCT-3' repeats and functioning as structural scaffolds to stabilize many enzymatic elements through DNA-protein interactions (58-60). For example, it interacts with AID and stabilizes AID on S region DNA, while recruiting protein kinase A (PKA) to the S region DNA (56). AID is phosphorylated at Ser38 of the N-terminal region by PKA at the S region, which is critical for its association with replication protein A (RPA) (57-59). RPA enhances AID binding to its substrate when AID levels are limiting (60). RPA is an abundant single strand binding protein, originally identified as a protein, which is essential for SV40 DNA replication and has demonstrated roles in cellular DNA replication, recombination and repair. PKA-mediated phosphorylation of AID at Ser38 *in situ* recruits RPA, which enhances AID deamination of deoxycytosines (61,62). RPA also has scaffold functions to recruit and stabilize CSR factors such as uracil DNA glycosylase (UNG), mismatch repair machinery (MMR) and the MRE11/RAD5-NBS1 complex in the generation of DSBs (63). The resulting deoxyuracils are removed by UNG, which is recruited to and stabilized on S regions in a manner dependent on the scaffold functions of 14-3-3 and the translesion DNA polymerase REV1. Excision of UNG-generated abasic sites by apurinic/apyrimidinic endonucleases (APEs) and/or the MRE11-RAD50 lyase results in

single stranded breaks (SSBs), which either directly form double-strand breaks (DSBs) owing to the close proximity of SSBs on opposite strands (as they occur in the S region core) or are converted to DSBs in an MSH2- and EXO I-dependent fashion (as occurring in the flanking area), as AID can also deaminate DNA flanking the S region though less efficiently owing to the paucity of 5'-AGCT-3' repeats (**Figure 1.3**). AID deamination in these regions lead to the generation of mainly SSBs, of which can be converted to DSBs in a manner that is dependent on key MMR proteins, such as MSH2, MSH6, and EXO1 (45).

The DNA lesions introduced by AID during the initial stage of CSR and SHM must be further processed and repaired (45). Once DSBs have been introduced in the donor and acceptor S regions, they must be repaired to complete DNA recombination. CSR and SHM share many factors and take advantage of DNA repair and replication protein that are responsible for genome stability and maintenance. The mutagenic activity of AID necessitates tight regulation to avoid chromosomal translocations and genomic instability in B cells and non-B cells (64). Accordingly, AID expression and activity is regulated at the transcriptional, post-transcriptional and post-translational levels to the extent where AID is virtually undetectable in naïve B cells, but is expressed at high levels in activated B cells undergoing CSR (65,66). GC B cells that have dysregulated AID expression underlie a higher frequency of oncogenic transformations (67). In addition to the *Ig* loci, AID can also off-target a large number of non-*Ig* genes (68-71), including oncogenes such as *c-myc*, that are frequently translocated to *Ig* in human and mouse B cells leading to tumorigenesis. Accordingly, B cells expressing AID^{S3A} mutants display higher AID levels and increased *c-myc/IgH* translocations (72).

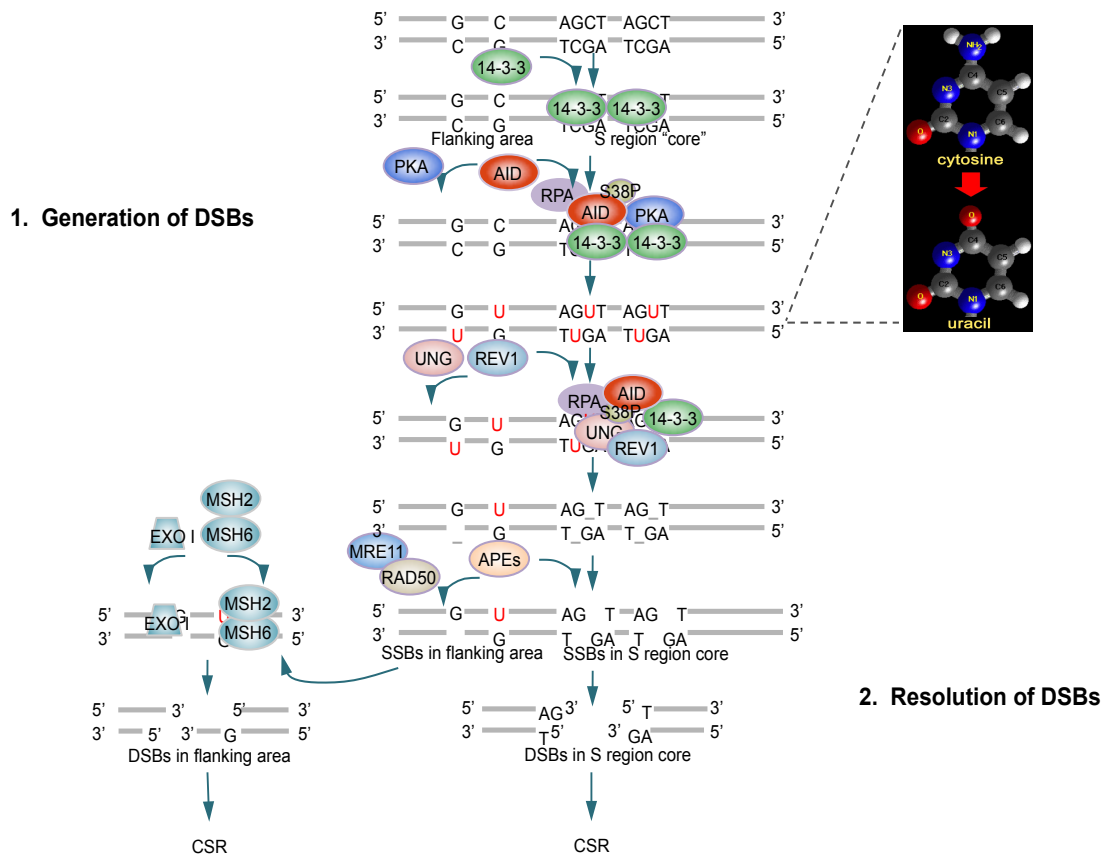


Figure 1.3. AID mediates the generation of DSBs. CSR is initiated by AID, which is recruited to S regions by 14-3-3 adaptors that specifically bind 5'-AGCT-3' repeats in the S region core and recruit AID and PKA to S region DNA. AID is phosphorylated at Ser38 of the N-terminal region by PKA. The resulting deoxyuracils are removed by UNG, which is recruited to and stabilized on S regions in a manner dependent on the scaffold functions of 14-3-3 and REV1. Excision of UNG-generated abasic sites by APEs and/or the MRE11–RAD50 lyase results in single stranded breaks, which owing to their close proximity either directly form double stranded breaks (as occurring in the S region core) or are converted to DSBs in an MSH2- and EXO I-dependent fashion (as occurring in the flanking area). DSB resolution by C-NHEJ or A-EJ leads to formation of S-S junctions and CSR. *Adapted from Xu et al., 2012 (45).*

1.6 Resolution of DSBs

Both CSR and SHM involve activation-induced cytidine deaminase (AID)-mediated generation of DNA lesions and subsequent DNA repair (26-28,73). CSR is completed upon resolution of DSB by S-S synapses, during which intervening DNA sequences are looped out into an extrachromosomal switch circle, generating circle transcripts and leading to the formation of an S-S junction (S-S synapsis), thereby juxtaposing the V_HDJ_H exons to a downstream C_H region exon (45,74). This results in a hyper-mutated, class-switched, antibody gene encoding a post recombination transcript (**Figure 1.4**).

In CSR, DSBs can occur in the S_μ and $S_\gamma1$ regions. For example, in switching for mu to gamma, DSBs are inserted by AID in the S_μ and $S_\gamma1$ regions. These breaks must be processed, by which the upstream region of S_μ is ligated to the downstream region of $S_\gamma1$. DNA DSBs generated by extrinsic DNA damaging agents, such as ionizing radiation are subject to repair in order to maintain genomic integrity by a common set of proteins. The DNA damage response factors ataxia-telangiectasia mutated (ATM), the histone variant H2AX, the MRN complex (Nbs1, Mre11 and Rad50), MDC1, and 53BP1 are recruited to undergo a highly coordinated process to promote appropriate repair and efficient long-range recombination (75). It has always been thought that the downstream DSB recognition, processing and joining steps occur due to non-homologous end joining (NHEJ).

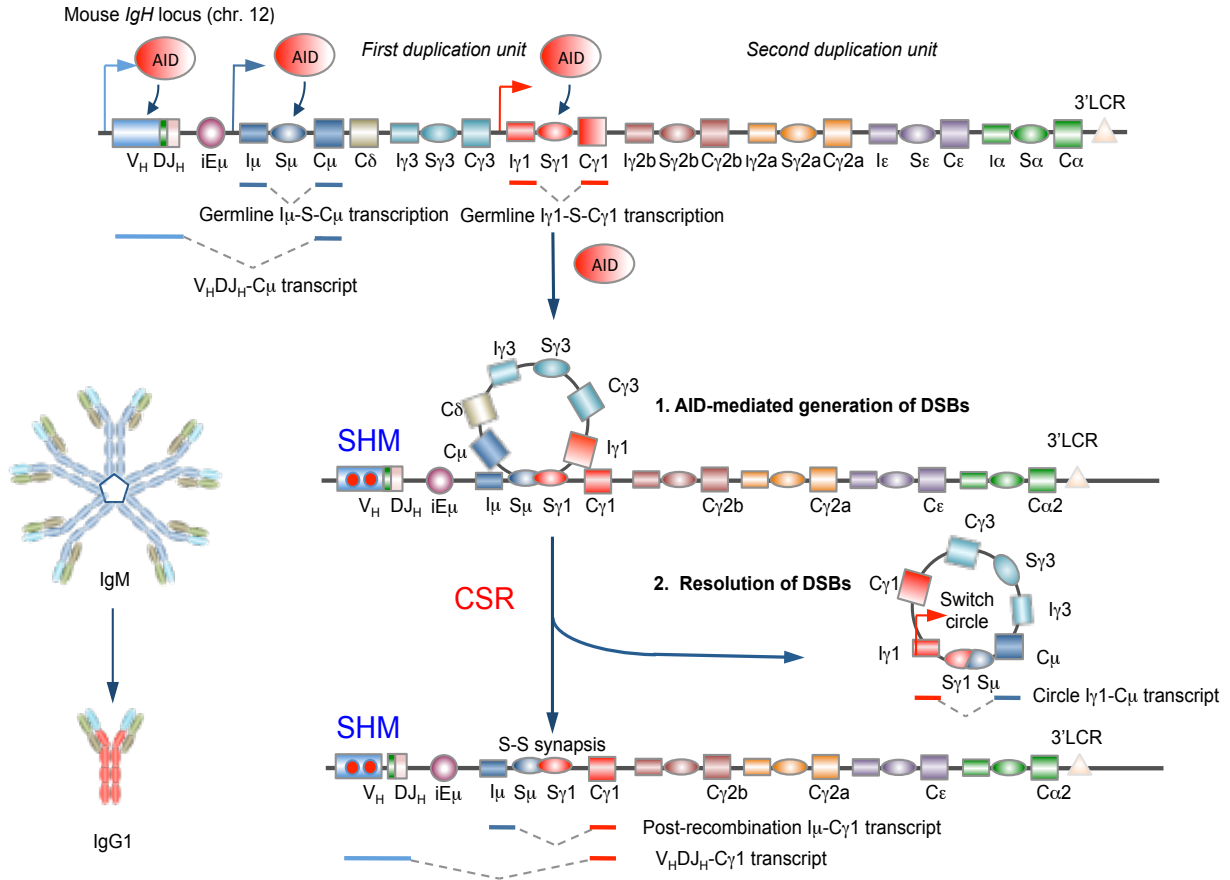


Figure 1.4. AID is critical for the initiation of SHM and CSR. AID is expressed in activated B cells, and deaminates deoxycytosine (dC) residues to yield deoxyuridine (dU); deoxyguanine (dG) mispairs. These mispairs trigger error prone translesion DNA polymerases such as Pol θ , Pol ζ , Pol ϵ , which introduce point mutations in the V(D)J regions during SHM. CSR entails a deletion recombination event in which a gene encoding an upstream immunoglobulin heavy chain constant region (C_H) is exchanged with one of a set of a downstream C_H gene. AID mediates CSR in two sequential steps; first, through the generation of double strand breaks (DSBs) in the upstream (donor) and downstream (acceptor) switch (S) regions. CSR is complete upon resolution of DSBs by S-S synapses, during which intervening DNA sequences are looped out into an extrachromosomal switch circle, thereby generating circle transcripts. The formation of an S-S junction juxtaposes the downstream C_H region DNA to the V(D)J region DNA. This

results in a hyper-mutated, class-switched antibody gene encoding a post-recombination transcript.

The mechanism synapsing S region DSBs uses most or all the elements of the NHEJ pathway, one of the two well-established mechanistic routes repairing DNA DSBs, the other being homologous recombination (HR). Unlike HR, which involves DSB ends with long overhangs and requires substantial DNA junctional homolog, NHEJ synapses DSBs with either blunt ends or short (5' or 3') complementary overhangs. The NHEJ process requires the Ku70/Ku86 heterodimer, the DNA-dependent protein kinase catalytic subunit DNA-PKcs, XRCC4, XLF and DNA Ligase IV (Lig IV) (68) (76-78). Ku is a heterodimer composed of Ku70 and Ku86 subunits, which are structure specific DNA binding proteins, that bind to the broken ends of the DNA based on its abundance and affinity for nicked DNA (69,70). The Ku70/Ku86 heterodimer binds to DNA DSBs, nicks, gaps and hairpin to activate DNA-PKcs, which recruits the XRCC4/Lig IV complex to complete the end joining process (71,79-81). A prominent role of C-NHEJ in CSR is supported by the predominant presence in the G1 phase of AID-dependent S region DSBs and *IgH* foci that contain the CSR factor NBS1. This Ku-dependent repair mechanism does not require substantial junctional homology. While Ku70/Ku86-mediated NHEJ plays an important role in the resolution of CSR-associated DSBs (82,83), it has been shown that a substantial amount of CSR occurred in the absence of critical components of NHEJ (Ku70 or XRCC4 and Lig IV) suggesting that a Ku-independent DSB repair pathway also plays a role in CSR (84-86). This pathway has been referred to as alternative-NHEJ. The precise mechanism of this Ku-independent DSB repair pathway remains to be defined.

This brings us to study the role of homology-mediated joining and HR elements in CSR. **Therefore, my dissertation work is focused on the role of an HR factor, Rad52 in the resolution of S region DSBs in CSR.**

1.7 References

1. Janeway, C. (2005) *Immunobiology : the immune system in health and disease*, 6th ed., Garland Science, New York
2. Janeway, C. A., Jr. (1992) The immune system evolved to discriminate infectious nonself from noninfectious self. *Immunology today* **13**, 11-16
3. Kabelitz, D., and Medzhitov, R. (2007) Innate immunity--cross-talk with adaptive immunity through pattern recognition receptors and cytokines. *Current opinion in immunology* **19**, 1-3
4. Medzhitov, R. (2007) Recognition of microorganisms and activation of the immune response. *Nature* **449**, 819-826
5. Lee, M. S., and Kim, Y. J. (2007) Signaling pathways downstream of pattern-recognition receptors and their cross talk. *Annual review of biochemistry* **76**, 447-480
6. Pone, E. J., Zhang, J., Mai, T., White, C. A., Li, G., Sakakura, J. K., Patel, P. J., Al-Qahtani, A., Zan, H., Xu, Z., and Casali, P. (2012) BCR-signalling synergizes with TLR-signalling for induction of AID and immunoglobulin class-switching through the non-canonical NF-kappaB pathway. *Nature communications* **3**, 767
7. Janeway, C. A., Jr., and Medzhitov, R. (2002) Innate immune recognition. *Annual review of immunology* **20**, 197-216
8. Akashi, K., Traver, D., Kondo, M., and Weissman, I. L. (1999) Lymphoid development from hematopoietic stem cells. *International journal of hematology* **69**, 217-226
9. MacLennan, I. C. (1994) Germinal centers. *Annual review of immunology* **12**, 117-139
10. Grawunder, U., Leu, T. M., Schatz, D. G., Werner, A., Rolink, A. G., Melchers, F., and Winkler, T. H. (1995) Down-regulation of RAG1 and RAG2 gene expression in preB cells after functional immunoglobulin heavy chain rearrangement. *Immunity* **3**, 601-608
11. Borowski, C., Li, X., Aifantis, I., Gounari, F., and von Boehmer, H. (2004) Pre-TCRalpha and TCRalpha are not interchangeable partners of TCRbeta during T lymphocyte development. *J. Exp. Med.* **199**, 607-615
12. Fazilleau, N., Mark, L., McHeyzer-Williams, L. J., and McHeyzer-Williams, M. G. (2009) Follicular helper T cells: lineage and location. *Immunity* **30**, 324-335
13. Casali, P., and Schettino, E. W. (1996) Structure and function of natural antibodies. *Curr. Top. Microbiol. Immunol.* **210**, 167-179
14. Klein, U., and Dalla-Favera, R. (2008) Germinal centres: role in B-cell physiology and malignancy. *Nat. Rev. Immunol.* **8**, 22-33
15. Allen, C. D., Ansel, K. M., Low, C., Lesley, R., Tamamura, H., Fujii, N., and Cyster, J. G. (2004) Germinal center dark and light zone organization is mediated by CXCR4 and CXCR5. *Nature immunology* **5**, 943-952
16. Renshaw, B. R., Fanslow, W. C., 3rd, Armitage, R. J., Campbell, K. A., Liggitt, D., Wright, B., Davison, B. L., and Maliszewski, C. R. (1994) Humoral immune responses in CD40 ligand-deficient mice. *J Exp Med* **180**, 1889-1900
17. Muramatsu, M., Kinoshita, K., Fagarasan, S., Yamada, S., Shinkai, Y., and Honjo, T. (2000) Class switch recombination and hypermutation require activation-

- induced cytidine deaminase (AID), a potential RNA editing enzyme. *Cell* **102**, 553-563
18. Zan, H., Tat, C., and Casali, P. (2014) MicroRNAs in lupus. *Autoimmunity* **47**, 272-285
 19. Cerutti, A., Puga, I., and Cols, M. (2011) Innate control of B cell responses. *Trends in immunology* **32**, 202-211
 20. Nimmerjahn, F., and Ravetch, J. V. (2007) Fc-receptors as regulators of immunity. *Advances in immunology* **96**, 179-204
 21. Rickert, R. C. (2005) Regulation of B lymphocyte activation by complement C3 and the B cell coreceptor complex. *Current opinion in immunology* **17**, 237-243
 22. Toapanta, F. R., and Ross, T. M. (2006) Complement-mediated activation of the adaptive immune responses: role of C3d in linking the innate and adaptive immunity. *Immunologic research* **36**, 197-210
 23. Revy, P., Muto, T., Levy, Y., Geissmann, F., Plebani, A., Sanal, O., Catalan, N., Forveille, M., Dufourcq-Labeuze, R., Gennery, A., Tezcan, I., Ersoy, F., Kayserili, H., Ugazio, A. G., Brousse, N., Muramatsu, M., Notarangelo, L. D., Kinoshita, K., Honjo, T., Fischer, A., and Durandy, A. (2000) Activation-induced cytidine deaminase (AID) deficiency causes the autosomal recessive form of the Hyper-IgM syndrome (HIGM2). *Cell* **102**, 565-575
 24. Stavnezer, J., Guikema, J. E., and Schrader, C. E. (2008) Mechanism and regulation of class switch recombination. *Annual review of immunology* **26**, 261-292
 25. Honjo, T. (2008) A memoir of AID, which engraves antibody memory on DNA. *Nature immunology* **9**, 335-337
 26. Casali, P., Pal, Z., Xu, Z., and Zan, H. (2006) DNA repair in antibody somatic hypermutation. *Trends Immunol* **27**, 313-321
 27. Xu, Z., Zan, H., Pone, E. J., Mai, T., and Casali, P. (2012) Immunoglobulin class switching: induction, targeting and beyond. *Nature Rev. Immunol.* **12**, 517-531
 28. Casali, P. (2014) Somatic recombination and hypermutation in the immune system. in *Lewin's Genes X* (Krebs, J. E., Goldstein, E. S., and Kilpatrick, S. T. eds.), 11 Ed., Jones & Bartlett, Sudbury, MA. pp 459-507
 29. Li, G., Zan, H., Xu, Z., and Casali, P. (2013) Epigenetics of the antibody response. *Trends Immunol.* **34**, 460-470
 30. Schuetz, C., Niehues, T., Friedrich, W., and Schwarz, K. (2010) Autoimmunity, autoinflammation and lymphoma in combined immunodeficiency (CID). *Autoimmunity reviews* **9**, 477-482
 31. Stavnezer, J., Guikema, J. E., and Schrader, C. E. (2008) Mechanism and regulation of class switch recombination. *Annu. Rev. Immunol.* **26**, 261-292
 32. Pone, E. J., Zhang, J., Sakakura, J., Mai, T., White, C. A., Patel, P. J., Longley, A. T., Al-Qahtani, A., Zan, H., Xu, Z., and Casali, P. (2012) BCR-signaling activates the non-canonical NF-kappaB pathway and synergizes with TLR1/2, TLR4, TLR7 or TLR9 to induce AID and immunoglobulin class-switching. *Nat. Commun.*, doi: 10.1038/ncomms1769
 33. Pone, E. J., Xu, Z., White, C. A., Zan, H., and Casali, P. (2012) B cell TLRs and induction of immunoglobulin class-switch DNA recombination. *Frontiers in bioscience* **17**, 2594-2615

34. Tangye, S. G., Ferguson, A., Avery, D. T., Ma, C. S., and Hodgkin, P. D. (2002) Isotype switching by human B cells is division-associated and regulated by cytokines. *J. Immunol.* **169**, 4298-4306
35. Deenick, E. K., Hasbold, J., and Hodgkin, P. D. (2005) Decision criteria for resolving isotype switching conflicts by B cells. *Eur. J. Immunol.* **35**, 2949-2955
36. Acosta-Rodriguez, E. V., Merino, M. C., Montes, C. L., Motran, C. C., and Gruppi, A. (2007) Cytokines and chemokines shaping the B-cell compartment. *Cytokine Growth Factor Rev.* **18**, 73-83
37. Ivashkiv, L. B. (2008) A signal-switch hypothesis for cross-regulation of cytokine and TLR signalling pathways. *Nat. Rev. Immunol.* **8**, 816-822
38. Cerutti, A., Zan, H., Schaffer, A., Bergsagel, L., Harindranath, N., Max, E. E., and Casali, P. (1998) CD40 ligand and appropriate cytokines induce switching to IgG, IgA, and IgE and coordinated germinal center and plasmacytoid phenotypic differentiation in a human monoclonal IgM⁺IgD⁺ B cell line. *J. Immunol.* **160**, 2145-2157
39. Szomolanyi-Tsuda, E., Brien, J. D., Dorgan, J. E., Welsh, R. M., and Garcea, R. L. (2000) The role of CD40-CD154 interaction in antiviral T cell-independent IgG responses. *J. Immunol.* **164**, 5877-5882
40. Park, S. R., Zan, H., Pal, Z., Zhang, J., Al-Qahtani, A., Pone, E. J., Xu, Z., Mai, T., and Casali, P. (2009) HoxC4 binds to the promoter of the cytidine deaminase AID gene to induce AID expression, class-switch DNA recombination and somatic hypermutation. *Nat. Immunol.* **10**, 540-550
41. Pone, E. J., Zan, H., Zhang, J., Al-Qahtani, A., Xu, Z., and Casali, P. (2010) Toll-like receptors and B-cell receptors synergize to induce immunoglobulin class-switch DNA recombination: relevance to microbial antibody responses. *Crit. Rev. Immunol.* **30**, 1-29
42. Pasare, C., and Medzhitov, R. (2005) Control of B-cell responses by Toll-like receptors. *Nature* **438**, 364-368
43. Pasare, C., and Medzhitov, R. (2005) Toll-like receptors: linking innate and adaptive immunity. *Adv. Exp. Med. Biol.* **560**, 11-18
44. Cerutti, A., Puga, I., and Cols, M. (2011) Innate control of B cell responses. *Trends Immunol.* **32**, 202-211
45. Xu, Z., Zan, H., Pone, E. J., Mai, T., and Casali, P. (2012) Immunoglobulin class-switch DNA recombination: induction, targeting and beyond. *Nature reviews. Immunology* **12**, 517-531
46. Haddad, D., Oruc, Z., Puget, N., Laviolette-Malirat, N., Philippe, M., Carrion, C., Le Bert, M., and Khamlichi, A. A. (2011) Sense transcription through the S region is essential for immunoglobulin class switch recombination. *The EMBO journal* **30**, 1608-1620
47. Nambu, Y., Sugai, M., Gonda, H., Lee, C. G., Katakai, T., Agata, Y., Yokota, Y., and Shimizu, A. (2003) Transcription-coupled events associating with immunoglobulin switch region chromatin. *Science* **302**, 2137-2140
48. Linehan, L. A., Warren, W. D., Thompson, P. A., Grusby, M. J., and Berton, M. T. (1998) STAT6 is required for IL-4-induced germline Ig gene transcription and switch recombination. *J. Immunol.* **161**, 302-310

49. Klein, J., Ju, W., Heyer, J., Wittek, B., Haneke, T., Knaus, P., Kucherlapati, R., Böttinger, E. P., Nitschke, L., and Kneitz, B. (2006) B cell-specific deficiency for Smad2 in vivo leads to defects in TGF-beta-directed IgA switching and changes in B cell fate. *J. Immunol.* **176**, 2389-2396
50. Watanabe, K., Sugai, M., Nambu, Y., Osato, M., Hayashi, T., Kawaguchi, M., Komori, T., Ito, Y., and Shimizu, A. (2010) Requirement for Runx proteins in IgA class switching acting downstream of TGF-beta 1 and retinoic acid signaling. *J. Immunol.* **184**, 2785-2927
51. Peng, S. L., Szabo, S. J., and Glimcher, L. H. (2002) T-bet regulates IgG class switching and pathogenic autoantibody production. *Proc. Natl. Acad. Sci. U.S.A.* **99**, 5545-5550
52. Rifkin, I. R., and Marshak-Rothstein, A. (2003) T-bet: the Toll-bridge to class-switch recombination? *Nat. Immunol.* **4**, 650-652
53. Xu, W., and Zhang, J. J. (2005) Stat1-dependent synergistic activation of T-bet for IgG2a production during early stage of B cell activation. *J. Immunol.* **175**, 7419-7424
54. Sellars, M., Reina-San-Martin, B., Kastner, P., and Chan, S. (2009) Ikaros controls isotype selection during immunoglobulin class switch recombination. *J. Exp. Med.* **206**, 1073-1087
55. Xu, Z., Fulop, Z., Wu, G., Pone, E. J., Zhang, J., Mai, T., Thomas, L. M., Al-Qahtani, A., White, C. A., Park, S. R., Steinacker, P., Li, Z., Yates, J. r., Herron, B., Otto, M., Zan, H., Fu, H., and Casali, P. (2010) 14-3-3 adaptor proteins recruit AID to 5'-AGCT-3'-rich switch regions for class switch recombination. *Nat. Struct. Mol. Biol.* **17**, 1124-1135
56. Lam, T., Thomas, L. M., White, C. A., Li, G., Pone, E. J., Xu, Z., and Casali, P. (2013) Scaffold functions of 14-3-3 adaptors in B cell immunoglobulin class switch DNA recombination. *PLoS one* **8**, e80414
57. Chaudhuri, J., Khuong, C., and Alt, F. W. (2004) Replication protein A interacts with AID to promote deamination of somatic hypermutation targets. *Nature* **430**, 992-998
58. Crouch, E. E., Li, Z., Takizawa, M., Fichtner-Feigl, S., Gourzi, P., Montano, C., Feigenbaum, L., Wilson, P., Janz, S., Papavasiliou, F. N., and Casellas, R. (2007) Regulation of AID expression in the immune response. *J. Exp. Med.* **204**, 1145-1156
59. Basu, U., Wang, Y., and Alt, F. W. (2008) Evolution of phosphorylation-dependent regulation of activation-induced cytidine deaminase. *Mol. Cell* **32**, 285-291
60. Chaudhuri, J., Khuong, C., and Alt, F. W. (2004) Replication protein A interacts with AID to promote deamination of somatic hypermutation targets. *Nature* **430**, 992-998
61. Basu, U., Chaudhuri, J., Phan, R. T., Datta, A., and Alt, F. W. (2007) Regulation of activation induced deaminase via phosphorylation. *Advances in experimental medicine and biology* **596**, 129-137
62. Basu, U., Franklin, A., and Alt, F. W. (2009) Post-translational regulation of activation-induced cytidine deaminase. *Philosophical transactions of the Royal Society of London. Series B, Biological sciences* **364**, 667-673

63. Rada, C., Di Noia, J. M., and Neuberger, M. S. (2004) Mismatch recognition and uracil excision provide complementary paths to both Ig switching and the A/T-focused phase of somatic mutation. *Molecular cell* **16**, 163-171
64. Robbiani, D. F., Bunting, S., Feldhahn, N., Bothmer, A., Camps, J., Deroubaix, S., McBride, K. M., Klein, I. A., Stone, G., Eisenreich, T. R., Ried, T., Nussenzweig, A., and Nussenzweig, M. C. (2009) AID produces DNA double-strand breaks in non-Ig genes and mature B cell lymphomas with reciprocal chromosome translocations. *Mol. Cell* **36**, 631-641
65. Xu, Z., Pone, E. J., Al-Qahtani, A., Park, S. R., Zan, H., and Casali, P. (2007) Regulation of aicda expression and AID activity: relevance to somatic hypermutation and class switch DNA recombination. *Crit. Rev. Immunol.* **27**, 367-397
66. Stavnezer, J. (2011) Complex regulation and function of activation-induced cytidine deaminase. *Trends Immunol.* **32**, 194-201
67. Pasqualucci, L., Bhagat, G., Jankovic, M., Compagno, M., Smith, P., Muramatsu, M., Honjo, T., Morse, H. C., 3rd, Nussenzweig, M. C., and Dalla-Favera, R. (2008) AID is required for germinal center-derived lymphomagenesis. *Nat. Genet.* **40**, 108-112
68. Wyman, C., and Kanaar, R. (2006) DNA double-strand break repair: all's well that ends well. *Annual review of genetics* **40**, 363-383
69. van Gent, D. C., Hoeijmakers, J. H., and Kanaar, R. (2001) Chromosomal stability and the DNA double-stranded break connection. *Nat Rev Genet* **2**, 196-206
70. Jackson, S. P. (2002) Sensing and repairing DNA double-strand breaks. *Carcinogenesis* **23**, 687-696
71. Paillard, S., and Strauss, F. (1991) Analysis of the mechanism of interaction of simian Ku protein with DNA. *Nucleic Acids Res.* **19**, 5619-5624
72. Dynan, W. S., and Yoo, S. (1998) Interaction of Ku protein and DNA-dependent protein kinase catalytic subunit with nucleic acids. *Nucleic acids research* **26**, 1551-1559
73. Casali, P., and Zan, H. (2004) Class switching and Myc translocation: how does DNA break? *Nat. Immunol.* **5**, 1101-1103
74. Casali, P., Pal, Z., Xu, Z., and Zan, H. (2006) DNA repair in antibody somatic hypermutation. *Trends Immunol.* **27**, 313-321
75. Ramiro, A., Reina San-Martin, B., McBride, K., Jankovic, M., Barreto, V., Nussenzweig, A., and Nussenzweig, M. C. (2007) The role of activation-induced deaminase in antibody diversification and chromosome translocations. *Adv Immunol* **94**, 75-107
76. Blier, P. R., Griffith, A. J., Craft, J., and Hardin, J. A. (1993) Binding of Ku protein to DNA. Measurement of affinity for ends and demonstration of binding to nicks. *The Journal of biological chemistry* **268**, 7594-7601
77. Lieber, M. R., Grawunder, U., Wu, X., and Yaneva, M. (1997) Tying loose ends: roles of Ku and DNA-dependent protein kinase in the repair of double-strand breaks. *Current opinion in genetics & development* **7**, 99-104

78. Yaneva, M., Kowalewski, T., and Lieber, M. R. (1997) Interaction of DNA-dependent protein kinase with DNA and with Ku: biochemical and atomic-force microscopy studies. *The EMBO journal* **16**, 5098-5112
79. Dynan, W. S., and Yoo, S. (1998) Interaction of Ku protein and DNA-dependent protein kinase catalytic subunit with nucleic acids. *Nucleic Acids Res.* **26**, 1551-1559
80. Lieber, M. R., Lu, H., Gu, J., and Schwarz, K. (2008) Flexibility in the order of action and in the enzymology of the nuclease, polymerases, and ligase of vertebrate non-homologous DNA end joining: relevance to cancer, aging, and the immune system. *Cell Res* **18**, 125-133
81. Walker, J. R., Corpina, R. A., and Goldberg, J. (2001) Structure of the Ku heterodimer bound to DNA and its implications for double-strand break repair. *Nature* **412**, 607-614
82. Manis, J. P., Gu, Y., Lansford, R., Sonoda, E., Ferrini, R., Davidson, L., Rajewsky, K., and Alt, F. W. (1998) Ku70 is required for late B cell development and immunoglobulin heavy chain class switching. *J. Exp. Med.* **187**, 2081-2089
83. Casellas, R., Nussenzweig, A., Wuerffel, R., Pelanda, R., Reichlin, A., Suh, H., Qin, X. F., Besmer, E., Kenter, A., Rajewsky, K., and Nussenzweig, M. C. (1998) Ku80 is required for immunoglobulin isotype switching. *EMBO J.* **17**, 2404-2411
84. Yan, C. T., Boboila, C., Souza, E. K., Franco, S., Hickernell, T. R., Murphy, M., Gumaste, S., Geyer, M., Zarrin, A. A., Manis, J. P., Rajewsky, K., and Alt, F. W. (2007) IgH class switching and translocations use a robust non-classical end-joining pathway. *Nature* **449**, 478-482
85. Boboila, C., Jankovic, M., Yan, C. T., Wang, J. H., Wesemann, D. R., Zhang, T., Fazeli, A., Feldman, L., Nussenzweig, A., Nussenzweig, M., and Alt, F. W. (2010) Alternative end-joining catalyzes robust IgH locus deletions and translocations in the combined absence of ligase 4 and Ku70. *Proc. Natl. Acad. Sci. USA.* **107**, 3034-3039
86. Boboila, C., Yan, C., Wesemann, D. R., Jankovic, M., Wang, J. H., Manis, J., Nussenzweig, A., Nussenzweig, M., and Alt, F. W. (2010) Alternative end-joining catalyzes class switch recombination in the absence of both Ku70 and DNA ligase 4. *J. Exp. Med.* **207**, 417-427

CHAPTER 2

The role of Rad52 in class switch DNA recombination

Contents:

2.1 Homologous Recombination	31
2.2 The role of Rad52 in CSR	35
2.3 Rad52 deficiency increases the class switched antibody response <i>in vivo</i>	39
2.4 Rad52 deficiency increases CSR <i>in vitro</i>	43
2.5 Enforced expression of Rad52 impairs CSR	48
2.6 Methods	50
2.7 Discussion	57
2.8 References	60

2.1 Homologous recombination

Homologous recombination (HR) is a high-fidelity DSB repair pathway which involves the exchange of sister chromosomes and utilizes a long, undamaged homologous template for repair. As previously mentioned, NHEJ is active primarily during the G1-early S phase of the cell cycle, as it does not require template DNA for repair. However, it can also be active throughout the cell cycle. As HR requires a homologous template, it occurs mainly during the S/G2 phase of the cell cycle, during DNA replication (17, 18). However, it has been recently challenged that HR may not require DNA replication to occur (Schatz).

Rad52 is an HR repair factor that binds to single-strand DNA ends and plays a central role in genetic recombination by recruiting Rad51, which mediates HR and promotes the annealing of complementary ssDNA (1-3). Rad52 interacts with not only Rad51, but also with replication protein A (RPA) (5), another ssDNA-binding protein that has been suggested to play a role in CSR by helping stabilize AID's ssDNA targets and associates preferentially with resected ssDNA in response to lesions created by AID (6, 7). RPA stimulates long patch base-excision repair or mismatch repair (**Figure 2.1**). Studies suggest Ku70/Ku86 preferentially binds to DNA with free, blunt ends, whereas Rad52 favors single stranded DNA with 3' overhangs (staggered ends) or protruding ends (19). If HR does not require DNA replication to occur, Rad52 can be recruited to the DSBs before the S phase and may preferentially bind to single strand protruding ends.

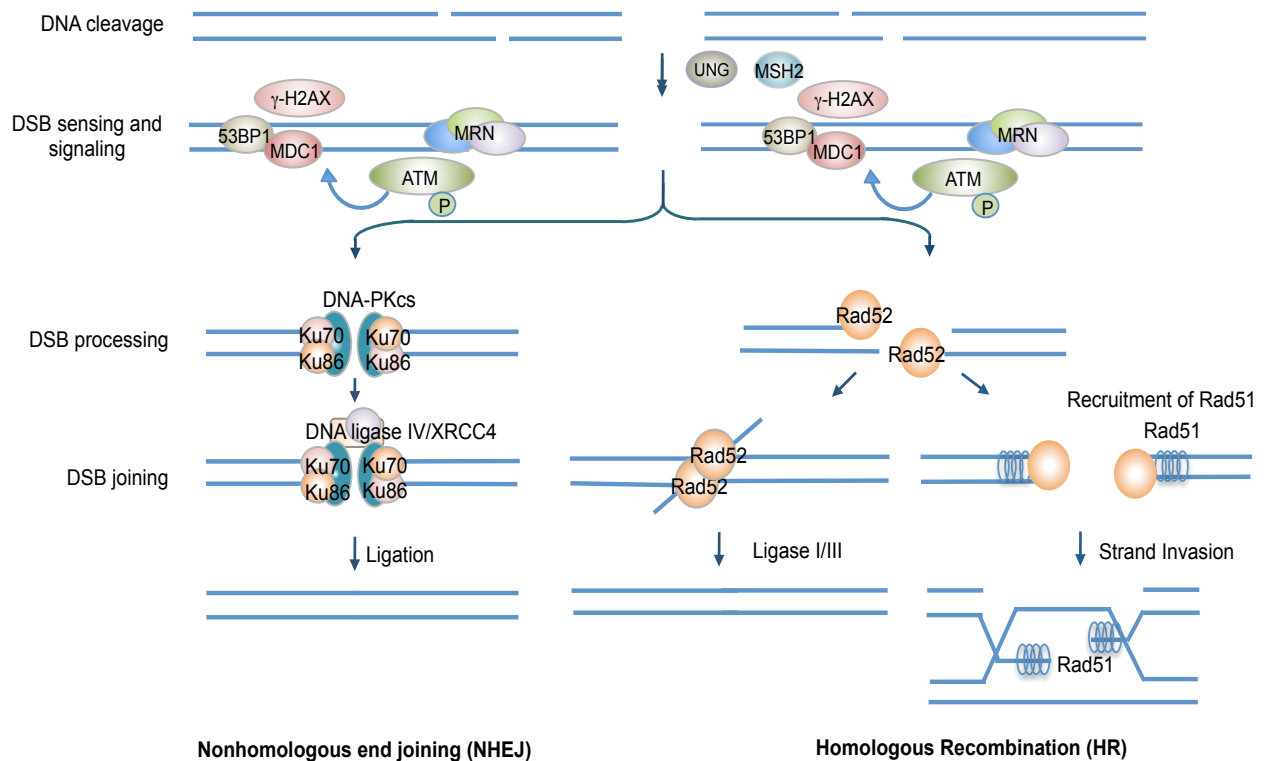


Figure 2.1. DSB Repair Process. DNA double strand breaks can be repaired by one of two main repair pathways: non-homologous end joining or homologous recombination. These two repair mechanisms employ distinct sets of proteins. Proteins involved in NHEJ include the Ku70/Ku86 heterodimer complex, DNA PKcs, and DNA ligase IV/XRCC4. HR is a high-fidelity DSB repair pathway which involves the exchange of sister chromosomes and utilizes a long, undamaged homologous template for repair. Rad52 is a single strand binding protein, which plays a central role in genetic recombination by recruiting Rad51, which mediates HR and promotes the annealing of complementary ssDNA. These two end-joining processes repair DSBs based on the ends generated after the break. Ku70/Ku86 preferentially binds to DNA with blunt ends. Rad52 preferentially binds single stranded DNA with 3' overhangs (staggered ends).

The structure of Rad52 exists as an undecameric subunit ring with extensive subunit contacts; a large, positively charged groove runs along the surface of the ring, suggesting a mechanism by which Rad52 presents the single strand reannealing with complementary single-stranded DNA (**Figure 2.2**). Rad52 is 46 kiloDalton protein that spans 418 residues. The single strand-binding domain resides in the N-terminal region (residues 24-177) of the protein and is highly conserved, whereas the non-conserved Rad51-interaction domain is located in the C-terminal region (178-209) and promotes single-strand annealing *in vitro* (**Figure 2.2**). Rad51 is expressed and localized to the nucleus of B cells undergoing CSR (3, 4). These processes may play important roles in repairing breaks in the *Ig* locus, by associating with and stabilizing resected free DNA ends that cannot easily be repaired by classical NHEJ, thereby facilitating salvage by homology-mediated repair pathways (7). The role of homology-mediated end joining and HR elements in CSR remains to be elucidated.

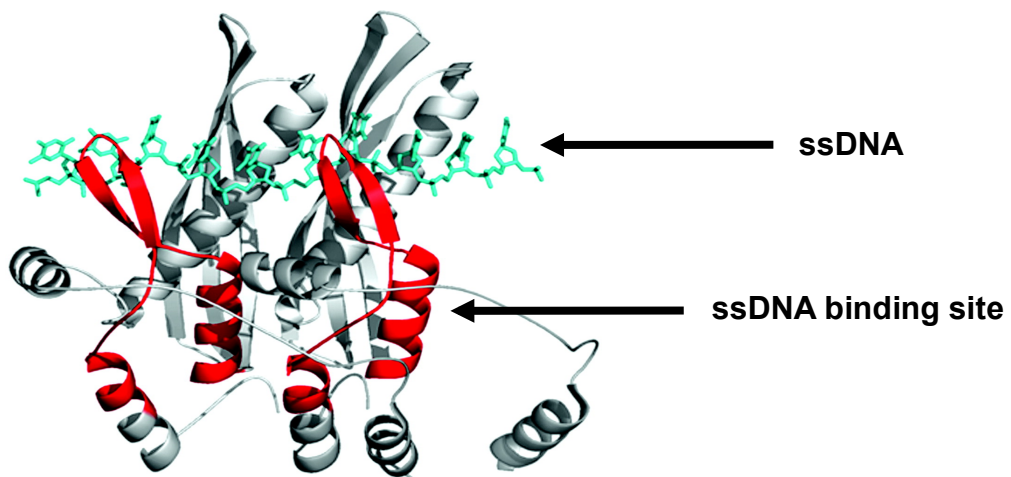
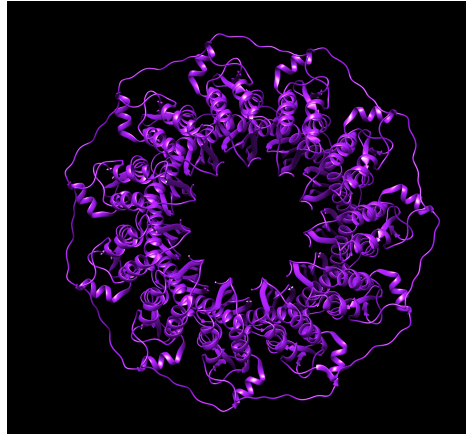


Figure 2.2. Structure of the Rad52 undecamer. Ribbon representation of Rad52 as an undecameric subunit with 11 monomers (top). A large, positively charged deep groove runs across the protein surface suggesting a mechanism for which Rad52 may play a critical role in DSB repair involving single strand annealing with complementary ssDNA. Structures were rendered using the UCSF Chimera Program. Ribbon representation of the proposed ssDNA-binding site for Rad52 on residues 39–80 of the protein (red) of the N-terminal region (residues 1–209), shown in gray. The ssDNA is overlaid in cyan. *Adapted from Singleton et al., 2002 (8).*

2.2 The role of Rad52 in CSR

In the absence of core NHEJ components, namely Ku70/Ku86, XRCC4, and Ligase IV, a substantial amount of CSR occurs; therefore we asked the question if Ku is not present, what is mediating CSR? There is only one other main mechanism, which is HR.

Although the mechanism of the Ku-independent DSB repair pathway remains to be defined, it can be postulated that given the long stretches of repetitive DNA sequences in S regions, some homology-mediated recombination process, potentially based on short or imprecise homologies, plays a role in CSR. Consistent with this notion, an increase in microhomologies has been observed in S-S junctions generated from residual CSR activity in Ku70- and Lig IV-deficient B cells (27,86-88), suggesting that the Ku- and Lig IV-independent mechanism recombining CSR DSB ends involves annealing of complementary single-strand DNA (**Figure 2.3**). Microhomology mediated end joining (MMEJ) is an error-prone method of repair and can often result in deletion mutations in the genetic code which may initiate the creation of oncogenes that could lead to the development of cancer. The Alt group found in addition to the increase in microhomologies, there was an increase in interchromosomal translocations in Ku-deficient B cells (86).

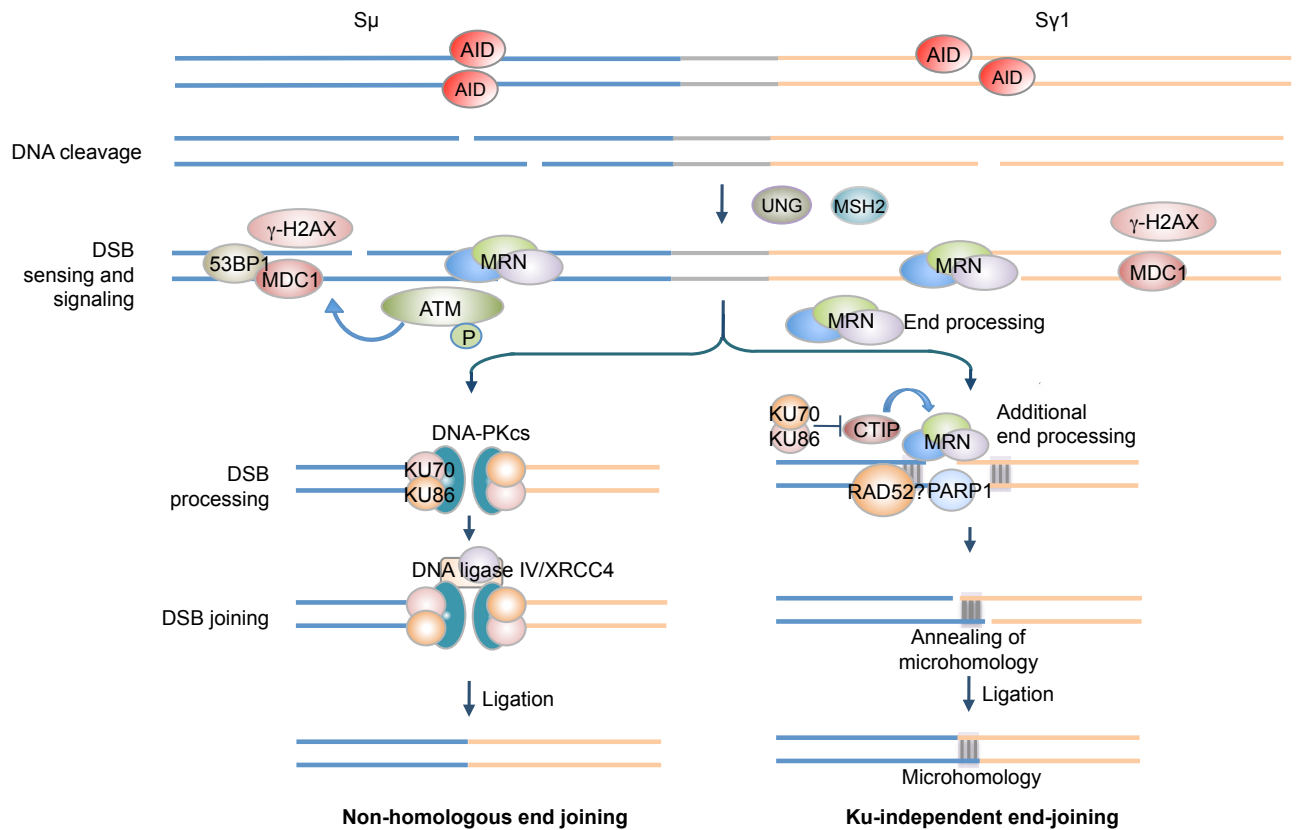


Figure 2.3. DSB repair process in CSR. AID mediates the generation of DSBs in CSR and is typically repaired by non-homologous end joining (NHEJ). CSR junctions mediated by the NHEJ pathway employ the Ku70/Ku86 heterodimer complex for DSB recognition and XRCC4/DNA ligase IV for ligation. A substantial amount of CSR occurred in the absence of critical components of NHEJ (Ku70 or XRCC4 and Ligase IV), suggesting that other DSB repair modalities are at work. This Ku-independent end joining mechanism is associated with an increase in microhomologies at the S-S junctions and *c-myc/IgH* interchromosomal translocations in Ku-deficient B cells.

Rad52 is a single strand binding protein that plays a critical role in the DSB repair process involving single-strand annealing. As a single strand binding protein, Rad52 plays a critical role in the DSB repair process involving single-strand annealing and may be linked to the increased microhomologies in Ku-deficient B cells, as Rad52 favors single strand breaks with protruding ends. Further, our previous findings suggest that Rad52 preferentially binds to protruding DSB ends in the *IgH* locus during antibody diversification (9). This led us to hypothesize that Rad52 mediates the resolution of S region DSBs in CSR.

To address the role of Rad52 in repairing AID-mediated DSBs in S region DNA during CSR, we first obtained *Rad52*^{-/-} mice (10). These mice were viable, fertile, and showed no gross abnormalities. Furthermore, the size of the spleens, and number and size of Peyer's patches in these mice were comparable to those of *Rad52*^{+/+} mice. To address the role of Rad52 in CSR, we first had to determine the impact of Rad52 deficiency on CSR by examining the specific class switched antibody response in *Rad52*^{-/-} mice. We proceeded by analyzing the specific and class-switched antibody response in *Rad52*^{-/-} mice and validated these findings obtained *in vitro* using *Rad52*^{-/-} B cells by molecular and genetic analysis. Finally, we enforced expression of Rad52 by retroviral transduction and analyzed CSR with the anticipation that this would give us the opposite effect.

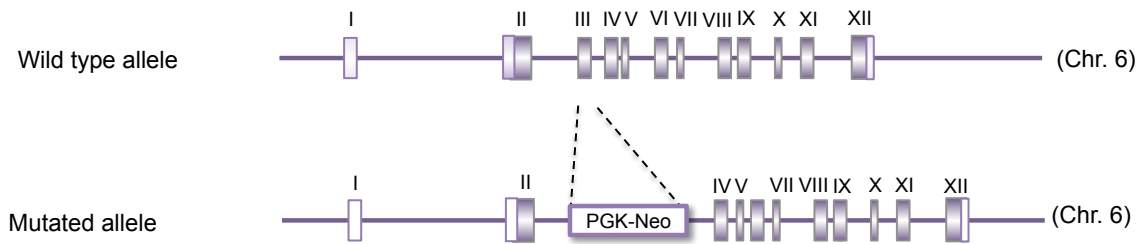


Figure 2.4. Disruption of the *MmRAD52* gene. Schematic representation of the disruption of the *MmRAD52* gene. Displayed is the targeted *MmRad52* gene, the targeting vector, and targeted locus. Roman numbered solid boxes indicate all coding exons, and noncoding (parts of) exons are shown as open boxes. In mouse ES cells, *MmRAD52* replaced exon 3 of the *Rad52* gene with the *neomycin* gene and an upstream mouse sequence (UMS) which functions as a transcription terminator. The *MmRAD52* gene spans approximately 18 kb on chromosome 6 and consists of 12 exons. These mice are viable, fertile and show no gross abnormalities. *Adapted from Rijkers et al., 1998 (10).*

2.3 Rad52 deficiency increases the class switched antibody response *in vivo*

To understand the role of Rad52 on a specific T-dependent response, we immunized *Rad52*^{+/+} and *Rad52*^{-/-} mice with the hapten NP (4-hydroxy-3-nitrophenylacetyl) coupled to chicken gamma globulin (CGG), which preferentially induces NP-binding IgG1. We found *Rad52*^{-/-} mice showed increased titers of total IgG1, NP₃₂-binding IgG1 and high affinity NP₄-specific binding IgG1, although levels of total IgM were normal (**Figure 2.5a**). The increased class-switched NP-binding IgG1 titers in *Rad52*^{-/-} mice were associated with a more than 75% increase of IgG1⁺ PNA^{hi}B220⁺ germinal center B cells compared to their *Rad52*^{+/+} littermates (**Figure 2.5b**). Consistently, in the Peyer's patches of unimmunized 10-12 week-old *Rad52*^{-/-} mice, the number of germinal center B cells class switched to IgA showed a twofold greater abundance than in *Rad52*^{+/+} B cells. Thus, Rad52 deficiency elevates a specific class-switched antibody response.

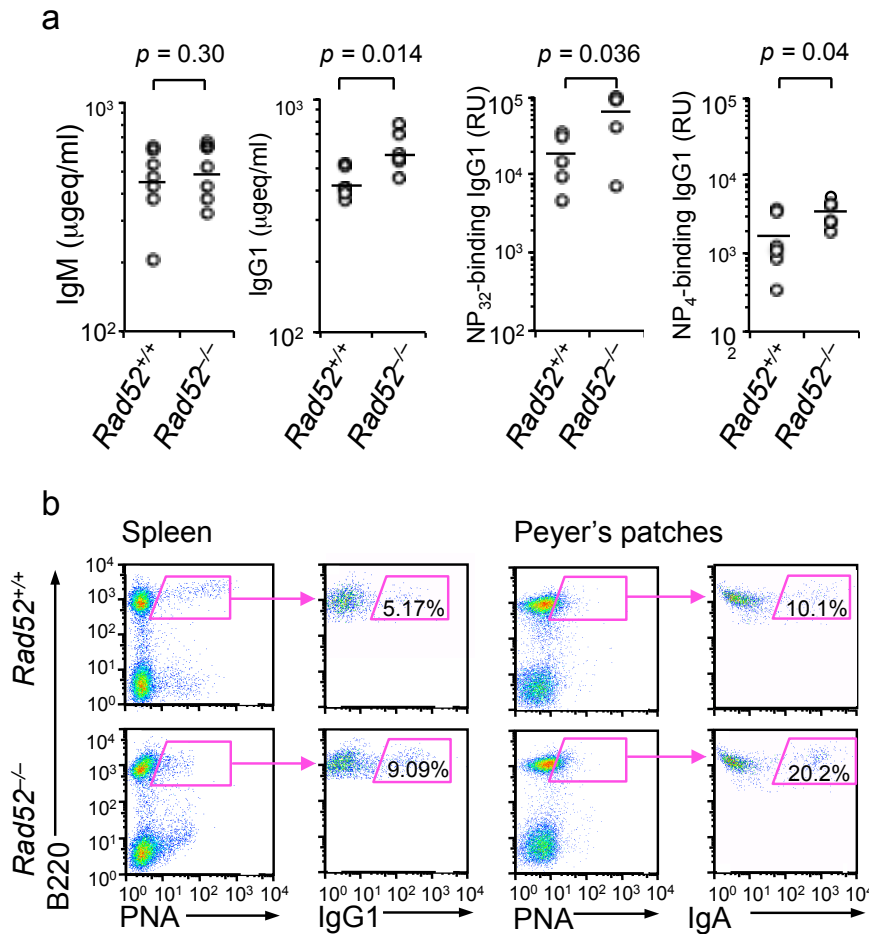


Figure 2.5. Rad52 deficiency increases the class-switched antibody response *in vivo*. (a) Titers of circulating IgM, IgG1, NP₃₂-binding IgM and IgG1, and high affinity NP₄-binding IgM and IgG1 in serum from *Rad52*^{+/+} and *Rad52*^{-/-} littermates 10 d after NP₁₆-CGG immunization, expressed as µg equivalent per ml (µgeq/ml) or the number of dilutions needed to reach 50% of saturation binding (relative units, RU). *n* = 5-6 pairs of mice, each symbol represents an individual mouse. *p* values, paired *t*-test. (b) Surface IgG1 expression in B220⁺PNA^{hi} GC B cells isolated from the spleens of *Rad52*^{+/+} and *Rad52*^{-/-} littermates 10 d after NP₁₆-CGG injection (left panels), and surface IgA expression in B220⁺PNA^{hi} GC B cells from the Peyer's Patches of unimmunized *Rad52*^{+/+} and *Rad52*^{-/-} littermates (right panels) were analyzed by flow cytometry. Data are from representative of three independent experiments.

The augmented antibody response to NP-CGG in *Rad52*^{-/-} mice was not due to obvious alterations in lymphoid differentiation. These mice demonstrate no gross morphological differences in regards to the size of the spleen or the number and size of the Peyer's patches in comparison to those in *Rad52*^{+/+} mice (not shown). The number of B and T cells, the proportion of CD4⁺ and CD8⁺ T cells, the proportion of PNA^{hi} GC B cells and B220^{low}CD138⁺ plasma cells in the spleen were also comparable to those of *Rad52*^{+/+} mice (**Figure 2.6a**). Analysis of incorporation of the thymidine analog BrdU (2-bromodeoxyuridine) into the DNA of rapidly proliferating B cells in *Rad52*^{-/-} mice was not different than in *Rad52*^{+/+} mice, as demonstrated by normal B cell proliferation, viability and cell cycle of total and GC B cells, as measured by BrdU incorporation and 7AAD staining in both mouse genotypes (**Figure 2.6b**). Therefore, Rad52 deficiency does not alter B cell, CD4⁺ or CD8⁺ T cell, and GC B cell numbers, plasma cell differentiation, or B cell proliferation, viability and cell division. The increased class-switched antibody response in *Rad52*^{-/-} mice was likely due to an intrinsic alteration to the CSR machinery.

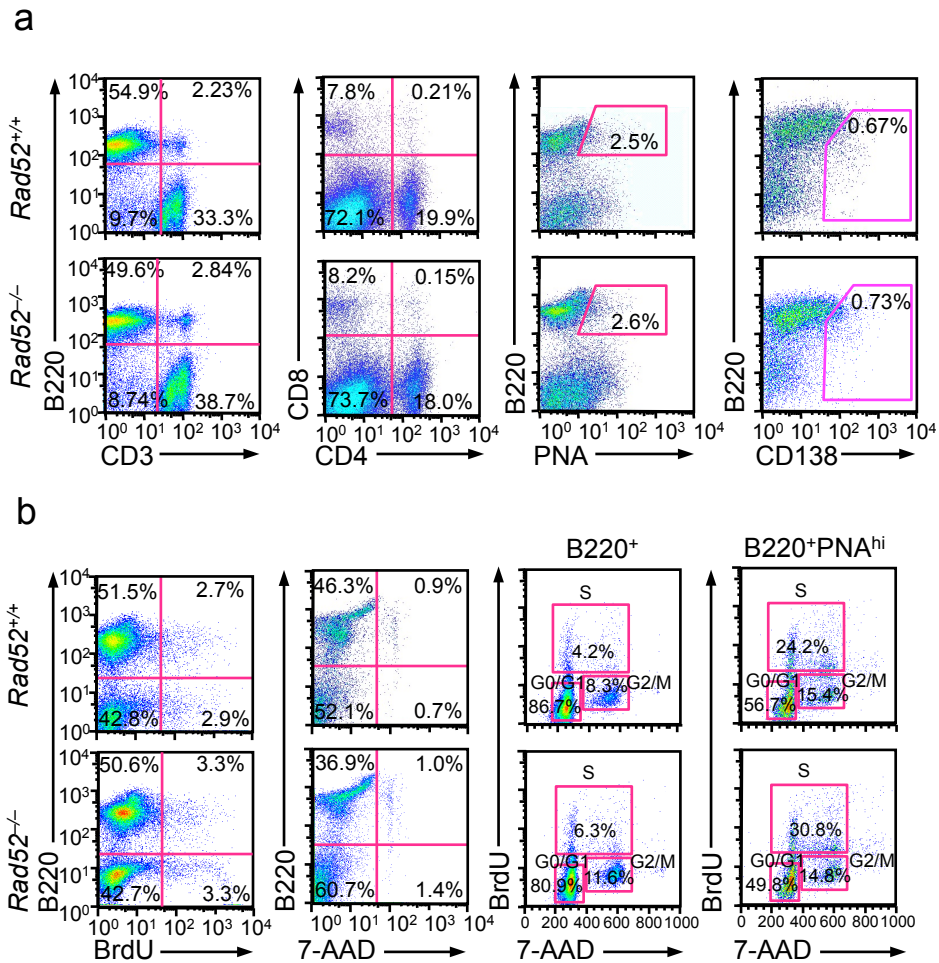


Figure 2.6. The augmented antibody response is not due to alterations in proportions of B and T cells, plasma cell differentiation, and B cell proliferation and survival. (a) Flow cytometry analysis of the spleen cells from *Rad52*^{+/+} and *Rad52*^{-/-} littermates for the proportion of: B220⁺ B cells and CD3⁺ T cells, CD4⁺ and CD8⁺ T cells, B220⁺PNA^{hi} GC B cells, B220^{lo}CD138⁺ plasma cells, proliferating B cells (BrdU-stained B220⁺ B cells), and viable (7-AAD⁻) B220⁺ B cells. **(b)** *In vivo* cell cycle analysis (the quadrant corresponding to the G0/G1, S and G2/M phase of the cell cycle) of B220⁺ B cells and B220⁺PNA^{hi} GC B cells from the spleens of *Rad52*^{+/+} and their *Rad52*^{-/-} littermates. Data are from representative of three independent experiments.

2.4 Rad52 deficiency increases CSR *in vitro*

To further determine the impact of Rad52 deficiency on CSR, we activated *Rad52*^{+/+} and *Rad52*^{-/-} spleen B cells *in vitro* with LPS (to induce switching to IgG3), LPS or CD154 plus IL-4 (IgG1), LPS plus IFN- γ (IgG2a), and LPS plus TGF- β , IL-5, IL-4, and anti- δ monoclonal antibody (mAb)/dex (IgA). After 4 days, there were 2.3, 2.1, 1.6, and 2.0 fold increased switched surface IgG1⁺, IgG2a⁺, IgG3⁺, and IgA⁺ B cells, respectively in *Rad52*^{-/-} mice relative to its expression in *Rad52*^{+/+} B cells (**Figure 2.7**). The increased CSR observed in *Rad52*^{-/-} B cells was not due to altered proliferation, as *Rad52*^{-/-} B cells completed a comparable number of cell divisions as their *Rad52*^{+/+} counterparts did after 3 days of culture upon stimulation with LPS or CD154 plus IL-4. However, the percentage of IgG1 positive B cells in *Rad52*^{-/-} B cells is virtually double that of *Rad52*^{+/+} B cells, which had undergone the same number of divisions (**Figure 2.8a**).

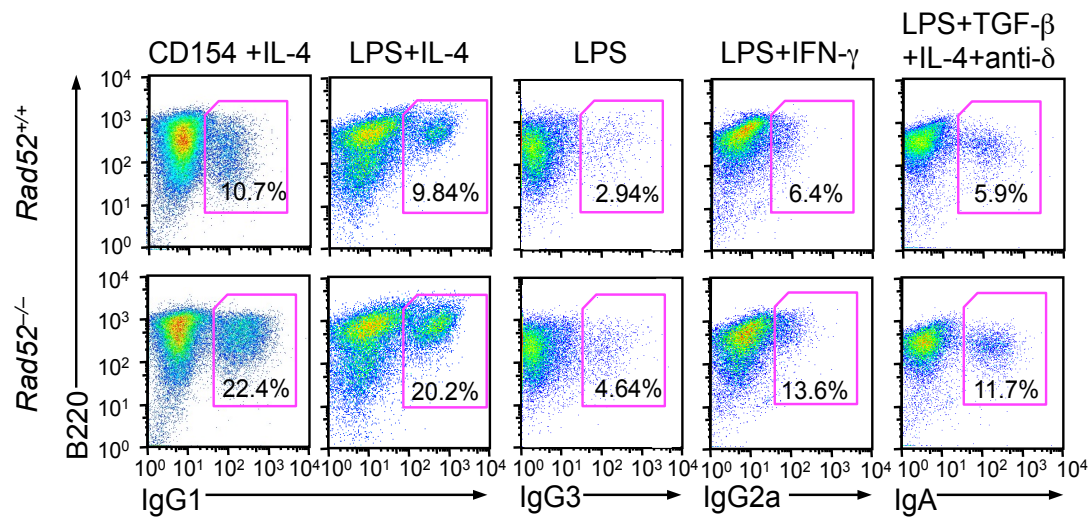


Figure 2.7. Rad52 deficiency increases CSR *in vitro*. *Rad52*^{+/+} and *Rad52*^{-/-} B cells were stimulated with CD154 or LPS plus IL-4 (for CSR to IgG1), LPS alone (for IgG3), LPS plus IFN γ (for IgG2a), and LPS plus TGF- β 1, IL-4, IL-5 and anti- δ mAb/dex (for IgA). After 4 d of culture, the cells were analyzed for surface B220 and IgG1, IgG3, IgG2a or IgA by flow cytometry.

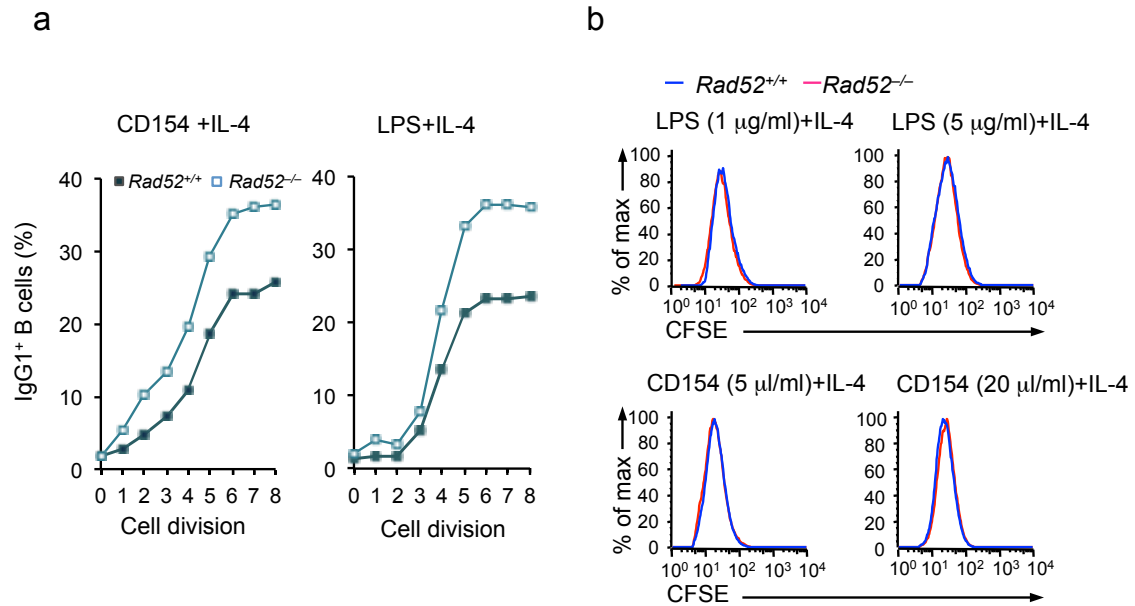


Figure 2.8. Rad52 deficiency increases CSR without affecting B cell division or proliferation. (a) Proliferation of *Rad52*^{+/+} and *Rad52*^{-/-} B cells labeled with the cell division tracking fluorochrome CFSE and stimulated with LPS plus IL-4 or CD154 plus IL-4 for 4 d. CFSE intensity and surface IgG1 expression were analyzed by flow cytometry. The proportion of surface IgG1⁺ B cells at each cell division is indicated. (b) Proliferation of *Rad52*^{+/+} and *Rad52*^{-/-} spleen B cells labeled with CFSE and stimulated for 3 d with LPS or LPS plus IL-4. Progressive left shift of fluorescence intensity indicates B220⁺ B cell division. Data are representative of three independent experiments.

At the molecular level, quantitative real-time PCR (qRT-PCR) analysis demonstrated that the increased CSR in *Rad52*^{-/-} B cells was not due to alterations of germline transcription of the intervening heavy-chain (I_H) region and constant heavy-chain (C_H) region (I_H-C_H), which is necessary for CSR, since the level of *Aicda* expression and abundance of germline I γ 1-C γ 1 and I γ 3-C γ 3 transcripts in *Rad52*^{-/-} B cells stimulated for 60 hr with LPS plus IL-4 or LPS alone were comparable to their *Rad52*^{+/+} B cell counterparts (**Figure 2.9b**). However, the circle I γ 1-C μ and I γ 3-C μ and post-recombination I μ -C γ 1 and I μ -C γ 3 transcripts, which are molecular indicators of ongoing and completed CSR respectively, were significantly increased in *Rad52*^{-/-} B cells as compared to *Rad52*^{+/+} B cells. This was more precisely confirmed by upregulated S μ -S γ 1 or S μ -S γ 3 DNA recombination, as detected by DC-PCR (**Figure 2.9d**). Further, after stimulation with LPS and IL-4, or CD154 and IL-4, *Rad52*^{-/-} B lymphocytes were comparable in their rate of cell division, as measured by vital CFSE incorporation to *Rad52*^{+/+} cells (**Figure 2.8b**). Thus, Rad52 deficiency enhances CSR, without affecting germline I_H-C_H and *Aicda* transcription.

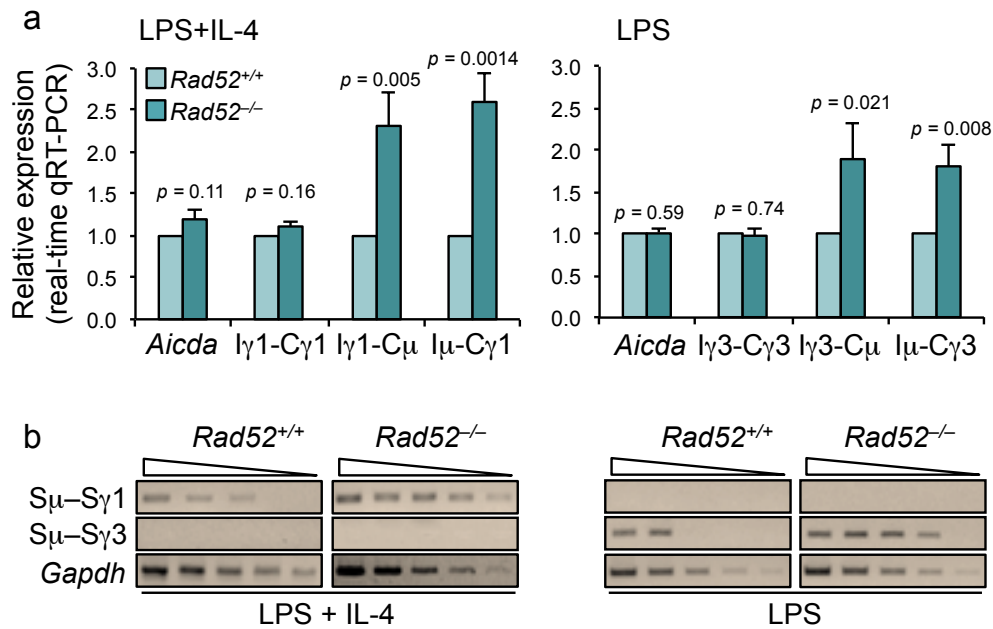


Figure 2.9. Rad52 deficiency increases CSR, as well as circle I_H-C_μ and post-recombination I_μ-C_H transcription but does not alter germline I_H-C_H transcription. (a) *Rad52*^{-/-} B cells display increased circle I_{γ1}-C_μ, I_{γ3}-C_μ and post-recombination I_μ-C_{γ1}, I_μ-C_{γ3} transcripts as well as switch recombination, but did not alter *Aicda* and germline I_{γ1}-C_{γ1}, I_{γ3}-C_{γ3} transcripts. Real-time qRT-PCR analysis of germline I_{γ1}-C_{γ1} and I_{γ3}-C_{γ3} transcripts, circle I_{γ1}-C_μ and I_{γ3}-C_μ transcripts, and post-recombination I_μ-C_{γ1} and I_μ-C_{γ3} transcripts in *Rad52*^{+/+} and *Rad52*^{-/-} B cells cultured for 60 hr with LPS (*Aicda*, I_{γ3}-C_{γ3}, I_{γ3}-C_μ and I_μ-C_{γ3}) or LPS plus IL-4 (*Aicda*, I_{γ1}-C_{γ1}, I_{γ1}-C_μ and I_μ-C_{γ1}). Expression was normalized to *Cd79b* expression and depicted relative to the expression in *Rad52*^{+/+} B cells, set as one. The *p* values were determined using a paired Student's *t* test. Data are from three independent experiments (mean and SEM). (b) Recombinant S_μ-S_{γ1} or S_μ-S_{γ3} DNAs analyzed by DC-PCR using serially 2-fold diluted *HindIII* digested and T4 DNA ligase-ligated genomic DNA from *Rad52*^{+/+} or *Rad52*^{-/-} B cells stimulated with LPS or LPS plus IL-4 for 4 days. The *Gapdh* gene was used as a control for ligation and DNA loading. Data are from one representative of three independent experiments.

2.5 Enforced expression of Rad52 impairs CSR

To further demonstrate the role of Rad52 in CSR, we enforced expression of Rad52 in B cells and analyzed CSR. We transduced LPS-activated spleen B cells with pMIG-Rad52, or an empty pMIG control retroviral vector, and stimulated them with LPS and IL-4 for 96 hr before analyzing CSR. The pMIG control retroviral construct encodes GFP while the pMIG-Rad52 retroviral constructs encode both GFP and Rad52, respectively. In contrast to what we found in *Rad52*^{-/-} B cells, CSR in the GFP⁺ cells was greatly reduced in B cells transduced with the pMIG-Rad52 retroviral construct compared to those transduced with the pMIG control retrovirus, while CSR in GFP⁻ B cells, which do not express the retroviral transduced genes, were virtually unchanged (**Figure 2.10**). Thus, enforced expression of Rad52 resulted in impaired CSR.

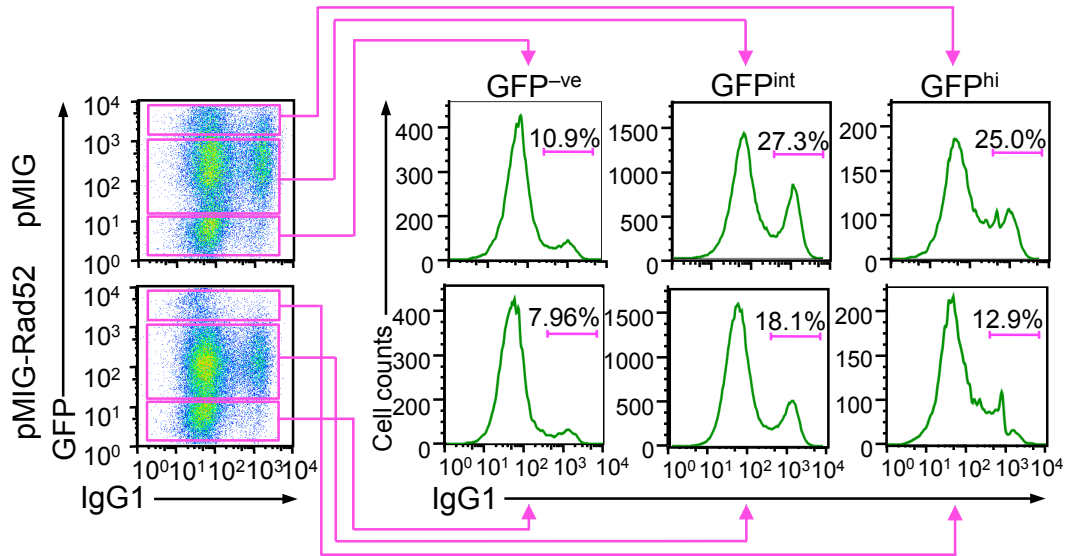


Figure 2.10. Enforced expression of Rad52 in B cells impairs CSR. B cells from C57BL/6 mice were activated with LPS for 12 hr prior to retroviral transduction, and then cultured for 48 hr with LPS plus IL-4 before retroviral transduction. CSR to IgG1 in B cells transduced with empty pMIG retrovirus or pMIG-Rad52 retrovirus expressing recombinant Rad52. CSR is assessed by surface IgG1 expression in transduced (B220⁺GFP^{int} or B220⁺GFP^{hi}) or non-transduced (B220⁺GFP^{-ve}) B cells. Histograms show the distribution of surface IgG1⁺ B cells among B220⁺GFP^{-ve}, B220⁺GFP^{int}, or B220⁺GFP^{hi} B cells. Data are from one representative experiment of five independent experiments.

2.6 Methods

Mice

Rad52^{-/-} mice were generated by Dr. Albert Pastink (Leiden University, Leiden, The Netherlands) by replacing exon 3 of the *Rad52* gene with a positive selection marker, neomycin, which is driven by the phosphoglycerate kinase (PGK) promoter and an upstream mouse sequence (UMS) which functions as a transcription terminator. No full length or truncated Rad52 protein was produced from the disrupted allele. These mice were viable and fertile, and show no gross abnormalities (10). *P53*^{-/-} (B6.129S2-*Trp53*^{tm1Tyj/J}) mice were purchased from the Jackson Laboratory (Bar Harbor, Maine). *P53*^{-/-}*Rad52*^{+/+} and *P53*^{-/-}*Rad52*^{-/-} mice were generated by us by crossbreeding *p53*^{-/-} with *Rad52*^{+/+} mice. *Aicda*^{-/-} mice (C57BL/6 background) (11) were obtained from Dr. T. Honjo (Kyoto University, Kyoto, Japan). All mice were housed under pathogen-free conditions, and were provided with autoclaved food and deionized water. The Institutional Animal Care and Use Committees of the University of Texas Health Science Center, San Antonio and the University of California, Irvine approved all animal protocols.

NP₁₆-CGG immunization and titration of total and NP-binding IgM and IgG1

Rad52^{+/+} and *Rad52*^{-/-} (8-12 weeks of age) were injected intraperitoneally (i.p.) with 100 µg of NP₁₆-CGG (average 16 molecules of 4-hydroxy-3-nitrophenyl acetyl coupled to 1 molecule of chicken γ-globulin; Biosearch Technologies) in 100 µl of alum (Imject[®] Alum, Pierce). Serum was collected 10 days later for titration of circulating total and NP-binding IgM and IgG1 using enzyme-linked immunosorbent assays (ELISAs), as we described (12-14).

B and T cells, cell cycle, and proliferation

B cells (B220⁺), CD4⁺ and CD8⁺ T cells, dead B cells, germinal center (GC) (PNA^{hi}B220⁺) B cells, plasma cells (B220^{lo}CD138⁺) were identified and analyzed by flow cytometry using a FACSCaliburTM or LSR-II flow cytometer (BD Biosciences) and data analysis was performed using FlowJo software (Tree Star). Single cell suspensions were prepared from spleens of *Rad52*^{+/+} and *Rad52*^{-/-} mice and stained with phycoerythrin (PE)-anti-B220 (CD45R; RA3-6B2; eBioscience), fluorescein isothiocyanate (FITC)-anti-CD3 (17A2; BioLegend), FITC-anti-CD4 (GK1.5; BioLegend) and/or allophycocyanin (APC)-anti-CD8 (53-6.7; BD Biosciences), Alexa Fluor® 647-peanut agglutinin (PNA; Invitrogen), biotin-anti-CD138 (281-2; BD Biosciences) followed by FITC-streptavidin (11-4317-87; eBioscience) or PE-streptavidin (12-4317-87; eBioscience), PE-anti-IgM (AF6-78; BD Biosciences), FITC-anti-IgG1 (A85-1; BD Biosciences), FITC-anti-IgG3 (R40-82; BD Biosciences), FITC-anti-IgA (C10-3; BD Biosciences), biotin-rat-anti-mouse IgG2a (R19-15; BD Pharmingen) followed by APC-streptavidin (550874; eBioscience), 7-aminoactinomycin D (7-AAD; BD Biosciences), as previously described (12, 14-16).

For analysis of B cell proliferation and total or GC B cell cycle *in vivo*, mice were immunized with NP₁₆-CGG. Ten days after NP₁₆-CGG immunization, the mice were injected i.p. with bromodeoxyuridine (BrdU) twice, at 1 mg (in 200 µl PBS) each time, within a 16 hr interval and sacrificed 4 hr after the last injection. Spleen cells stained with PE-anti-B220 mAb, and incorporated (intracellular) BrdU stained with APC-anti-BrdU mAb using the APC BrdU Flow Kit (BD Biosciences) were analyzed for BrdU incorporation by flow cytometry. To analyze cell cycle of B220⁺ B cells or PNA^{hi}B220⁺

GC B cells, spleen cells were stained for surface B220 and PNA with PE-anti-B220 mAb (clone RA3-6B2, Invitrogen) and Alexa Fluor® 647-labeled PNA (Invitrogen), APC-anti-BrdU mAb before being fixed/permeabilized and stained with APC-anti-BrdU mAb and 7-AAD using the APC BrdU Flow Kit according to manufacturer's instructions. DNA contents as indicated by 7-AAD staining and BrdU incorporation in B220⁺ B cells or PNA^{hi}B220⁺ GC B cells were analyzed by flow cytometry. B cell division was analyzed by CFSE dilution using the CellTrace™ CFSE Cell Proliferation Kit (Invitrogen). Briefly, B cells were incubated for 5 min at 37°C in 3 ml PBS with 2.5 μM CFSE at a density of 1 x 10⁷ cells/ml and then washed in FBS-RPMI. Cells were then cultured in the presence LPS plus IL-4 or CD154 plus IL-4 for 3 d, before being stained with PE-anti-B220 mAb, 7-AAD and APC-anti-IgG1 mAb (X56; BD Biosciences), and then analyzed by flow cytometry.

CSR analysis in vitro and in vivo

B cells isolated from red blood cell (RBC)-depleted splenocytes of mice were purified by negative selection of cells expressing CD43, CD4, CD8, CD11b, CD49b, CD90.2, Gr-1 or Ter-119 using the EasySep™ Mouse B cell Isolation kit (Stemcell Technologies). B cells were resuspended in RPMI 1640 medium with 10% FBS, 50 mM β-mercaptoethanol and 1x antibiotic-antimycotic mixture (15240-062; Invitrogen) (FBS-RPMI) at 37°C in 48-well plates and stimulated with the following reagents: lipopolysaccharide (LPS) (1 or 5 μg/ml) from *Escherichia coli* (055:B5; Sigma-Aldrich) for CSR to IgG3; LPS (3 μg/ml) or CD154 (1 U/ml; obtained from membrane fragments of baculovirus-infected Sf21 insect cells (17) plus IL-4 (5 ng/ml; R&D Systems) for CSR to IgG1; LPS (3 μg/ml) plus TGF-β (2 ng/ml; R&D Systems), IL-4 (5 ng/ml), IL-5 (3

ng/ml; R&D Systems) and anti-IgD dextran (Fina Biosolutions) for CSR to IgA; LPS (3 μ g/ml) plus IFN- γ (50 ng/ml) for CSR to IgG2a. After 4 days, cells were analyzed for surface Ig after being stained with FITC-labeled rat mAb to mouse IgG1 (clone A85-1), mouse IgG2a (clone R19-15), mouse IgG3 (clone R40-82) mouse IgA (clone C10-3), or PE-labeled rat mAb to mouse B220 (clone RA3-6B2; all from BD Biosciences). Stained cells were analyzed by flow cytometry.

The numbers of (class-switched) GC (PNA^{hi} B220⁺) B cells expressing IgG1 or IgA were determined by flow cytometry. Single cell suspensions were prepared from spleen of *Rad52*^{+/+} and *Rad52*^{-/-} mice 14 days after immunization with NP₁₆-CGG, or Peyer's patches of unimmunized *Rad52*^{+/+} and *Rad52*^{-/-} mice and stained with PE-labeled anti-mouse B220 mAb or Alexa Fluor® 647-labeled PNA, as well as FITC-labeled anti-mouse IgG1 (clone A85-1) or FITC-labeled anti-mouse IgA (clone C10-3) mAbs (BD Biosciences). Stained cells were analyzed using a LSR-II flow cytometer (BD Biosciences).

Quantitative RT-PCR (qRT-PCR) analysis of transcripts

Total RNA was extracted from 2-5 x 10⁶ cells pelleted B cells using the RNeasy Mini Kit (Qiagen). Residual DNA was removed from the extracted RNA with gDNA eliminator columns (Qiagen). cDNA was synthesized from 1-2 μ g total RNA with the SuperScript™ III First-Strand Synthesis System (Invitrogen) using oligo-dT primer. The expression of germline I γ 1-C γ 1 and I γ 3-C γ 3, circle I γ 1-C μ and I γ 3-C μ , post-recombination I μ -C γ 1 and I μ -C γ 3, *Cd79b* and *Gapdh* transcripts was measured by real-time qPCR with appropriate primers as described previously (12, 14, 16, 18). A Bio-Rad MyiQ™ Real-Time PCR Detection System (Bio-Rad Laboratories) was used to measure

SYBR Green (IQ™ SYBR® Green Supermix, Bio-Rad Laboratories) incorporation with the following protocol: 95°C for 15 sec, 40 cycles of 94°C for 10 sec, 60°C for 30 sec, 72°C for 30 sec. Data acquisition was performed during 72°C extension step. Melting curve analysis was performed from 72°C-95°C. The change in cycling threshold ($\Delta\Delta Ct$) method was used to analyze levels of transcripts and data were normalized to the level of Cd79b, which encodes the BCR Ig β chain constitutively expressed in B cells, or *Gapdh*.

Digestion-circularization PCR (DC-PCR) analysis

B cells were stimulated with LPS or LPS plus IL-4 for 4 days for isolation of genomic DNA. The genomic DNA was digested with HindIII before being ligated with T4 DNA ligase to generate circularized DNA (14). S μ -S γ 1 and S μ -S γ 3 HindIII fragments were amplified by nested PCR using Phusion® High-Fidelity DNA polymerase (New England BioLabs) with reported primers (19). The completeness of HindIII digestions and ligations was verified by PCR with a primer set specific to the *Gapdh* gene. First round PCR was carried out for 25 cycles at 94°C for 30 sec; 58°C for 30 sec; 72°C for 35 sec. 1 μ l of the first round PCR product was used as template for the second round of PCR for 32 cycles at 94°C for 30 s; 60°C for 30 sec; 72°C for 30 sec.

Rad52 retroviral construct and enforced expression

Rad52 cDNA was amplified from mouse spleen B cells using the appropriate primers (Supplemental Table 1), and cloned into the pMIG retroviral expression vector (GFP translation is initiated by the IRES in the pMIG vector; GFP⁺ B cells indicate transduced B cells). To generate the retrovirus, the empty pMIG vector, pMIG-Rad52 constructs were transfected along with the pCL-Eco retrovirus-packaging vector (Imgenex) into

HEK293T cells using a calcium phosphate-mediated transfection procedure from the ProFection® Mammalian Transfection System (Promega). The retroviral constructs were used to transduce spleen B cells from C57BL/6 mice as we reported (12, 14). Briefly, B cells were activated with LPS for 12 hr and transduced with retrovirus. Transduced B cells were then stimulated with LPS plus IL-4 for 96 hr before analyzing GFP⁺ and IgG1⁺ B cells by flow cytometry, as described previously (12, 14). Dead (7-AAD⁺) cells were excluded from analysis.

Table 2.1: Oligonucleotide sequences for qRT-PCR, ChIP Assays, and analysis of S-S junctions, *c-Myc/IgH* translocations.

Supplemental Table S1. Oligonucleotide sequences.		
Primers for qRT-PCR		
	Forward primer	Reverse primer
<i>Aicda</i>	5'- AGAAAGTCACGCTGGAGACC -3'	5'- CTCTCTTCACCACGTAGCA -3'
<i>Iγ1-Cγ1</i>	5'- TCGAGAAGCCTGAGGAATGTG -3'	5'- ATGGAGTTAGTTTGGGCAGCA -3'
<i>Iγ1-Cμ</i>	5'- GGCCCTTCCAGATCTTTGAG -3'	5'- GAAGACATTTGGGAAGGACTGAC -3'
<i>Iμ-Cγ1</i>	5'- ACCTGGGAATGTATGGTTGTGGCTT -3'	5'- ATGGAGTTAGTTTGGGCAGCA -3'
<i>Iγ3-Cγ3</i>	5'- AACTACTGCTACCACCACCACCAG -3'	5'- ACCAAGGGATAGACAGATGGGG -3'
<i>Iγ3-Cμ</i>	5'- TCGAGAAGCCTGAGGAATGTG -3'	5'- GGTACTTGCCCCCTGTCCTCAG -3'
<i>Iμ-Cγ3</i>	5'- ACCTGGGAATGTATGGTTGTGGCTT -3'	5'- AGCCAGGACCAAGGGATAGAC-3'
<i>CD79b</i>	5'- CCACACTGGTGTCTTCC-3'	5'- GGGCTTCCTTGAAATTCAG-3'
<i>Gapdh</i>	5'- ATCACTGCCACCCAGAAGACTG-3'	5'- CCCTGTTGCTGTAGCCGTATTC -3'
Primers for ChIP assays		
Sμ	5'- GCTAAACTGAGGTGATTACTCTGAGGTAAG -3'	5'- GTTTAGCTTAGCGGCCAGCTCATTCCAGT-3'
Sγ1	5'- ATAAGTAGTAGTTGGGGATTC -3'	5'- CTCAGCCTGGTACCTTATACA -3'
Sγ3	5'- AATCTACAGAGAGCCAGGTGG -3'	5'- TGGTTTTCCATGTTCCCACTT -3'
Cμ	5'- CAGCACCATTTCTTCACCTGGAACCTACCA -3'	5'- GGCTAGGTAAGTTGCCCCCTGTCCTCAGTGT -3'
Primers for S-S junction		
Sμ-Sγ1	Sμ	Sγ1
1 st round	5'- AACTCTCCAGCCACAGTAATGACC -3'	5'- CTGTAACCTACCCAGGAGACC-3'
2 nd round	5'- ACGCTCGAGAAGGCCAGCCTCATAAAGCT-3'	5'- GTCGAATTCCTCCATCCTGTACCTATA -3'
Sμ-Sα	Sμ	Sα
1 st round	5'- ATAAGTAGTAGTTGGGGATTC -3'	5'- TCCAGCAAAGCTCAGGCTAGAAC -3'
2 nd round	5'- CAGCACCATTTCTTCACCTGGAACCTACCA -3'	5'- AGTCCAGTCATGCTAATTCACC -3'
Primers for <i>c-Myc/IgH</i> translocations		
	<i>IgH</i>	<i>c-Myc</i>
1 st round	5'- TGAGGACCAGAGAGGGATAAAAAGAGAA -3'	5'- GTTTAGCTTAGCGGCCAGCTCATTCCAGT-3'
2 nd round	5'- CACCCTGCTATTTCTTGTGCTAC -3'	5'- GACACCTCCCTTCTACACTCTAAACCG -3'

2.7 Discussion

In the first part of this study, we have addressed an important role of Rad52 in the antibody response. In *Rad52*^{-/-} mice injected with the T-dependent NP-CGG, specific class switching to IgG1 was observed. This was consistent with an increase in class switching to IgG1 and IgA in the germinal center B cells (PNA^{hi}) of the spleens and Peyer's patches of *Rad52*^{-/-} mice compared to their *Rad52*^{+/+} littermates. This augmented antibody response was not due to alterations in the proportions of B and T cells, germinal center B cells, plasma cell differentiation, or B cell proliferation, viability, and cell cycle. *Rad52*^{-/-} B cells displayed normal cell cycle and proliferation, indicating that the increase in CSR reflected an inherent effect on the CSR machinery. In purified *Rad52*^{+/+} and *Rad52*^{-/-} B cells stimulated with the appropriate cytokines, class switching to IgG1, IgG3, IgG2a and IgA virtually doubled. Consistently, at the molecular level, CSR is enhanced in *Rad52*^{-/-} B cells as indicated by the increased circle I_H-C_μ and post-recombination I_μ-C_H transcripts, which are molecular indicators of ongoing CSR and completed CSR respectively. The normal levels of *Aicda* and germline I_H-C_H transcripts in *Rad52*^{-/-} B cells suggest that Rad52 deficiency enhances CSR without affecting germline I_H-C_H transcription. This was further confirmed by an increase in S_μ-S_γ1 (IgM to IgG1) and S_μ-S_γ3 switch DNA recombination (IgM to IgG3). Conversely, enforced expression of Rad52 by retroviral transduction impaired CSR, contrary to the increase in CSR observed in *Rad52*^{-/-} B cells.

Collectively, the phenotypic data assessed by cellular and molecular parameters suggest that B cell Rad52 deficiency increases CSR *in vivo* and *in vitro*. This is an intriguing and unexpected phenomenon, which lends to the second part of this thesis. Although CSR increases in *Rad52*^{-/-} B cells, the mechanism by which it mediates S region DSB repair remains to be defined.

Based on previous findings by others in Ku- and Lig IV- deficient B cells (19-22), there was an observed increase in microhomologies in S-S junctions generated from residual CSR activity in Ku70- and Lig IV-deficient B cells suggesting that the Ku- and Lig IV-independent mechanism recombining the DSB ends exists in CSR. Although this microhomology-mediated end joining process accounts for a minor amount of DNA repair during CSR, it could provide an explanation for the residual CSR activity that occurs in the absence of Ku70 and Ligase IV (22). Microhomologies are short 5-25 complementary base pairs, which align to the broken ends of the DNA to align the strands with mismatched ends in the switch junction. Unfortunately, microhomology mediated end joining is an error-prone method of repair which may result in deletion mutations in the genetic code, thereby initiating translocations between oncogenes, leading to the development of cancer. This is substantiated by the fact that alternative end joining catalyzes robust *IgH* locus deletions and interchromosomal *c-myc/IgH* translocations in the combined absence of Ku70 and Ligase IV (21). Therefore, we postulated that the single strand binding protein, Rad52 plays a critical role in the DSB repair process involving single-strand annealing and may be linked to the increased microhomologies and chromosomal translocations in Ku-deficient B cells.

Furthermore, both Ku and Rad52 bind to DNA ends and facilitate end-to-end interactions (19). Rad52 and Ku have been suggested to bind to different DNA structures produced early in DSB repair, as Rad52 binds more effectively to long ssDNA. It has been suggested that the binding of Ku or Rad52 to the DNA ends would lead to different DSB repair processes. However, like Ku70/Ku86, Rad52 can also bind to blunt or short protruding DNA ends (19). This lead us to hypothesize that the increase in CSR observed in *Rad52*^{-/-} B cells may be due to the presence of Ku70/Ku86, which facilitates non-homologous end joining and leads to productive CSR. Moreover, it suggests that the absence of Rad52 may result in increased recruitment of Ku70/Ku86 to the S region, which provides an explanation for the twofold greater class switched antibody response. Accordingly, this suggests that Rad52 may compete with Ku70/Ku86 in binding to S region DSB ends to modulate immunoglobulin class switch DNA recombination.

In the next chapter, we explore the mechanism(s) by which Rad52 mediates S region DSB repair, including the potential competition between Rad52 and Ku70/Ku86 for binding to switch region DSB ends in CSR.

2.8 References

1. Mortensen, U. H., C. Bendixen, I. Sunjevaric, and R. Rothstein. 1996. DNA strand annealing is promoted by the yeast Rad52 protein. *Proceedings of the National Academy of Sciences of the United States of America* 93: 10729-10734.
2. Parsons, C. A., P. Baumann, E. Van Dyck, and S. C. West. 2000. Precise binding of single-stranded DNA termini by human RAD52 protein. *The EMBO journal* 19: 4175-4181.
3. Li, M. J., M. C. Peakman, E. I. Golub, G. Reddy, D. C. Ward, C. M. Radding, and N. Maizels. 1996. Rad51 expression and localization in B cells carrying out class switch recombination. *Proceedings of the National Academy of Sciences of the United States of America* 93: 10222-10227.
4. Peakman, M. C., and N. Maizels. 1998. Localization of splenic B cells activated for switch recombination by in situ hybridization with Igamma1 switch transcript and Rad51 probes. *J Immunol* 161: 4008-4015.
5. Sugiyama, T., and N. Kantake. 2009. Dynamic regulatory interactions of rad51, rad52, and replication protein-a in recombination intermediates. *J. Mol. Biol.* 390: 45-55.
6. Vuong, B. Q., M. Lee, S. Kabir, C. Irimia, S. Macchiarulo, G. S. McKnight, and J. Chaudhuri. 2009. Specific recruitment of protein kinase A to the immunoglobulin locus regulates class-switch recombination. *Nat Immunol* 10: 420-426.
7. Yamane, A., D. F. Robbiani, W. Resch, A. Bothmer, H. Nakahashi, T. Oliveira, P. C. Rommel, E. J. Brown, A. Nussenzweig, M. C. Nussenzweig, and R. Casellas. 2013. RPA accumulation during class switch recombination represents 5'-3' DNA-end resection during the S-G2/M phase of the cell cycle. *Cell Rep.* 3: 138-147.
8. Singleton, M. R., L. M. Wentzell, Y. Liu, S. C. West, and D. B. Wigley. 2002. Structure of the single-strand annealing domain of human RAD52 protein. *Proc Natl Acad Sci U S A* 99: 13492-13497.
9. Zan, H., X. Wu, A. Komori, W. K. Holloman, and P. Casali. 2003. AID-dependent generation of resected double-strand DNA breaks and recruitment of Rad52/Rad51 in somatic hypermutation. *Immunity* 18: 727-738.
10. Rijkers, T., J. Van Den Ouweland, B. Morolli, A. G. Rolink, W. M. Baarends, P. P. Van Sloun, P. H. Lohman, and A. Pastink. 1998. Targeted inactivation of mouse RAD52 reduces homologous recombination but not resistance to ionizing radiation. *Mol. Cell Biol.* 18: 6423-6429.
11. Muramatsu, M., K. Kinoshita, S. Fagarasan, S. Yamada, Y. Shinkai, and T. Honjo. 2000. Class switch recombination and hypermutation require activation-induced cytidine deaminase (AID), a potential RNA editing enzyme. *Cell* 102: 553-563.
12. Park, S.-R., H. Zan, J. Zhang, A. Al-Qahtani, E. J. Pone, Z. Xu, T. Mai, and P. Casali. 2009. HoxC4 binds to the promoter of the cytidine deaminase AID gene to induce AID expression, class-switch DNA recombination and somatic hypermutation. *Nat Immunol* 10: 540-550.
13. White, C. A., J. Seth Hawkins, E. J. Pone, E. S. Yu, A. Al-Qahtani, T. Mai, H. Zan, and P. Casali. 2011. AID dysregulation in lupus-prone MRL/Fas(lpr/lpr)

- mice increases class switch DNA recombination and promotes interchromosomal c-Myc/IgH loci translocations: modulation by HoxC4. *Autoimmunity* 44: 585-598.
14. Zan, H., C. A. White, L. M. Thomas, T. Mai, G. Li, Z. Xu, J. Zhang, and P. Casali. 2012. Rev1 recruits Ung to switch regions and enhances dU glycosylation for immunoglobulin class switch DNA recombination. *Cell Rep.* 2: 1220-1232.
 15. Zan, H., and P. Casali. 2008. AID- and Ung-dependent generation of staggered double-strand DNA breaks in immunoglobulin class switch DNA recombination: a post-cleavage role for AID. *Mol. Immunol.* 46: 45-61.
 16. Mai, T., H. Zan, J. Zhang, J. S. Hawkins, Z. Xu, and P. Casali. 2010. Estrogen receptors bind to and activate the promoter of the HoxC4 gene to potentiate HoxC4-mediated AID induction, immunoglobulin class-switch DNA recombination and somatic hypermutation. *J. Biol. Chem.* 285: 37797-37810.
 17. Van Dyck, E., A. Z. Stasiak, A. Stasiak, and S. C. West. 1999. Binding of double-strand breaks in DNA by human Rad52 protein. *Nature* 398: 728-731.
 18. Wang, L., R. Wuerffel, S. Feldman, A. A. Khamlichi, and A. L. Kenter. 2009. S region sequence, RNA polymerase II, and histone modifications create chromatin accessibility during class switch recombination. *J. Exp. Med.* 206: 1817-1830.
 19. Ristic, D., M. Modesti, R. Kanaar, and C. Wyman. 2003. Rad52 and Ku bind to different DNA structures produced early in double-strand break repair. *Nucleic Acids Res.* 31: 5229-5237.
 20. Yan, C. T., C. Boboila, E. K. Souza, S. Franco, T. R. Hickernell, M. Murphy, S. Gumaste, M. Geyer, A. A. Zarrin, J. P. Manis, K. Rajewsky, and F. W. Alt. 2007. IgH class switching and translocations use a robust non-classical end-joining pathway. *Nature* 449: 478-482.
 21. Boboila, C., M. Jankovic, C. T. Yan, J. H. Wang, D. R. Wesemann, T. Zhang, A. Fazeli, L. Feldman, A. Nussenzweig, M. Nussenzweig, and F. W. Alt. 2010. Alternative end-joining catalyzes robust IgH locus deletions and translocations in the combined absence of ligase 4 and Ku70. *Proc. Natl. Acad. Sci. USA.* 107: 3034-3039.
 22. Boboila, C., C. Yan, D. R. Wesemann, M. Jankovic, J. H. Wang, J. Manis, A. Nussenzweig, M. Nussenzweig, and F. W. Alt. 2010. Alternative end-joining catalyzes class switch recombination in the absence of both Ku70 and DNA ligase 4. *J. Exp. Med.* 207: 417-427.

CHAPTER 3

Rad52 competes with Ku70/Ku86 to modulate immunoglobulin class switch DNA recombination

Contents:

3.1 Introduction	63
3.2 Rad52 deficiency is associated with a reduction in the frequency and length of microhomologies at the S-S junctions	66
3.3 Rad52 deficient B cells activated for CSR results in reduced <i>c-Myc/IgH</i> translocations	71
3.4 Rad52 deficiency increases recruitment of Ku70/Ku86 to S region DSB	74
3.5 Rad52 competes with Ku70/Ku86 in binding to S region dsDNA ends	76
3.6 Rad52 mediated repair favors intra-S region rejoining	80
3.7 Methods	82
3.8 The potential role of Pol θ in CSR	87
3.9 Discussion	93
3.10 References	100

3.1 Introduction

The nature of the switch junctions following CSR reflects the end-joining processes that ligate DSBs. CSR can be affected by the type of nonhomologous end-joining using either the classical or alternate pathways, which is determined by the microhomology length of the joined products. Classical end-joining is characterized by blunt or short overlapping sequences, whereas Ku-independent end-joining uses longer overlaps (32). It has been shown that B cells deficient in Ku or other key NHEJ factors, such as XRCC4 and Lig IV, displayed greatly increased microhomologies at the S-S junctions (1-3).

To determine if there is an association of Rad52 with the increase in microhomologies in the S-S junctions of Ku-deficient and Ligase IV-deficient B cells, we analyzed the frequency and length of microhomologies in the S-S junctions of *Rad52*^{+/+} and *Rad52*^{-/-} B cells during CSR.

Furthermore, as previously mentioned, microhomology mediated end joining is error-prone and may result in genomic instability, which may lead to translocations between oncogenes. DSB repair is essential to maintaining genome integrity, and deficiencies in NHEJ can lead to an increase in the frequency of chromosomal translocations and neoplastic transformation (4). Differences in microhomologies in *Rad52*^{+/+} and *Rad52*^{-/-} B cells would suggest that repair of DSB ends by microhomology can lead to interchromosomal translocations. Specifically, the increased CSR in *Rad52*^{-/-} B cells upon AID-induced DSB may suggest an improved NHEJ activity which may impair *c-Myc/IgH* translocations.

To determine the role of Rad52 in modulating interchromosomal translocations, we examined the frequency of *c-myc/IgH* translocations in *Rad52*^{+/+} and *Rad52*^{-/-} B cells on a

p53 deficient background, as the tumor suppressor *p53* is essential for protecting B cells from *c-Myc/IgH* translocations but has no detectable effect on CSR. Since *p53* inhibits inter-chromosomal translocation, *p53* deficiency will significantly amplify AID-dependent *c-Myc/IgH* translocations (5). *Rad52*^{+/+}*p53*^{-/-} and *Rad52*^{-/-}*p53*^{-/-} B cells were stimulated with LPS plus IL-4 and the frequency of *c-myc/IgH* translocations were examined by long-range PCR, and confirmed by Southern blotting and sequence analysis.

Substantial differences in the frequency and length of microhomologies in the S-S junctions of *Rad52*^{+/+} and *Rad52*^{-/-} B cells would indicate a difference in end joining processes utilized for repair in CSR. The different end joining processes function downstream of the core components used in DSB recognition. It is known that Rad52 and Ku70/Ku86 bind to and interact with different DNA substrates produced early in DNA double-strand break repair (25). Since it is postulated that either Rad52 or Ku70/Ku86 are recruited to the S region DNA after DSBs, we hypothesized that they may compete and therefore examined the competition between Rad52 and Ku70/Ku86 for binding to S region DSB ends by performing chromatin immunoprecipitation (ChIP) assays and electrophoretic mobility shift assays (EMSAs) using purified human recombinant Ku70/Ku86 or Rad52 protein incubated with an S μ DNA probe.

Although we contend that Rad52 competes with Ku70/Ku86 in binding to S region DNA ends in CSR, there must also be a deeper explanation for the increase in CSR in *Rad52*^{-/-} B cells. Multiple DSBs are introduced into S μ during CSR, with some being rejoined or joined to each other during intra-S-region recombination, this is recombination within the upstream and downstream S regions, which lead to internal switch region deletions (ISD). It has been shown that B cell activation for CSR generates

substantial ISD in the S μ region and that ISD were greatly increased in the absence of C-NHEJ (3). Furthermore, *IgH* chromosomal translocations to the *c-myc* oncogene were also augmented in the combined absence of Ku70 and Ligase IV. To determine if Rad52 mediates DSB repair by intra-S region rejoining, we analyzed the frequency of intra-S region recombination using specific S μ primers which flank upstream and downstream of the S region core by PCR amplification followed by colony PCR screening of individual clones generated from the amplification of genomic DNA of stimulated *Rad52*^{+/+} and *Rad52*^{-/-} B cells. This experiment would finally provide a potential mechanism to corroborate the increase in CSR observed in *Rad52*^{-/-} B cells, as intra-S region rejoining does not lead to productive CSR.

3.2 Rad52 deficiency is associated with a reduction in the frequency and length of microhomologies at the S-S junctions

To determine if Rad52 may be linked to increased microhomologies in the S-S junctions of Ku-deficient and Ligase IV-deficient B cells, we amplified, sequenced and analyzed the frequency and length of microhomologies in the S μ -S α (IgM to IgA) junctions *in vivo* from DNA of GC B cells from the Peyer's patches and S μ -S γ 1 junctions (IgM to IgG1) from the DNA of *Rad52*^{+/+} and *Rad52*^{-/-} B cells stimulated with LPS plus IL-4 for 4 days. Consistent with our previous studies (6,7), the majority of S μ -S α and S μ -S γ 1 junctions in the *Rad52*^{+/+} cells carried microhomology. Almost 71% of S μ -S α junctions in the *Rad52*^{+/+} and over 80% of the S μ -S γ 1 junctions B cells had microhomology between one to nine nucleotides (**Figures 3.1 and 3.2**), among them, more than 43% of S μ -S α junctions and 47 % of S μ -S γ 1 junctions showed microhomology of four nucleotides or more.



Figure 3.1. Rad52 deficiency is associated with reduced microhomology at the Sμ-Sα junctions in CSR *in vivo*. Junctional Sμ-Sα DNAs from the Peyer's patches of 3 *Rad52*^{+/+} and 3 *Rad52*^{-/-} mice were amplified, cloned, and sequenced. Eighteen sequences from *Rad52*^{+/+} mice and eighteen sequences *Rad52*^{-/-} mice are shown. The germline Sμ or Sα sequences are aligned above and below the recombination switch junctional sequences. Microhomologies (bold and underlined) were determined by identifying the longest region at the switch junction of perfect uninterrupted donor/acceptor identity, or the longest overlap region at the switch junction with no more than one mismatch on either side of the breakpoint. Zero (0) indicates no microhomology and no insertions are observed at the junction.



Figure 3.2. Rad52 deficiency is associated with reduced microhomology at the $\Sigma\mu$ -Syl1 junctions in CSR *in vitro*. $\Sigma\mu$ -Syl1 junctions from *Rad52*^{+/+} and *Rad52*^{-/-} B cells *in vitro* stimulated with LPS plus IL-4 for 4 d were analyzed. Junctional $\Sigma\mu$ -Syl1 DNAs from stimulated cells were amplified, cloned, and sequenced. Twenty-five sequences from *Rad52*^{+/+} B cells and twenty-five sequences *Rad52*^{-/-} B cells are shown. The germline $\Sigma\mu$ or Syl1 sequences are aligned above and below the recombination switch junctional sequences. Microhomologies (bold and underlined) were determined by identifying the longest region at the switch junction of a perfect uninterrupted donor/acceptor identity, or the longest overlap region at the switch junction with no more than one mismatch on either side of the breakpoint. Zero (0) indicates no microhomology and no insertions are observed at the junction.

The frequency and length of microhomologies in the S μ -S α and S μ -S γ 1 junctions were significantly reduced in *Rad52*^{-/-} B cells (**Figure 3.3**). None of the S μ -S α junctions in the *Rad52*^{-/-} B cells and only 3.47% of the S μ -S γ 1 junctions had microhomology lengths of four nucleotides or more. Remarkably, there was a significant increase in the frequency of junctions with direct (blunt) joins that is without microhomology. The number of junctions with blunt joins in the S μ -S α and S μ -S γ 1 junctions increased from 14.3% and 13.2% in *Rad52*^{+/+} B cells to approximately 42.1% and 42.9% in *Rad52*^{-/-} B cells, respectively. Overall, the average microhomology length decreased from 3.07 nucleotides (S μ -S α) or 3.58 nucleotides (S μ -S γ 1) in *Rad52*^{+/+} B cells to 0.789 nucleotides (S μ -S α) or 0.357 nucleotides (S μ -S γ 1) in *Rad52*^{-/-} B cells (**Figure 3.3**). Thus, in the absence of Rad52, DNA ends generated during CSR are primarily processed through an end-joining mechanism not relying on microhomology. The difference in frequency and length of microhomologies at the S-S junctions between *Rad52*^{+/+} and *Rad52*^{-/-} B cells, suggest that the increase in CSR in *Rad52*^{-/-} B cells may be due to differences in end-joining.

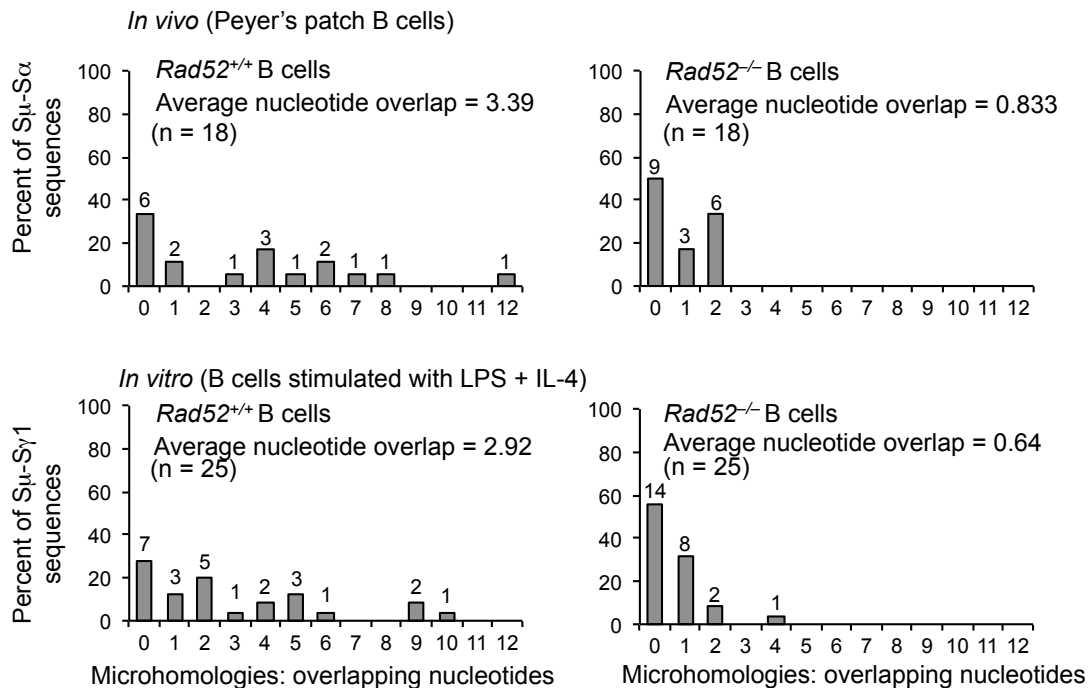


Figure 3.3. Total microhomologies at switch recombination junctions of *Rad52*^{+/+} and *Rad52*^{-/-} B cells in CSR. Histograms showing the percentage of S μ -S α junction sequences (as in Figure 3) with indicated numbers of nucleotide overlaps in *Rad52*^{+/+} (n = 18) and *Rad52*^{-/-} B cells (n = 18) from the Peyer's patches of three pairs of *Rad52*^{+/+} and *Rad52*^{-/-} littermates are shown. S μ -S γ 1 junction sequences (as in Figure 3) with indicated numbers of nucleotide overlaps (microhomologies) in *Rad52*^{+/+} (n = 25) and *Rad52*^{-/-} B cells (n = 25) stimulated with LPS plus IL-4 for 4 d are shown. The mean length of overlap in base pairs and the number of sequences analyzed (n) is indicated. The white portion of bars indicates the percentage of sequences with small (1-4 nt) insertions.

3.3 Rad52 deficient B cells activated for CSR display reduced

c-Myc/IgH translocations

As AID can off target a large number of non-*Ig* genes, and DSBs can instigate translocations between S μ on chromosome 12 and exon 1 of the *c-myc* protooncogene on chromosome 15 (**Figure 3.4**). To determine the role of Rad52 in modulating *c-Myc/IgH* translocations during CSR, we generated *p53*^{-/-}*Rad52*^{+/+} and *p53*^{-/-}*Rad52*^{-/-} mice (5) and stimulated *p53*^{-/-}*Rad52*^{+/+} and *p53*^{-/-}*Rad52*^{-/-} B cells with LPS plus IL-4 *in vitro*. After 96 hr in culture, we determined that the frequency of *c-Myc/IgH* translocations by long-range PCR, and confirmed these by Southern blot hybridization with *c-Myc* and *IgH* probes and sequence analysis (**Figure 3.5**). Consistent with previous reports (5), *c-Myc/IgH* translocations were induced at a frequency of 3.2 x 10⁻⁷ translocations/cell in *p53*^{-/-} *Rad52*^{+/+} B cells (**Figure 3.5**). Under these conditions, the frequency of *c-Myc/IgH* translocations is about three-fold higher than in *p53*^{-/-}*Rad52*^{-/-} mice (1.2 x 10⁻⁷ translocations/cell), suggesting that *Rad52* plays an active role in mediating *c-Myc/IgH* translocations in CSR. The greatly reduced *c-Myc/IgH* translocations in LPS and IL-4 stimulated B cells from *p53*^{-/-}*Rad52*^{-/-} mice compared to the B cells from their *p53*^{-/-}*Rad52*^{-/-} littermates suggest a role for Rad52 in Ku-independent end joining. Furthermore, our data show that *Rad52*^{+/+} B cells carried microhomology, and owing to the error-prone nature of microhomologies may be associated with an increase in the frequency of *c-myc/IgH* translocations, which supports the role for Rad52 in repairing DSBs through a microhomology mediated end joining process.

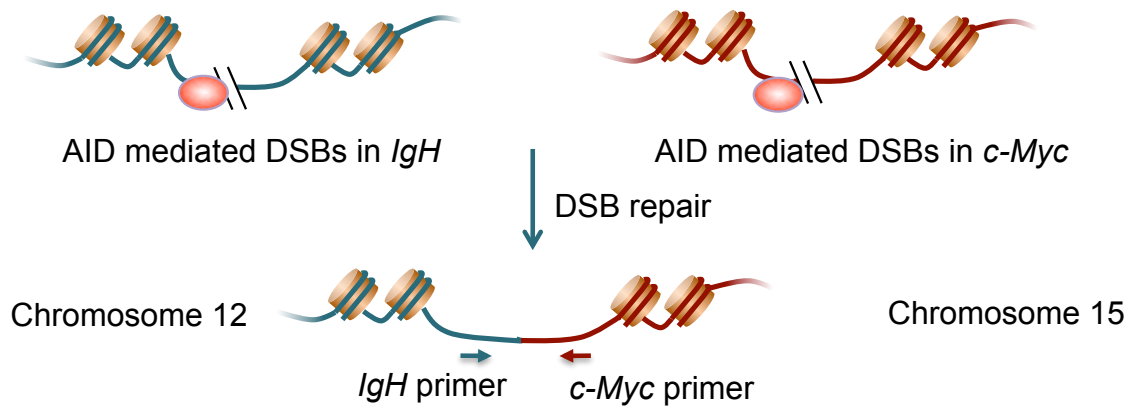


Figure 3.4. Schematic of the *IgH* and *c-myc* loci with the location of the primers used for PCR amplification to detect interchromosomal *c-myc/IgH* translocations are indicated. Green primers: S μ region of the *IgH* locus on chromosome 12. Red primers: exon 1 of the *c-myc* gene on chromosome 15.

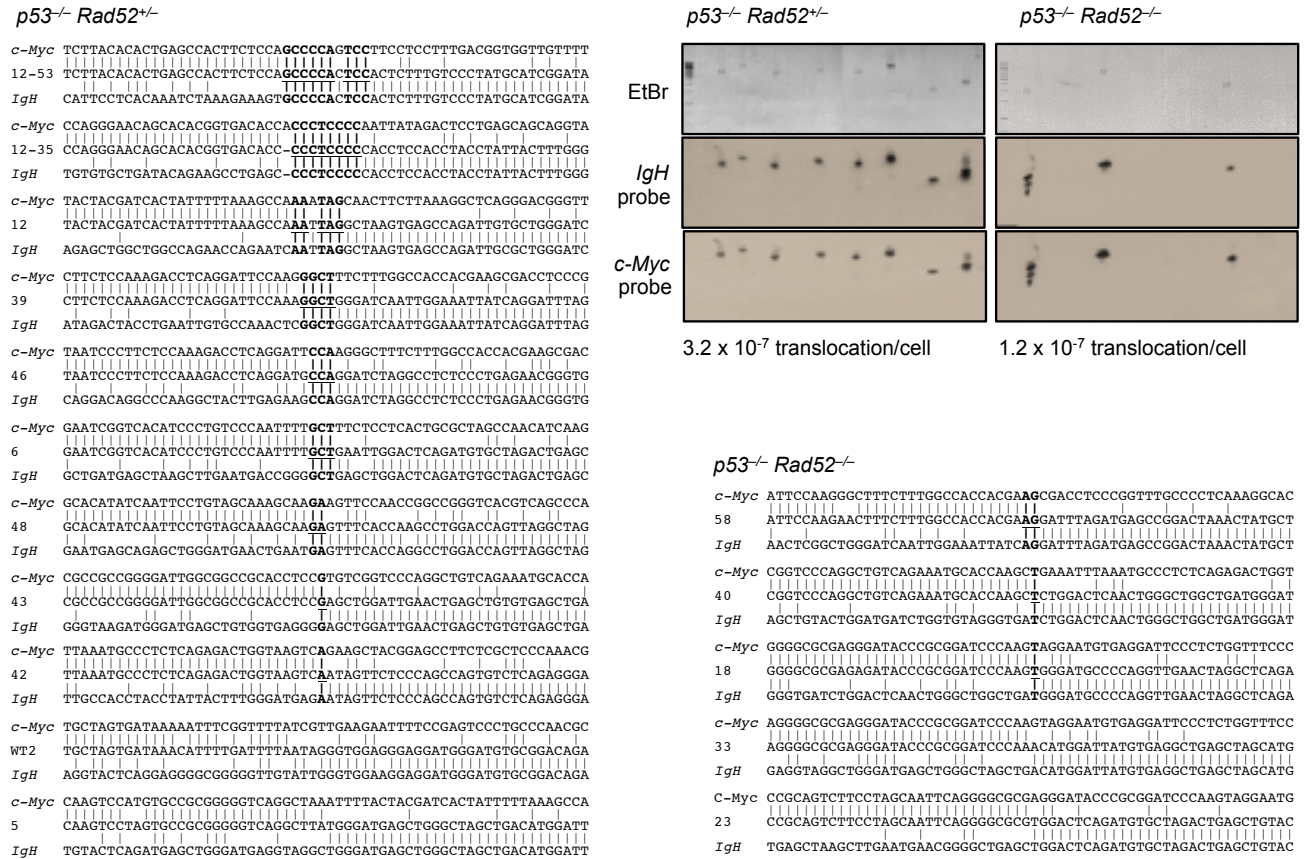


Figure 3.5. *Rad52^{-/-}* B cells activated for CSR on a *p53* deficient background display reduced *c-Myc/IgH* translocations. *c-Myc/IgH* junction DNA were amplified from *Rad52^{+/+}p53^{-/-}* and *Rad52^{-/-}p53^{-/-}* B cells stimulated with LPS plus IL-4 for 4 days, then cloned and sequenced. *c-Myc/IgH* translocations were detected by long-range nested PCR using primers specific to the *IgH* and *c-Myc* locus, and verified by Southern blot hybridization to an *IgH* or *c-myc* specific probe. Each individual PCR assay was performed using a DNA template corresponding to 1 × 10⁶ cells. The corresponding frequency of translocations per cell is indicated underneath each panel. Sequences of the *c-Myc/IgH* translocation junctions compared with germline *c-Myc* and germline *IgH* sequences. Microhomologies are bold and underlined. Data are representative of independent experiments with 3 sets of mice.

3.4 Rad52 deficiency increases recruitment of Ku70/Ku86 to S region

DSBs

To understand how Rad52 is involved in the DNA repair process of CSR, we carried out ChIP experiments to assess whether Rad52 could be detected at the S region DNA. Like Ku70/Ku86, Rad52 was specifically recruited to the S μ and S γ 1, but not S γ 3, in LPS plus IL-4 stimulated B cells, which undergo CSR to IgG1 but not IgG3, and to S μ and S γ 3, but not S γ 1, in LPS stimulated B cells, which undergo CSR to IgG3 but not IgG1. While Rad52 and Ku70/Ku86 could be readily detected at S μ and S γ 1 or S γ 3, but not C μ in wild-type B cells stimulated with LPS plus IL-4 or LPS alone, they failed to associate with the S regions in similarly activated *Aicda*^{-/-} B cells (**Figure 3.6a,b**). The AID-dependency of Rad52 and Ku70/Ku86 recruitment to activated S regions suggest that both Rad52 and Ku70/Ku86 associate with broken S region DNA.

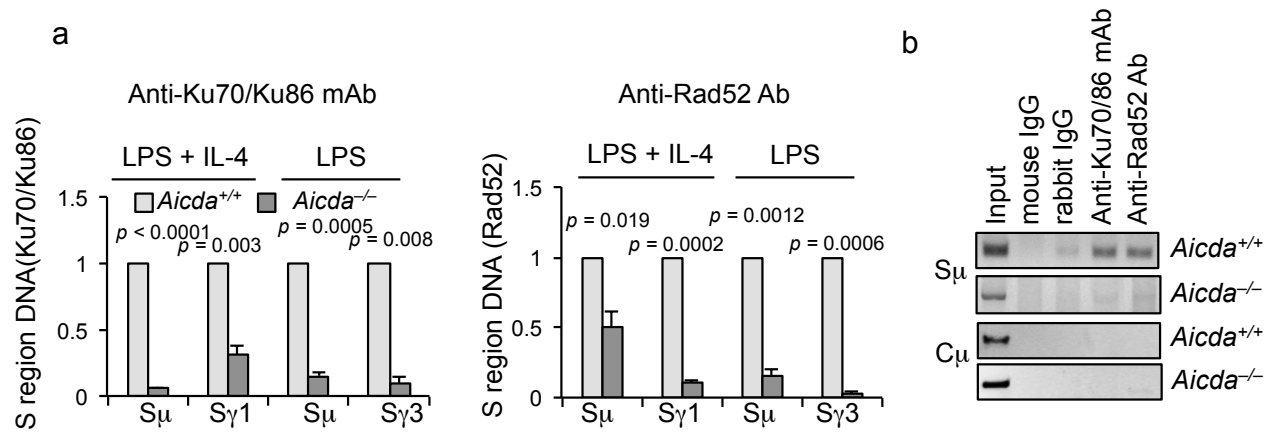


Figure 3.6. Rad52 deficiency increases recruitment of Ku70/Ku86 to S region DSBs. (a,b) *Aicda*^{+/+} and *Aicda*^{-/-} B cells were stimulated with LPS or LPS plus IL-4 for 60 hr. Cross-linked chromatin was precipitated using rabbit Ab specific to Rad52 or mouse mAb to Ku70/Ku86, or irrelevant rabbit or mouse IgG control. The precipitated S_μ, S_{γ1} and S_{γ3} DNA were quantified by real-time qPCR. Shown is the recruitment of S region DNA relative to *Aicda*^{+/+} samples. The *p* values were determined using a paired Student's *t* test. Data are representative of at least three independent experiments. Error bars indicate standard deviation (SD). The precipitated S_μ and C_μ DNA were quantified by PCR. Data are representative of three independent experiments.

3.5 Rad52 competes with Ku70/Ku86 in binding to S region dsDNA ends

As the binding of Rad52 or Ku70/Ku86 to DSBs lead to different repair processes, it is possible that Ku70/Ku86 might be prevented from accessing S region DNA in switched B cells in the presence of Rad52. Indeed, there was a remarkable 7.6-fold increase in the levels of Ku70/Ku86 bound to S γ 1 and S γ 3 DNA in *Rad52*^{-/-} B cells upon stimulation with LPS plus IL-4 or LPS, suggesting that depletion of Rad52 enhances the recruitment of Ku70/Ku86 S region DNA (**Figure 3.7a**).

The association of Ku70/Ku86 to broken S region DNA and facilitation of this association by Rad52 deficiency were further defined by *in situ* DNA end labeling by bio-dUTP (7) followed by ChIP with anti-Ku Ab, and capture of the biotin-labeled DNA fragments with streptavidin magnetic beads (**Figure 3.8**). This approach allows us to specifically detect the recruitment of Ku to DNA ends. As expected, Ku70/Ku86 were recruited to broken S μ and S γ 1 or S γ 3 DNA asymmetric around DSB ends in B cells stimulated with LPS plus IL-4 or LPS alone. This recruitment was enhanced by Rad52 deficiency (**Figure 3.7b**).

To test the possibility that Rad52 and Ku70/Ku86 compete with each other in binding to S region DNA ends, we analyzed the binding Rad52 and Ku70/Ku86 using single purified protein components of human recombinant Rad52 or Ku70/Ku86 and incubated them with biotin-labeled S region DNA ends followed by an electrophoretic mobility shift assay (EMSA). Incubation of the biotinylated S μ DNA probe with Ku70/Ku86 and Rad52 alone gave rise to a Ku70/Ku86 or Rad52 protein-S μ DNA complex (**Figure 3.7c**). Upon increasing incremental picomol amounts of human recombinant Rad52

protein and stable amounts of Ku70/Ku86, we observed increased binding of Rad52 to the S μ region DNA. This suggests that Rad52 competes with Ku70/Ku86 in binding to S region DNA ends.

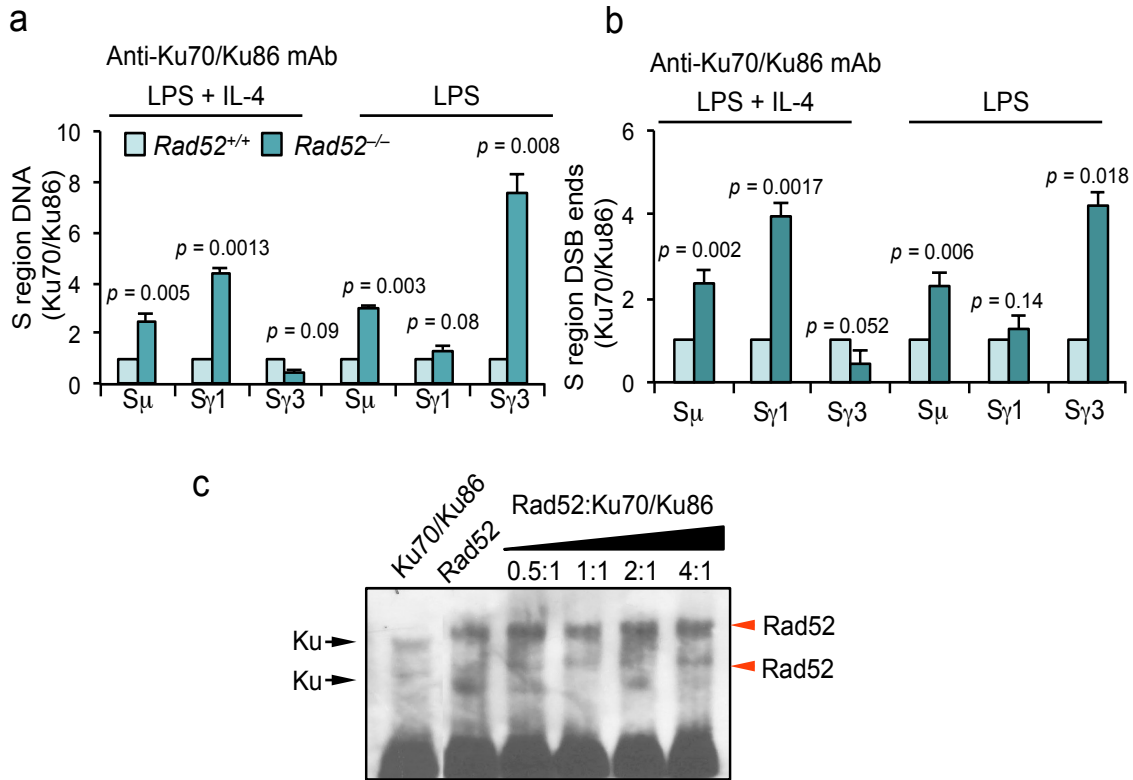


Figure 3.7. Rad52 competes with Ku70/Ku86 in binding to S region dsDNA ends (a,b) *Rad52*^{+/+} and *Rad52*^{-/-} B cells were stimulated with LPS or LPS plus IL-4 for 60 hr. Cross-linked chromatin was precipitated using rabbit Ab specific to mouse mAb to Ku70/Ku86, or irrelevant rabbit or mouse IgG control. The precipitated S μ , S γ 1 and S γ 3 DNA were quantified by real-time qPCR. Shown is the recruitment of S region DNA relative to *Rad52*^{+/+} samples. Data are representative of at least three independent experiments. Error bars indicate standard deviation (SD). The *p* values were determined using a paired Student's *t* test. **(c)** Single purified protein components of human recombinant Ku70/Ku86 and Rad52 were incubated at increasing picomol amounts of Rad52 with 20 pmol biotin-labeled S μ DNA probes during an electrophoretic mobility shift assay.

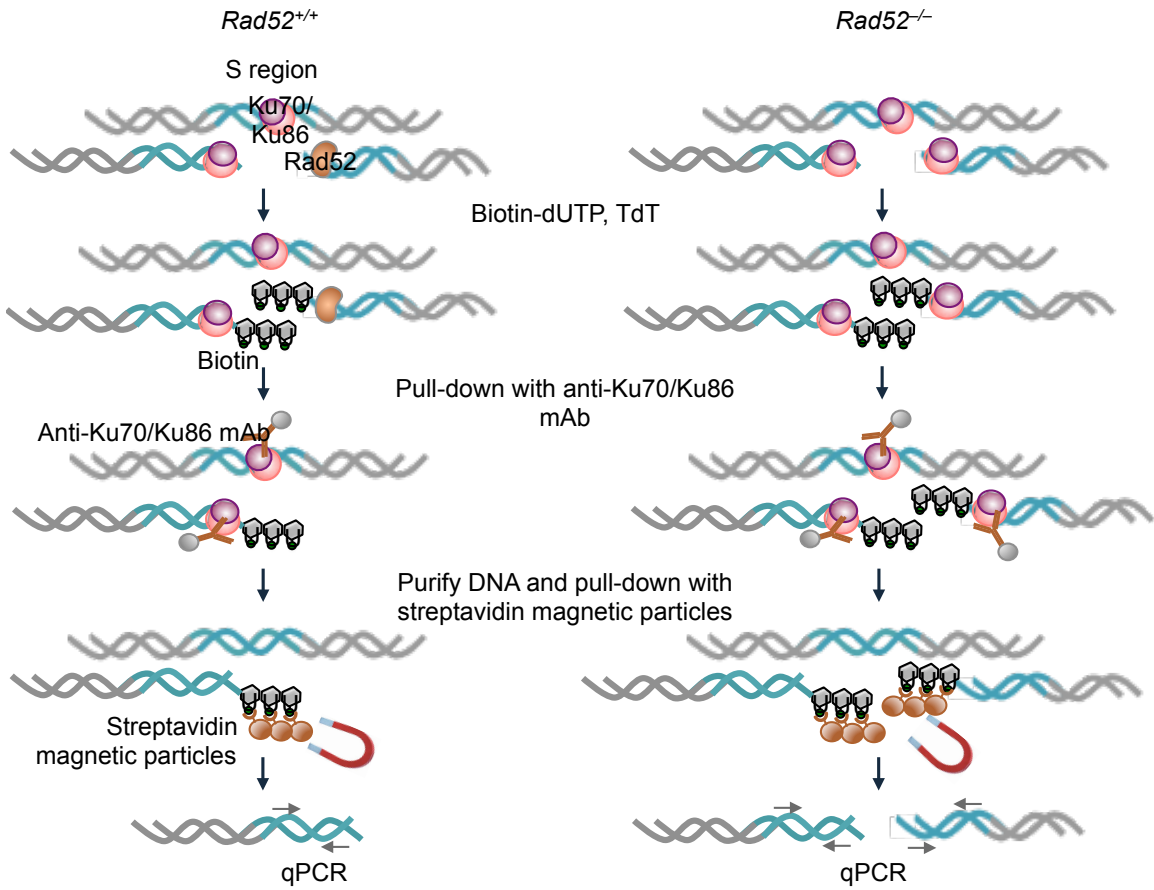


Figure 3.8: DNA end-labeling assay to detect recruitment of Ku70/Ku86 to DSB free ends. DNA ends were labeled *in situ* with bio-dUTP using TdT. Cross-linked chromatin was precipitated using mAb specific to Ku70/Ku86. The precipitated DNA with broken ends was pulled down with streptavidin magnetic beads. S_{μ} , $S_{\gamma 1}$ and $S_{\gamma 3}$ DNA levels were quantified by quantitative real-time PCR.

3.6 Rad52 mediated repair favors intra-S region DNA rejoining

AID activity can generate multiple DSBs within a given S region (4-6). These DSBs can be re-ligated, joined to another DSB in the same S region (intra-switch region recombination) which does not lead to productive CSR, or (for S μ) joined to a DSB in a downstream S region to effect CSR (inter-switch recombination). Rejoining DSBs within an S region is accompanied by resection or joining of two DSBs within an S region, leading to internal switch deletions (ISDs). Studies have shown that large ISDs occur far more frequently in S μ than in downstream target S regions (6,12,13).

To determine the role of Rad52 in AID-mediated DSB repair in CSR, we assayed for ISDs within the S μ region of genomic DNA generated from splenic *Rad52*^{+/+} and *Rad52*^{-/-} B cells activated for CSR to IgG1. To assay for internal S μ ISDs and distinguish them from CSR, genomic DNA that bind to S μ primers that flank both sides of S μ were amplified by PCR and cloned into a TOPO cloning vector. The S μ region deletions from individual clones were amplified by PCR and bands smaller than the germline S μ were scored as ISD events. By comparing the frequency of smaller PCR fragments to the germline S μ regions, we found a substantial level of S μ ISDs in *Rad52*^{+/+} B cells (45%) compared to *Rad52*^{-/-} B cells (12.5%). Together, these findings suggest that ISD at S μ can occur robustly in *Rad52*^{+/+} B cells in comparison with *Rad52*^{-/-} B cells (**Figure 3.9**). It is suggested that Rad52 mediated repair may favor intra-S region DNA rejoining.

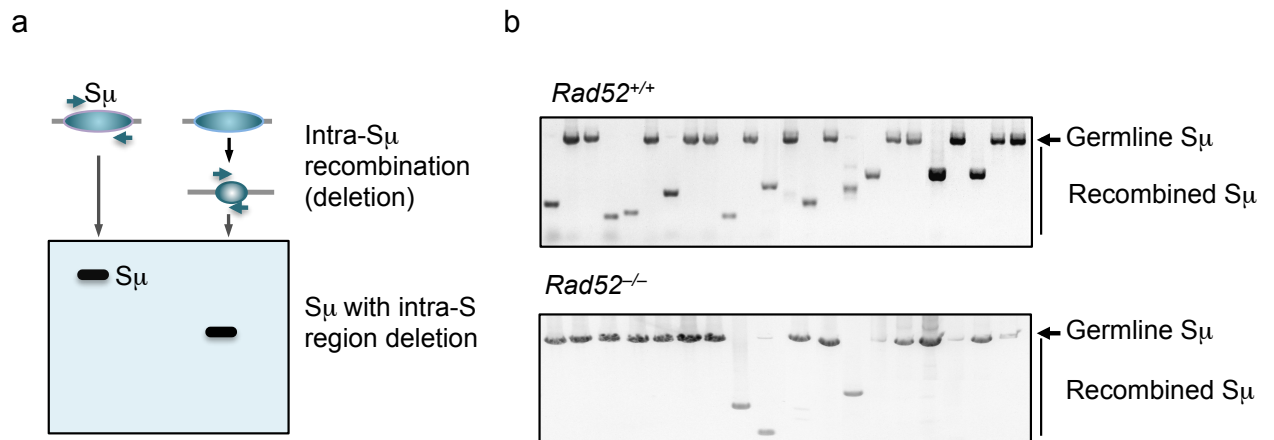


Figure 3.9. Rad52 mediated repair favors intra-S region DNA recombination. (a) Schematic representation of the detection of intra-S region recombination (deletion) in S μ region by PCR amplification. DNA ends that have undergone intra-S region DNA recombination products are much shorter in length than S μ products in the germline S μ region (b) *Rad52*^{+/+} and *Rad52*^{-/-} B cells were stimulated with LPS plus IL-4 for 4 d. S μ region DNA was amplified by PCR and cloned into the TOPO cloning vector. The S μ region deletions from individual clones were amplified by PCR. PCR products smaller than the amplified germline S μ region sequence indicate intra-S region deletions.

3.6 Methods

S-S DNA junction sequences

Genomic DNA was prepared from spleen B cells cultured for 4 days with LPS and rmIL-4, GC (PNA^{hi}B220⁺) B cells from the Peyer's patches. S μ -S γ 1 or S μ -S α DNA were amplified by two sequential rounds of specific PCR using PhusionTM high-fidelity DNA polymerase (New England BioLabs) and the following nested oligonucleotide primers (6,7): forward 5'-AACTCTCCAGCCACAGTAATGACC-3' (S μ 1-4942) and reverse 5'-CTGTAACCTACCCAGGAGACC-3' (S γ 1) or 5'-TCCAGCAAAGCTCAGGCTAGAAC-3' (S α) for the first round PCR; and forward 5'-ACGCTCGAGAAGGCCAGCCTCATAAAGCT-3' (S μ 2-4972) and reverse 5'-GTCGAATCCCCCATCCTGTCACCTATA-3' (S γ 1-NS) or 5'-AGTCCAGTCATGCTAATTCACC-3' (S α -NS) for the second round PCR. The first and second rounds of PCR were performed at 94°C for 45 s, 55°C for 45 s, 72°C for 4 min, 30 cycles. PCR products were purified using a QIAquick PCR purification kit (Qiagen) and cloned into the pCR-Blunt II-TOPO[®] vector (Invitrogen) for sequencing. Sequence alignment was done by comparing the sequences of PCR products with S μ , S γ 1 and S α genomic sequences with the use of National Center for Biotechnology Information (NCBI) Blast (www.ncbi.nih.gov/BLAST).

c-Myc/IgH translocations

Genomic DNA was isolated from *p53^{-/-}Rad52^{-/-}* and *p53^{-/-}Rad52^{+/-}* B cells stimulated with LPS plus IL-4 for 4 days. Nested PCRs for translocations were performed on genomic DNA from 1 x 10⁶ cells with GoTaq[®] Long PCR Master Mix (Promega) using

the following primers: 5'-TGAGGACCAGAGAGGGATAAAAAGAGAA-3' (IgH1) and 5'-GGGGAGGGGGTGTCAAATAATAAGA-3' (c-Myc-1) for the first round; 5'-GCAGGCAGGGCTAGATATGG -3' (IgH2) and 5'-GACACCTCCCTTCTACTCTAAACCG-3' (c-Myc-2) for the second round. PCR conditions were as follows: 95°C for 2 min followed by 25 cycles (95°C, 10 s; 62°C, 45 s; and 65°C, 6 min) for both the first and second round. Amplified DNA were fractionated through 1.0% agarose, blotted onto Hybond-N⁺ membranes and hybridized to biotin labeled *IgH*- or *c-Myc*-specific oligonucleotide probes 5'-GACGCCACTGCACCAGAGACCCTGCAGCGATTCAG -3', or 5'-CCTGGTATACAGGACGAAACTGCAGCAG-3', respectively, using Streptavidin-HRP as the detection system. To analyze the *c-Myc-IgH* junction sequences, PCR products were gel purified, cloned into the pCR-Blunt II-TOPO vector (Invitrogen) and sequenced. Sequence alignment was done by comparing the sequences of PCR products with germline *c-Myc* and *IgH* genomic sequences using NCBI *BLAST* <http://www.ncbi.nih.gov/BLAST>.

Chromatin Immunoprecipitation assays

Chromatin Immunoprecipitation (ChIP) assays were performed as previously described (8-11). The biotin labeled or unlabeled B cells (1×10^7) were treated with formaldehyde (1% v/v) for 10 min at 25°C to crosslink chromatin. After quenching with 100 mM of glycine (pH 8.0) and washing with cold PBS containing protease inhibitors (Roche), B cells were resuspended in lysis buffer (20 mM Tris-HCl, 200 mM NaCl, 2 mM EDTA, 0.1% w/v SDS and protease inhibitors, pH 8.0). Chromatin was sonicated to yield DNA fragments (about 200 to 1,000 bp in length), pre-cleared with Pierce Protein A beads

(Thermo Scientific) and incubated with rabbit anti-Rad52 Ab (H-300; Santa Cruz Biotechnology), anti-Ku70/86 mAb (MA1-21818, Thermo Scientific) or control rabbit or mouse IgG with irrelevant specificities at 4°C overnight. Immune complexes were precipitated by Protein A agarose beads, washed and eluted (50 mM Tris-HCl, 0.5% SDS, 200 mM NaCl, 100 µg/ml proteinase K, pH 8.0), followed by incubation at 65°C for 4 hr. DNA was purified using a QIAquick PCR purification kit (Qiagen). Biotin-labeled DNA or DNA from unlabeled B cells was used as a template for analysis of S μ , S γ 1 and S γ 3 by qPCR using specific primers (11) (Table 3.1).

in situ DNA end-labeling with biotin

The DNA break ends were labeled with biotin as previously described by us and others (7,12,13). *Rad52*^{+/+} and *Rad52*^{-/-} B cells were stimulated with LPS or LPS plus IL-4 for 72 hr. Live B cells were separated through a Ficoll[®] gradient, followed by fixation, permeabilization and *in situ* DNA end-labeling with biotin-16-dUTP (bio-dUTP) using TdT. Chromatin was pulled down with anti-Ku70/Ku86 mAb or control rabbit IgG with irrelevant specificities. Genomic DNA was prepared using a QIAquick PCR purification kit (Qiagen). Biotin labeled DNA fragments were captured by streptavidin magnetic beads (Promega) before being analyzed by qPCR.

Electrophoretic mobility shift assays

Biotinylated double strand DNA probes were generated by PCR with biotin-16-dUTP. The PCRs were performed using GoTaq[®] DNA polymerase (Promega). An oligonucleotide S μ 1F, which consist of a part of mouse S μ region sequence 5'-

CATTAATCTAGGTTGAATAGAGCTAAACTCTACTGCCTACACTGGACTGTTCT GAGCTGAGATGAGCTGGGGTG-3' was used as template. To generate the blunt ended DNA probe, a forward primer S μ 3F (5'-GTACCAACTTCATTAATCTAGGTTGAATAG-3') and a reverse primer S μ 3R (5'-GTACCTGAGCTCACCCCAGCTCATCTCAGCT-3') were used. The DNA probe with 4 nt overhangs at 3' ends of both strands (staggered probe) was generated by KpnI digestion of the PCR product amplified with the forward S μ 3F-Kpn (5'-GAACTGGTACCAACTTCATTAATCTAGGTTGAATAG-3') and reverse S μ 3R-Kpn (5'-CGTACGGTACCTGAGCTCACCCCAGCTCATCTCAGC-3') primers. Electrophoretic mobility shift assays (EMSAs) were performed using the LightShift Chemiluminescent EMSA Kit (Thermo Scientific) according to manufacturer's instructions. Biotinylated probes were used in a concentration of 5 fmol per reaction and incubated with 0.16 or 0.32 pmol of human recombinant Ku70/Ku86 (Cell Sciences), or 0.5 or 1.0 pmol of human recombinant Rad52 (Axxora). Electrophoresis of the DNA-protein complexes was carried out on a 5% non-denaturing polyacrylamide gel with 0.5x TBE. Afterwards, the samples were transferred to Hybond-N⁺ membranes with a semi-dry transfer followed by UV cross-linking. Detection was done with the Chemiluminescent Nucleic Acid Detection Module (Thermo Fisher Scientific) according to the manufacturer's instructions.

Analysis of intra-S μ region recombinations

Intra-S μ region DNA recombination was analyzed by specific PCR and Southern blotting of the amplified DNAs using a specific S μ probe. S μ DNA was amplified using mouse S μ -specific primer (forward, moS μ F1 5'-AACTCTCCAGCCACAGTAATGACC-3';

reverse, moS μ R1 5'-AGGGTAGGAGGAAGGTGGGTTATG-3') from genomic DNA isolated from *Rad52*^{+/+} and *Rad52*^{-/-} B cells stimulated with LPS plus IL-4 for 3 d. Amplified DNA was fractionated through a 0.8% agarose gel, blotted onto Hybond-N⁺ membranes (GE Healthcare) and hybridized to biotinylated S μ specific oligonucleotide probe moS μ Pro1 5'-TAGTAAGCGAGGCTCTAAAAAGCAT-3'. Recombined intra-S μ DNA, that is an S μ region with internal deletions, were identified by comparing the lengths of the amplified and hybridized DNAs with those derived from amplification of the respective germline S μ regions. The amplified S μ region DNAs were cloned into pCR-Blunt II-TOPO[®] vector (Qiagen) and sequenced.

Statistical analysis

Statistical analysis was performed using Excel software to determine *p* values by paired and unpaired Student's *t*-test, and *p* values less than 0.05 were considered significant.

3.8 The potential role of Pol θ in CSR

Pol θ is an error-prone translesion DNA polymerase that exhibits low fidelity on templated DNA and also displays a terminal transferase-like activity that catalyzes nucleotide addition in a template-independent manner (1). The relevance of Pol θ has been highlighted in *Drosophila melanogaster*, where Pol θ is shown to stimulate nucleotide insertions during DSB repair by A-NHEJ, and *C. elegans* in which Pol θ promotes end joining of replication-associated DSBs, and more recently in mammalian cells by stimulating the end-joining reaction. As previously mentioned, homology-directed repair (HDR) is prevalent during the S/G2 phases of the cell cycle, which coincides with the peak of A-NHEJ activity. Specifically, these authors found that Pol θ mediated A-NHEJ is essential for the survival of human 293T cells, epithelial ovarian cancer cells (EOCs), and various other human cancer cell lines with a compromised HDR pathway (1), (2).

Our data demonstrate that Rad52 can repair DSB through a microhomology mediated end joining mechanism which leads to inter-switch (S) region rejoining, thereby resulting in efficient CSR. It is postulated that through this route, the recruitment of single strand binding proteins RPA and Rad51 to Rad52 promotes HDR-mediated repair (3,4). An opposing activity is likely to be exerted by Pol θ . It has been shown by others that Pol θ negatively regulates HR. Pol θ is a RAD51-interacting protein, which negatively affects RAD51-ssDNA assembly through its RAD51 binding and ATPase activities (2). Hence, Pol θ is an error-prone polymerase that participates in A-NHEJ and acts as part of a second compensatory DNA repair pathway that antagonizes HR and promotes error-

prone repair. Polθ may exploit both template-independent and template-dependent activities to stabilize the annealed intermediate structure and influence repair towards A-NHEJ (1). Similarly, our data show that Rad52 can also resolve inter-S region DSBs, possibly as part of an A-NHEJ pathway in CSR albeit through a microhomology-mediated end joining process; this lead us to hypothesize that there may be some correlation or antagonizing relationship between Polθ and Rad52 in repairing DSBs by A-NHEJ in CSR.

Our laboratory has conducted extensive studies on error-prone translesion DNA polymerases and have demonstrated an important role for Polθ in somatic hypermutation (5), therefore we asked whether Polθ may also be involved in CSR.

To examine the role of Polθ in CSR, we obtained *Polθ^{+/+}* and *Polθ^{-/-}* mice. To determine the impact of Polθ deficiency on CSR, we stimulated *Polθ^{+/+}* and *Polθ^{-/-}* spleen B cells with LPS plus IL-4 (to induce class switching to IgG1), LPS (IgG3), or LPS plus IFNγ (IgG2a), and LPS plus TGFB, IL-5, IL-4 and anti-δ monoclonal antibody (mAb)/dex (IgA). After 4 days, there was virtually no change in switched surface IgG1⁺, IgG3⁺, IgG2a⁺, IgA⁺ B cells among *Polθ^{+/+}* and *Polθ^{-/-}* mice (**Figure 3.10a**). Consistent with the unaltered surface expression of class switched B cells, *Polθ^{-/-}* B cells underwent the same number of cell divisions as their *Polθ^{+/+}* counterparts after 3 days of culture with LPS plus IL-4 (**Figure 3.10b**). Further, the total percentage of IgG1 positive B cells was unchanged.

At the molecular level, we quantified germline Iγ1-Cγ1, Iγ3-Cγ3, circle Iγ1-Cμ, Iγ3-Cμ and post-recombination Iμ-Cγ1 and Iμ-Cγ3 transcripts of *Polθ^{+/+}* and *Polθ^{-/-}* B cells

stimulated with LPS plus IL-4 by quantitative real-time PCR. qRT-PCR analysis revealed that the level of germline $I\gamma 1-C\gamma 1$, $I\gamma 3-C\gamma 3$, circle $I\gamma 1-C\mu$, $I\gamma 3-C\mu$ and post-recombination $I\mu-C\gamma 1$ and $I\mu-C\gamma 3$ transcripts were unaltered in $Pol\theta^{+/+}$ and $Pol\theta^{-/-}$ B cells (**Figure 3.10c**).

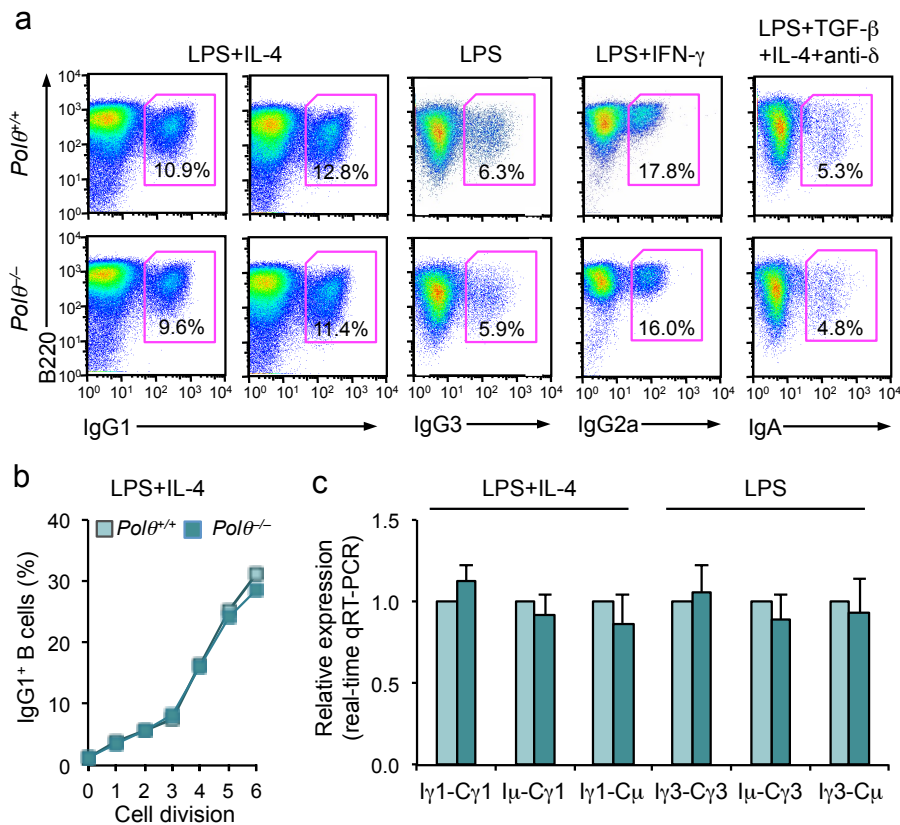


Figure 3.10. $Pol\theta$ deficiency does not affect CSR. (a) $Pol\theta^{+/+}$ and $Pol\theta^{-/-}$ B cells were stimulated with LPS plus IL-4 (for CSR to IgG1), LPS alone (for IgG3), LPS plus IFN- γ (for IgG2a), and LPS plus TGF- β 1, IL-4, IL-5 and anti- δ mAb/dex (for IgA). After 4 d of culture, the cells were analyzed for surface B220 and IgG1, IgG3, IgG2a or IgA by flow cytometry. (b) Proliferation of $Pol\theta^{+/+}$ and $Pol\theta^{-/-}$ B cells were labeled with the cell division tracking fluorochrome CFSE and stimulated with LPS plus IL-4 for 4 d. CFSE intensity and surface IgG1 expression were analyzed by flow cytometry. The proportion of surface IgG1⁺ B cells at each cell division is indicated. Data are from one representative of three independent experiments. (c) Real time qPCR analysis of germline I γ 1-C γ 1, I γ 3-C γ 3 transcripts, circle I γ 1-C μ , I γ 3-C μ , and post-recombination I μ -C γ 1, I μ -C γ 3 transcripts in $Pol\theta^{+/+}$ and $Pol\theta^{-/-}$ B cells cultured for 60 hr with LPS plus IL-4 (*Aicda*, I γ 1-C γ 1, I γ 1-C μ and I μ -C γ 1) or LPS (*Aicda*, I γ 3-C γ 3, I γ 3-C μ and I μ -C γ 3). Expression of germline I_H-C_H, circle I_H-C μ , and post-recombination I μ -C_H transcripts were normalized to *Cd79b* expression and depicted relative to the expression in $Pol\theta^{+/+}$ B cells, set as one. The *p* values were determined using a paired Student's *t* test. Data are from three independent experiments (mean and SEM).

As Polθ has been shown to promote A-NHEJ, which is thought to be associated with an increase in microhomologies at the S-S junctions in CSR, we amplified, cloned, and sequenced DNA from *Polθ*^{+/+} and *Polθ*^{-/-} B cells stimulated with LPS plus IL-4 and analyzed the frequency and length of microhomologies at the S μ -S γ 1 junctions (**Figure 3.11**). It was determined that *Polθ* deficiency does not affect the frequency or length of microhomology at the S μ -S γ 1 junctions in CSR.

Polθ^{+/+} and *Polθ*^{-/-} B cells stimulated with LPS plus IL-4 undergo the same number of cell divisions, which suggest no obvious defects in proliferation, suggesting that CSR can occur (**Figure 3.11b**). The total percentage of class switched IgG1⁺ were comparable in *Polθ*^{+/+} and *Polθ*^{-/-} B cells. This was consistent with the fact that there were no significant alterations in class switching to IgG1, IgG3, IgG2a, and IgA at the cellular level as assessed by flow cytometry (**Figure 3.10a**). Analysis of germline I γ 1-C γ 1, I γ 3-C γ 3, circle I γ 1-C μ , I γ 3-C μ and post-recombination I μ -C γ 1 and I μ -C γ 3 transcripts, hallmarks of ongoing and completed CSR respectively, further confirm this result at the molecular level. Altogether, our results suggest that although Polθ can mediate DNA repair in HR-deficient tumors (2) through alternative NHEJ, it does not appear to have a role in CSR.

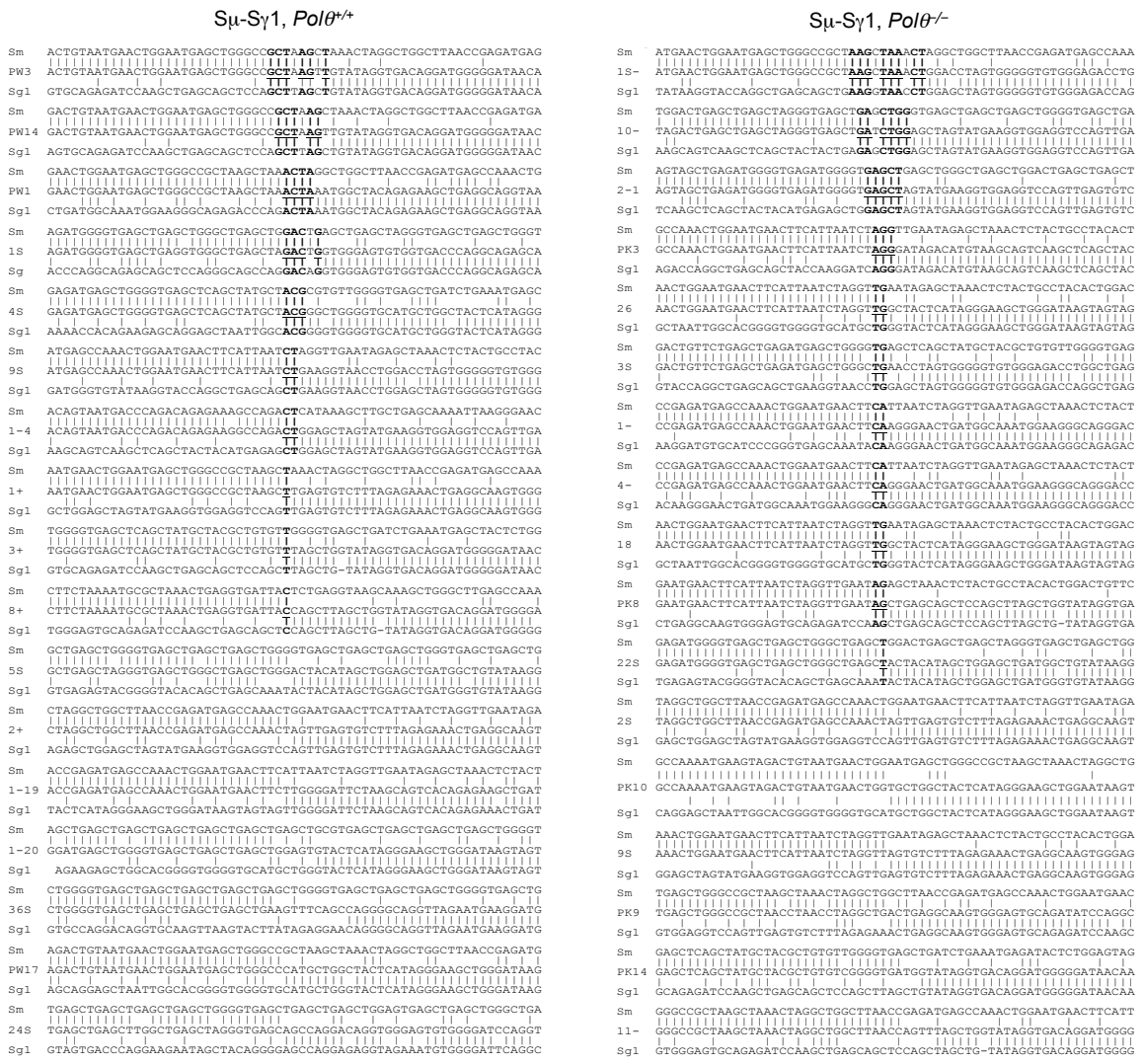


Figure 3.11. Polθ deficiency does not affect the frequency or length of microhomology at switch recombination junctions in CSR. Sμ-Sγ1 junctions from *in vitro* stimulated *Polθ*^{+/+} and *Polθ*^{-/-} B cells were analyzed. B cells from *Polθ*^{+/+} and *Polθ*^{-/-} mice were stimulated by LPS plus IL-4 for 4 d. Junctional Sμ-Sγ1 DNAs from stimulated cells were amplified, cloned, and sequenced. Seventeen sequences from *Polθ*^{+/+} B cells and seventeen sequences from *Polθ*^{-/-} B cells are shown. The germline Sμ or Sγ1 sequences are aligned above and below the recombination switch junctional sequences. Microhomologies (bold and underlined) were determined by identifying the longest region at the switch junction of perfect uninterrupted donor/acceptor identity, or the longest overlap region at the switch junction with no more than one mismatch on either side of the breakpoint.

3.9 Discussion

CSR entails AID-mediated generation of multiple DSBs in highly repetitive S regions and the resolution of these DSB (6-9). During CSR in B cells, S region DSBs are joined by NHEJ, which employs the Ku70/86 complex (Ku) for DSB recognition and the XRCC4/Lig IV complex for ligation, to form junctions either with short microhomologies or no homologies. Previous work has shown that in the absence of core NHEJ components such as Ku70/Ku86, XRCC4 or Lig IV, substantial CSR occurs albeit generating largely microhomology-mediated end joins. The mechanisms underlying NHEJ-independent S region DSB repair remain to be fully understood. In this study, we show that the DNA repair protein Rad52, which binds single-stranded DNA ends, and mediates the DNA-DNA interaction necessary for the annealing of complementary DNA strands, plays an important role in repairing S region DSBs. As with Ku70/Ku86 (10), Rad52 binds to DNA with DSB ends in the upstream and downstream S regions that are involved in CSR. Deficiency of Rad52 resulted in an increased recruitment of Ku70/Ku86 to S region DSBs, thereby leading to increased CSR. This was accompanied by decreased microhomologies in the S-S junctions and decreased inter-chromosomal *c-Myc/IgH* translocations in *Rad52*^{-/-} B cells *in vivo* and *in vitro* which is inversely consistent with that in Ku-deficient B cells (11,12). Our findings demonstrate that Rad52 competes with Ku70/Ku86 in binding to S region DSBs, facilitating a Ku-independent repair pathway for AID-mediated S region DSBs and mediates CSR at a much-reduced level (**Figure 3.12**).

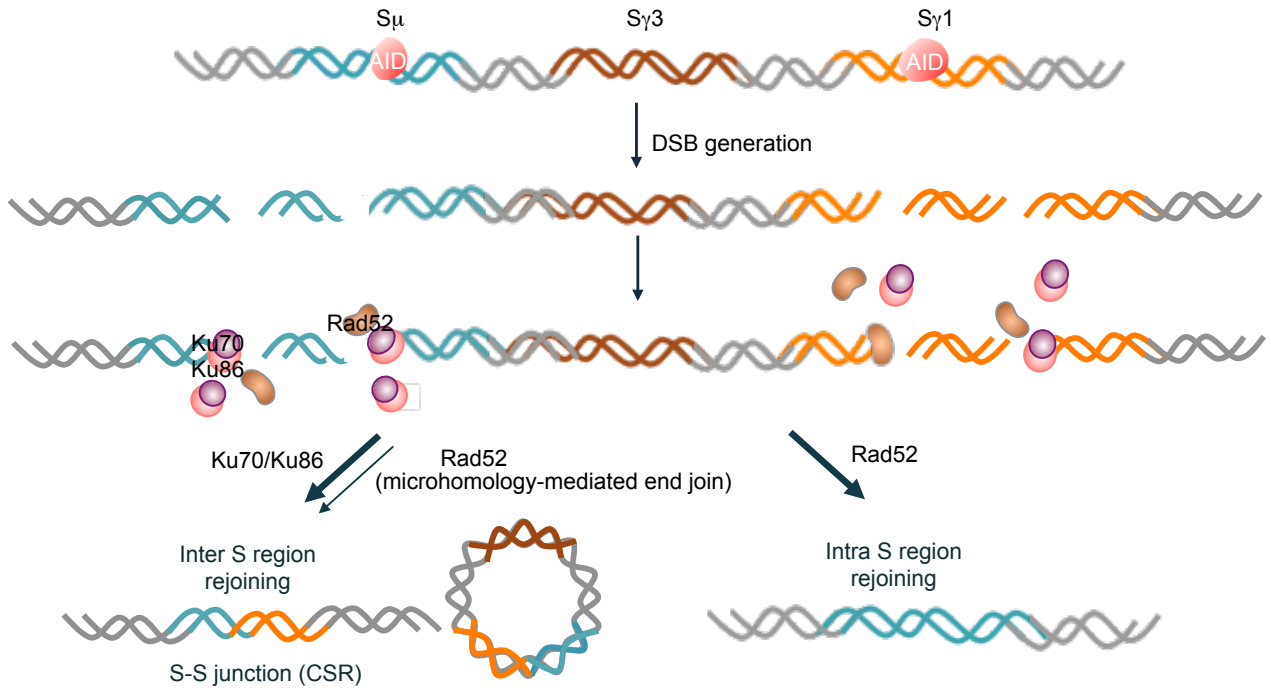


Figure 3.12. Schematic representation to show that Rad52 competes with Ku70/Ku86 for binding to S region DNA ends to modulate class switch DNA recombination. AID mediated S region breaks can be processed in a Ku70/Ku86 dependent manner leading to efficient CSR. Rad52 can also bind to S region DSBs ends to facilitate a Ku-independent process which favors intra-S region rejoining and does not lead to CSR, or can repair these ends through a microhomology mediated end joining process, which can resolve DSBs through inter-S region rejoining, possibly as part of an alternative NHEJ pathway.

The resolution of S region DSBs in CSR is a highly coordinated process that uses the DNA repair machinery to maintain genomic integrity. As mentioned previously, there are two well-characterized DSB repair pathways in mammalian cells. HR accurately repairs post-replicative DSBs via a long, homologous template from a sister chromatid, while NHEJ fuses DSB ends that lack substantial junctional homology to form mainly “direct” joins. It is suggested by our results that the increase in CSR in *Rad52*^{-/-} B cells may be due to an increase of Ku70/Ku86 recruitment to the S region DSBs, as NHEJ repairs paired DSBs in heterologous S regions yields predominantly productive recombination between two switch regions, resulting in CSR. The increase in CSR and translocations appear to be the result of defects in nonhomologous recombination pathways, as evidenced by the increase in microhomology lengths in *Rad52*^{+/+} B cells compared to their *Rad52*^{-/-} littermates. It is suggested that on considerable occasion, productive recombination fails mainly during alternative, or microhomology-mediated, end-joining, which is often associated with intraswitch recombination within an S region, thereby producing no CSR (13-16). In B cell activation for CSR, multiple DSBs are introduced into each S region that are involved in CSR, with some being rejoined or joined to each other to generate intra-S region deletions (11). The greatly increased intra-S region deletions in B cells lacking Ku and/or Lig IV (11,12) strongly suggest that the Ku-dependent NHEJ lead to effective CSR, while a Rad52-dependent end-joining process may be prone to introduce intra-S region deletions, which does not lead to productive CSR (**Figure 3.10**).

In the absence of the core NHEJ components, such as Ku70, XRCC4 or Lig IV, a majority of S-S junctions contain microhomologies, which are, on average, longer than

those observed in normal S-S junctions (11,12,17). Thus, the Ku- (or XRCC4-/Lig IV-) independent end joining process can be characterized as microhomology-mediated end joining, which likely involve protruding DSB ends and utilize a mechanism that share features of both NHEJ and HR. The reduced number and length of microhomologies in the S-S junctions in the *Rad52*^{-/-} B cells strongly suggest an important role of Rad52 in the Ku- (or XRCC4-/Lig IV-) independent end joining process. Rad52 functions as a recombination mediator that is involved in the maintenance of genomic integrity. It binds and wraps ssDNA and promotes annealing of complementary DNA strands as well as annealing between ssDNA-RPA complexes (18). Both Ku and Rad52 bind to DNA ends and facilitate end-to-end interactions (19). It has been suggested that Rad52 and Ku bind to different DNA structures produced early in DSB repair, and lead to different DSB repair processes. Rad52 binds more effectively to long ssDNA (20). Ku protein that binds to the DSB ends may block the access of terminal deoxynucleotidyl transferase (TdT) to the DSB ends, and the amount of Ku that binds to DSB could be even higher than what is detected. Similar to Ku70/Ku86, Rad52 can also bind to blunt or short protruding DNA ends (20). In our study, competition for binding to DNA ends by Ku and Rad52 was demonstrated by an increased recruitment of Ku to S region DNA asymmetric around DSB ends in *Rad52*^{-/-} B cells as measured by DNA end labeling with bio-dUTP using TdT.

By employing competing but overlapping repair pathways, eukaryotic cells ensure a level of redundancy for DSB repair, which allow one repair pathway to compensate for loss of the other which is beneficial to the cell. The effect of the competition is likely to be influenced by a number of factors, such as the affinities of Rad52 or Ku for binding

DNA ends, and the relative abundance of these proteins in B cells (21). Although NHEJ is most important during G1 or early S phase when no homologous template for recombination is available, it is active throughout the cell cycle. Given the important role of Rad52 in HR in yeast, it is, in general, recruited to DSB sites and readily form Rad52 foci in response to DNA damage during S and G2/M phase when a sister chromatid become available (22). Nevertheless, Rad52 can be accumulated at DNA damage sites immediately after DSB-induction (23). It has been recently suggested that AID-mediated DNA damage can lead to intra- and inter-genic deletions through HR-like recombination of sequence repeats in the same or different S region(s) (24). This recombination occurs in the same chromatin and is apparently independent of DNA replication and can function throughout the cell cycle.

It has been suggested that the mechanism leading to intra-S region deletion is mediated by S region microhomology uncovered by DNA-end resection and RPA recruitment (14,15,25). When Rad52 binds to DSB ends, this could lead to an intra-S region deletion, which does not result in productive CSR, owing to homologous recombination of sequence repeats (24). In the absence of Rad52, the DSB ends which are suppose to be bound by Rad52 could be bound by Ku70/Ku86 directly, if they are blunt or possess short overhangs, or after processing (removal of overhangs or fill-in by polymerases), and lead to a NHEJ process that can result in a productive CSR. This is consistent with the robust intra-S region recombination occurring in Ku70- and Ku70/Lig IV-deficient B-cell (11) and would explain the increased CSR in *Rad52*^{-/-} B cells.

A number of studies suggest that AID-mediated DSBs could be repaired by HR without introducing productive CSR (15,24). Inhibition of HR reduced the viability of B

cells that express AID and induced widespread DSBs (26,27). The AID co-factor RPA, another ssDNA-binding DSB repair protein that associates with resected DSBs, can also be recruited to the sites of AID-mediated damage in S regions (15). RPA can interact with AID and promotes the deamination of transcribed substrates by AID by stabilizing its interaction with ssDNA. It has been suggested that RPA can associate with and stabilize resected DSBs that cannot easily be repaired by classical NHEJ, by facilitating salvage by homology-mediated repair pathways (15). It is known that Rad52 associates with DNA-bound RPA and contributes to the recombination mediator activity. Additionally, it has been shown that the RPA that accumulated at AID-mediated DNA damage sites is associated with the Rad51. The interaction between Rad52 and RPA produces a Rad52–RPA–ssDNA complex, which recruits Rad51 into ssDNA and is important for the enhancement of annealing of complementary ssDNAs. We speculate that RPA may facilitate Rad52 binding to AID-mediated DSBs and lead to microhomology-mediated end joining, HR-like repeat recombination, which can result in inter-S recombination or a low frequency of CSR, or error-free HR, which do not introduce CSR.

Although Rad52 preferentially binds ssDNA or DNA ends with a long single-strand overhang, it can also bind blunt or small overhang DSBs more efficiently than Ku (20). It has been suggested that the structure of the DSB end will direct the substrate into differential use of end-processing factors, and that Ku and Rad52 direct the choice of DSB repair through two different repair pathways (41), (19), (20). Specifically, Rad52 accumulates on the DNA ends of single and double strand breaks to protect end degradation from exonucleases (19,28-30). Ku can bind to viral long terminal repeat

(LTR) DNA and plays an important role in the post-integration repair and circularization of viral cDNA during retroviral infection (31). Rad52 has been shown to compete with Ku for binding to HIV LTR DNA and suppress retroviral infection (32). Repair can also occur through gene conversion, although this may lead to chromosome rearrangements.

In addition, the Ku70/Ku86- and Lig IV-independent DSB repair mechanism also generates substantial levels of chromosomal *IgH* translocations in activated B cells in response to AID-induced DNA breaks (17,33). The greatly reduced AID-dependent *c-Myc/IgH* translocation in B cells in the absence of Ku70, XRCC4 or Lig IV (34), suggest an important role for the Ku- (or XRCC4-/Lig IV-) independent end joining process in mediating inter-chromosomal translocation. We reason here that if Rad52 is important for the DNA end joining process independent of the core NHEJ factors, deficiency of Rad52 would result in the reduction of *c-Myc/IgH* translocations. The greatly reduced *c-Myc/IgH* translocations in LPS and IL-4 stimulated B cells from *p53^{-/-}Rad52^{-/-}* mice compared to the B cells from their *p53^{-/-}Rad52^{-/-}* littermates strongly support the role for Rad52 in the Ku-independent end joining. These inter-chromosomal translocations, for instance in this case, *c-Myc/IgH* translocations result from the misjoining of DSBs caused by AID-mediated DNA lesions and can lead to tumorigenesis in humans and mice. Identification of the DSB repair factors and pathways required for translocation formation is important for understanding tumor formation and developing strategies for tumor prevention (35).

3.10 References

1. Mateos-Gomez, P. A., Gong, F., Nair, N., Miller, K. M., Lazzarini-Denchi, E., and Sfeir, A. (2015) Mammalian polymerase theta promotes alternative NHEJ and suppresses recombination. *Nature* **518**, 254-257
2. Ceccaldi, R., Liu, J. C., Amunugama, R., Hajdu, I., Primack, B., Petalcorin, M. I., O'Connor, K. W., Konstantinopoulos, P. A., Elledge, S. J., Boulton, S. J., Yusufzai, T., and D'Andrea, A. D. (2015) Homologous-recombination-deficient tumours are dependent on Poltheta-mediated repair. *Nature* **518**, 258-262
3. Chen, H., Lisby, M., and Symington, L. S. (2013) RPA coordinates DNA end resection and prevents formation of DNA hairpins. *Molecular cell* **50**, 589-600
4. Deng, S. K., Gibb, B., de Almeida, M. J., Greene, E. C., and Symington, L. S. (2014) RPA antagonizes microhomology-mediated repair of DNA double-strand breaks. *Nature structural & molecular biology* **21**, 405-412
5. Zan, H., Shima, N., Xu, Z., Al-Qahtani, A., Evinger Iii, A. J., Zhong, Y., Schimenti, J. C., and Casali, P. (2005) The translesion DNA polymerase theta plays a dominant role in immunoglobulin gene somatic hypermutation. *The EMBO journal* **24**, 3757-3769
6. Casali, P., and Zan, H. (2004) Class switching and Myc translocation: how does DNA break? *Nat Immunol* **5**, 1101-1103
7. Casali, P., Pal, Z., Xu, Z., and Zan, H. (2006) DNA repair in antibody somatic hypermutation. *Trends Immunol* **27**, 313-321
8. Xu, Z., Zan, H., Pone, E. J., Mai, T., and Casali, P. (2012) Immunoglobulin class switching: induction, targeting and beyond. *Nature Rev. Immunol.* **12**, 517-531
9. Casali, P. (2014) Somatic recombination and hypermutation in the immune system. in *Lewin's Genes X* (Krebs, J. E., Goldstein, E. S., and Kilpatrick, S. T. eds.), 11 Ed., Jones & Bartlett, Sudbury, MA. pp 459-507
10. Lee-Theilen, M., Matthews, A. J., Kelly, D., Zheng, S., and Chaudhuri, J. (2011) CtIP promotes microhomology-mediated alternative end joining during class-switch recombination. *Nat. Struct. Mol. Biol.* **18**, 75-79
11. Boboila, C., Jankovic, M., Yan, C. T., Wang, J. H., Wesemann, D. R., Zhang, T., Fazeli, A., Feldman, L., Nussenzweig, A., Nussenzweig, M., and Alt, F. W. (2010) Alternative end-joining catalyzes robust IgH locus deletions and translocations in the combined absence of ligase 4 and Ku70. *Proc. Natl. Acad. Sci. USA.* **107**, 3034-3039
12. Boboila, C., Yan, C., Wesemann, D. R., Jankovic, M., Wang, J. H., Manis, J., Nussenzweig, A., Nussenzweig, M., and Alt, F. W. (2010) Alternative end-joining catalyzes class switch recombination in the absence of both Ku70 and DNA ligase 4. *J. Exp. Med.* **207**, 417-427
13. Zarrin, A. A., Del Vecchio, C., Tseng, E., Gleason, M., Zarin, P., Tian, M., and Alt, F. W. (2007) Antibody class switching mediated by yeast endonuclease-generated DNA breaks. *Science* **315**, 377-381
14. Bothmer, A., Robbiani, D. F., Feldhahn, N., Gazumyan, A., Nussenzweig, A., and Nussenzweig, M. C. (2010) 53BP1 regulates DNA resection and the choice between classical and alternative end joining during class switch recombination. *J. Exp. Med.* **207**, 855-865

15. Yamane, A., Robbiani, D. F., Resch, W., Bothmer, A., Nakahashi, H., Oliveira, T., Rommel, P. C., Brown, E. J., Nussenzweig, A., Nussenzweig, M. C., and Casellas, R. (2013) RPA accumulation during class switch recombination represents 5'-3' DNA-end resection during the S-G2/M phase of the cell cycle. *Cell Rep.* **3**, 138-147
16. Zanotti, K. J., Maul, R. W., Castiblanco, D. P., Yang, W., Choi, Y. J., Fox, J. T., Myung, K., Saribasak, H., and Gearhart, P. J. (2015) ATAD5 Deficiency Decreases B Cell Division and Igh Recombination. *J Immunol* **194**, 35-42
17. Yan, C. T., Boboila, C., Souza, E. K., Franco, S., Hickernell, T. R., Murphy, M., Gumaste, S., Geyer, M., Zarrin, A. A., Manis, J. P., Rajewsky, K., and Alt, F. W. (2007) IgH class switching and translocations use a robust non-classical end-joining pathway. *Nature* **449**, 478-482
18. Grimme, J. M., Honda, M., Wright, R., Okuno, Y., Rothenberg, E., Mazin, A. V., Ha, T., and Spies, M. (2010) Human Rad52 binds and wraps single-stranded DNA and mediates annealing via two hRad52-ssDNA complexes. *Nucleic Acids Res.* **38**, 2917-2930
19. Van Dyck, E., Stasiak, A. Z., Stasiak, A., and West, S. C. (1999) Binding of double-strand breaks in DNA by human Rad52 protein. *Nature* **398**, 728-731
20. Ristic, D., Modesti, M., Kanaar, R., and Wyman, C. (2003) Rad52 and Ku bind to different DNA structures produced early in double-strand break repair. *Nucleic Acids Res.* **31**, 5229-5237
21. Hiom, K. (1999) Dna repair: Rad52 - the means to an end. *Curr. Biol.* **9**, R446-448
22. Barlow, J. H., and Rothstein, R. (2009) Rad52 recruitment is DNA replication independent and regulated by Cdc28 and the Mec1 kinase. *EMBO J.* **28**, 1121-1130
23. Koike, M., Yutoku, Y., and Koike, A. (2013) The C-terminal region of Rad52 is essential for Rad52 nuclear and nucleolar localization, and accumulation at DNA damage sites immediately after irradiation. *Biochem. Biophys. Res. Commun.* **435**, 260-266
24. Buerstedde, J. M., Lowndes, N., and Schatz, D. G. (2014) Induction of homologous recombination between sequence repeats by the activation induced cytidine deaminase (AID) protein. *eLife* **3**, e03110
25. Bothmer, A., Robbiani, D. F., Di Virgilio, M., Bunting, S. F., Klein, I. A., Feldhahn, N., Barlow, J., Chen, H. T., Bosque, D., Callen, E., Nussenzweig, A., and Nussenzweig, M. C. (2011) Regulation of DNA end joining, resection, and immunoglobulin class switch recombination by 53BP1. *Mol. Cell* **42**, 319-329
26. Hasham, M. G., Donghia, N. M., Coffey, E., Maynard, J., Snow, K. J., Ames, J., Wilpan, R. Y., He, Y., King, B. L., and Mills, K. D. (2010) Widespread genomic breaks generated by activation-induced cytidine deaminase are prevented by homologous recombination. *Nat Immunol* **11**, 820-826
27. Lamont, K. R., Hasham, M. G., Donghia, N. M., Branca, J., Chavaree, M., Chase, B., Breggia, A., Hedlund, J., Emery, I., Cavallo, F., Jasin, M., Ruter, J., and Mills, K. D. (2013) Attenuating homologous recombination stimulates an AID-induced antileukemic effect. *J. Exp. Med.* **210**, 1021-1033

28. Aylon, Y., Liefshitz, B., Bitan-Banin, G., and Kupiec, M. (2003) Molecular dissection of mitotic recombination in the yeast *Saccharomyces cerevisiae*. *Mol. Cell Biol.* **23**, 1403-1417
29. Mortensen, U. H., Bendixen, C., Sunjevaric, I., and Rothstein, R. (1996) DNA strand annealing is promoted by the yeast Rad52 protein. *Proc. Natl. Acad. Sci. USA* **93**, 10729-10734
30. Parsons, C. A., Baumann, P., Van Dyck, E., and West, S. C. (2000) Precise binding of single-stranded DNA termini by human RAD52 protein. *EMBO J.* **19**, 4175-4181
31. Masson, C., Bury-Mone, S., Guiot, E., Saez-Cirion, A., Schoevaert-Brossault, D., Brachet-Ducos, C., Delelis, O., Subra, F., Jeanson-Leh, L., and Mouscadet, J. F. (2007) Ku80 participates in the targeting of retroviral transgenes to the chromatin of CHO cells. *J. Virol.* **81**, 7924-7932
32. Lau, A., Kanaar, R., Jackson, S. P., and O'Connor, M. J. (2004) Suppression of retroviral infection by the RAD52 DNA repair protein. *EMBO J.* **23**, 3421-3429
33. Wang, J. H., Gostissa, M., Yan, C. T., Goff, P., Hickernell, T., Hansen, E., Difilippantonio, S., Wesemann, D. R., Zarrin, A. A., Rajewsky, K., Nussenzweig, A., and Alt, F. W. (2009) Mechanisms promoting translocations in editing and switching peripheral B cells. *Nature* **460**, 231-236
34. Simsek, D., and Jasin, M. (2010) Alternative end-joining is suppressed by the canonical NHEJ component Xrcc4-ligase IV during chromosomal translocation formation. *Nat. Struct. Mol. Biol.* **17**, 410-416
35. Zhang, Y., and Jasin, M. (2011) An essential role for CtIP in chromosomal translocation formation through an alternative end-joining pathway. *Nat. Struct. Mol. Biol.* **18**, 80-84

CHAPTER 4

Conclusion, Future Directions, and Perspectives on Rad52

Contents:

4.1 Future directions	104
4.2 The significance of Rad52 mediated repair in CSR	107
4.3 Implications for Rad52 in human health and disease	108
4.4 References	111

4.1 Future directions

AID-mediated resections of DSBs generate blunt ends and ends with short hangovers. DSBs that are blunt ended are typically repaired through NHEJ, as indicated by the recruitment of Ku70/Ku86 and other elements of the MRN complex. It has been shown in early studies in yeast and our studies in mouse and in human cell lines, that resected ends including 3'-protruding ends, recruit Rad52 to bind and protect the end. The resulting complex directs the terminal 3' sequences on a local complementarity search, beginning from the opposing end of the DSB. Since Rad52 is important an single strand binding protein, it initiates the single strand annealing of short homologous sequences (1). To test whether Rad52 preferentially binds to blunt or staggered ends, one future experiment we intend to perform are EMSAs incubating single purified protein components of human recombinant Ku70/Ku86 and Rad52 with a biotinylated S μ DNA probe designed to contain blunt and staggered ends and determine if there is indeed preferential binding of Ku70/Ku86 to blunt ends and Rad52 to staggered ends, fitting and more specifically defining our hypothesis that though Rad52 competes with Ku70/Ku86 for binding to S region DSB ends, Rad52 preferentially binds to staggered ends to promote single strand annealing, leading to a microhomology mediated end-joining process. At the same time, it has been shown that Rad52 can also bind to blunt ends (), most likely those containing homology, thereby leading to intra-S region recombination as an alternative mechanism for repair.

Since HR requires a homologous template from a sister chromatid, it occurs mainly during the S and G2/M phases of the cell cycle, however it has been shown that Rad52 can be recruited to the DNA damage site right after DSB induction. However it has been shown by us and others that AID-mediated DNA damage can lead to intra-S region recombination through HR-like recombination of sequence repeats independent of DNA replication (2,3). Therefore with the need for DNA replication, HR can occur throughout the cell cycle. NHEJ occurs mainly in the G1 and S phases of the cell cycle, as no homologous template for recombination is required, although it is active throughout the cell cycle. This provides a basis for the competition between Rad52 and Ku70/Ku86 in binding to S region DSBs to modulate CSR.

To determine whether or not Rad52 is involved in an HR mediated repair process, a future experiment that could be performed is a ChIP experiment using anti-Rad52 Ab followed by cell cycle analysis to determine which phase of the cell cycle Rad52 is recruited in during S region DSB. This experiment would allow us to determine whether Rad52 repairs DSB through HR, which predominates in the S and G2 phases of the cell cycle or throughout- indicating that it may not require DNA replication, suggesting an alternative mechanism of repair.

Our data show that in the absence of Rad52, CSR increases which we contend is due to the recruitment of Ku70/Ku86 to S region DSBs. To definitely define the role of each crucial element in CSR, one essential experiment to further assess the efficiency of Ku70/Ku86 and Rad52 in resolving DSBs involves inhibiting Ku70/Ku86 (by short hairpin RNA) in *Rad52^{+/+}* and *Rad52^{-/-}* B cells during CSR. It is anticipated that CSR may occur in *Rad52^{+/+}* B cells, albeit at an even lower frequency than observed by

Boboila et al., (4) based on our conclusion that Rad52 can mediate DSBs in CSR at a lower efficiency owing to utilization of intra-S region recombination. The combined inhibition of Ku70/Ku86 and Rad52 should completely abolish CSR in B cells and strengthen our contention that Rad52 competes with Ku70/Ku86 in binding to S region DSBs ends and validate that Rad52 plays a significant role in immunoglobulin class switch DNA recombination.

Our findings suggest that Rad52 plays a potential role in A-NHEJ, a pathway that is still poorly characterized. If substantial CSR activity occurs in the absence of these two critical components, this would suggest that other DSB repair factors are involved. These future experiments would provide further insights into potential upstream and downstream interaction partners of Rad52 and elucidate their involvement in A-NHEJ to provide a clearer understanding of the mechanism at hand.

4.2. The significance of Rad52 mediated repair in CSR

Historically, Rad52 was first discovered in *S. cerevisiae* and its' function was absolutely indispensable for DNA repair. Although the Ku70 complex has been shown to play an important role in telomerase regulation and protection in *C. albicans*, alluding to its role eventual role in end joining, early studies centering on Ku70 reveal interesting similarities and differences in the mechanism of the Ku complex in disparate systems (5). Seminal findings suggesting the importance of the Ku (Ku70/Ku86) heterodimer was first noted in the auto-antigens of patients with autoimmune disorders (6).

Therefore, the absence of Ku70/Ku86 could lead to autoimmune disorders such as lupus and genomic instability due to the inability to support V(D)J recombination as witnessed in *Ku70^{-/-}* mice (7). Though Ku70/Ku86 eventually displaced Rad52 as an essential DNA repair factor in the mammalian system, the absence of Ku results in residual CSR activity. With respect to our findings, we have demonstrated that Rad52 is still functionally significant and repairs DSBs leading to CSR. We have redefined the role of Rad52 in an A-NHEJ pathway mediated by microhomologies, given the lack of a safer means to repair breaks. Although this may lead to some level of genomic instability given the chromosomal translocations associated with microhomology mediated repair, effective repair is more tolerable to the cell.

This suggests an important role of Rad52 in the resolution of these DSBs in A-NHEJ, which functions as a backup choice for DSB repair when a core C-NHEJ factor is absent. The maintenance of genomic integrity is essential as AID can off target a large number of non-*Ig* genes, leading to chromosomal translocations, lymphomagenesis and autoimmunity (8-10).

4.3. Implications for Rad52 in human health and disease

In humans, DNA-PK activity and increased expression of Ku70 and Ku86 have been shown to correlate with resistance to therapeutic molecules notably in the context of chronic lymphoblastic leukemia (CLL) (11). Minor defects in the NHEJ pathway have been shown to confer predisposition to leukemia (12). Immunodeficiencies with abnormal DNA repair and genetic polymorphisms of NHEJ components (13) have been associated with the increased susceptibility to the development of lymphoid malignancies, suggesting that an aberrant NHEJ pathway could lead to lymphomagenesis. Acute lymphoblastic leukemia (ALL) cells were found to express high levels of DNA-PKcs, Ku70 and Ku86 protein, whereas CLL cells displayed a lower expression of DNA-PKcs and Ku86 but not Ku70 (14). As has been shown by qRT-PCR in several lymphoproliferative disorders (LPD), a lower expression of Ku70-encoding *XRCC6* gene was observed compared with reactive lymph nodes.

Similarly, data harvested from a human database (Zan et al., *unpublished data*) suggests a decrease in Rad52 expression in patients with active system lupus erythematosus (SLE). Lupus is a systemic autoimmune disease caused by genetic and environmental factors, which drive the development of multi-organ damage such as tissue damage in the kidney, skin, joints, brain, blood cells, lung and heart due to the emergence of pathogenic autoantibodies (15). These pathogenic autoantibodies are heavily mutated (16-22) emerging from unmutated V(D)J templates of naturally autoantibody-producing cell precursors in the primary repertoire (23,24). Reversion of hypermutated V(D)J sequences of anti-double strand DNA (dsDNA) autoantibodies to germline sequences result in the loss of dsDNA binding, suggesting that SHM is an important driver in the

generation of autoantibodies. In healthy individuals, tolerance mechanisms prevent the generation of autoantibodies, which are highly specific to double-strand DNA (25,26). Lupus is tightly associated with an increased risk for certain cancers. For example, lupus patients display a higher frequency of B cell lymphomas (27-30). These malignancies are derived from GC B cells, where AID is upregulated (9,31,32). As AID expression is important in the generation of interchromosomal translocations, the role of Rad52 can be explored for their potential in preventing B cell neoplasias and lymphomagenesis. As decreased expression of Ku70 is associated with autoantibody production LPD, particularly CLL, this may suggest a role for Rad52 in leukemia and B cell lymphoma.

One finding suggested that myeloproliferative disorders (MPD), or stem cell derived clonal diseases arise as a consequence of chromosomal aberrations between oncogenic fusion proteins such as BCR/ABL. Single strand annealing (SSA) can greatly attribute to these chromosomal aberrations, as this DSB repair mechanism is highly error-prone. BCR/ABL stimulates SSA activity, and such activity was accompanied by enhanced nuclear localization of RAD52 and ERCC1, which play a key role in DNA repair (33). These findings suggest that BCR/ABL and other fusion tyrosine kinases (FTKs) can cause disease progression in MPDs by inducing chromosomal instability through the production of DSBs and stimulation of SSA repair, which include factors such as RAD52 in hematopoietic cell lines and leukemic stem/progenitor cells from patients with chronic myelogenous leukemia (CML).

Our study suggests an important role of Rad52 in an alternative end joining pathway to mediate AID induced lesions in CSR to maintain genomic stability and can be applied in a broader context to B cell related diseases and cancers, such as B cell lymphoma and CML.

4.5 References

1. Zan, H., Wu, X., Komori, A., Holloman, W. K., and Casali, P. (2003) AID-dependent generation of resected double-strand DNA breaks and recruitment of Rad52/Rad51 in somatic hypermutation. *Immunity* **18**, 727-738
2. Barlow, J. H., and Rothstein, R. (2009) Rad52 recruitment is DNA replication independent and regulated by Cdc28 and the Mec1 kinase. *The EMBO journal* **28**, 1121-1130
3. Koike, M., Yutoku, Y., and Koike, A. (2013) The C-terminal region of Rad52 is essential for Rad52 nuclear and nucleolar localization, and accumulation at DNA damage sites immediately after irradiation. *Biochemical and biophysical research communications* **435**, 260-266
4. Boboila, C., Yan, C., Wesemann, D. R., Jankovic, M., Wang, J. H., Manis, J., Nussenzweig, A., Nussenzweig, M., and Alt, F. W. (2010) Alternative end-joining catalyzes class switch recombination in the absence of both Ku70 and DNA ligase 4. *The Journal of experimental medicine* **207**, 417-427
5. Chico, L., Ciudad, T., Hsu, M., Lue, N. F., and Larriba, G. (2011) The *Candida albicans* Ku70 modulates telomere length and structure by regulating both telomerase and recombination. *PloS one* **6**, e23732
6. Mimori, T., Akizuki, M., Yamagata, H., Inada, S., Yoshida, S., and Homma, M. (1981) Characterization of a high molecular weight acidic nuclear protein recognized by autoantibodies in sera from patients with polymyositis-scleroderma overlap. *The Journal of clinical investigation* **68**, 611-620
7. Gu, Y., Jin, S., Gao, Y., Weaver, D. T., and Alt, F. W. (1997) Ku70-deficient embryonic stem cells have increased ionizing radiosensitivity, defective DNA end-binding activity, and inability to support V(D)J recombination. *Proceedings of the National Academy of Sciences of the United States of America* **94**, 8076-8081
8. Liu, M., Duke, J. L., Richter, D. J., Vinuesa, C. G., Goodnow, C. C., Kleinstein, S. H., and Schatz, D. G. (2008) Two levels of protection for the B cell genome during somatic hypermutation. *Nature* **451**, 841-845
9. Pasqualucci, L., Bhagat, G., Jankovic, M., Compagno, M., Smith, P., Muramatsu, M., Honjo, T., Morse, H. C., 3rd, Nussenzweig, M. C., and Dalla-Favera, R. (2008) AID is required for germinal center-derived lymphomagenesis. *Nat. Genet.* **40**, 108-112
10. Robbiani, D. F., Bunting, S., Feldhahn, N., Bothmer, A., Camps, J., Deroubaix, S., McBride, K. M., Klein, I. A., Stone, G., Eisenreich, T. R., Ried, T., Nussenzweig, A., and Nussenzweig, M. C. (2009) AID produces DNA double-strand breaks in non-Ig genes and mature B cell lymphomas with reciprocal chromosome translocations. *Mol. Cell* **36**, 631-641
11. Muller, C., Christodoulopoulos, G., Salles, B., and Panasci, L. (1998) DNA-Dependent protein kinase activity correlates with clinical and in vitro sensitivity of chronic lymphocytic leukemia lymphocytes to nitrogen mustards. *Blood* **92**, 2213-2219
12. Riballo, E., Critchlow, S. E., Teo, S. H., Doherty, A. J., Priestley, A., Broughton, B., Kysela, B., Beamish, H., Plowman, N., Arlett, C. F., Lehmann, A. R., Jackson,

- S. P., and Jeggo, P. A. (1999) Identification of a defect in DNA ligase IV in a radiosensitive leukaemia patient. *Current biology : CB* **9**, 699-702
13. Hill, D. A., Wang, S. S., Cerhan, J. R., Davis, S., Cozen, W., Severson, R. K., Hartge, P., Wacholder, S., Yeager, M., Chanock, S. J., and Rothman, N. (2006) Risk of non-Hodgkin lymphoma (NHL) in relation to germline variation in DNA repair and related genes. *Blood* **108**, 3161-3167
 14. Holgersson, A., Erdal, H., Nilsson, A., Lewensohn, R., and Kanter, L. (2004) Expression of DNA-PKcs and Ku86, but not Ku70, differs between lymphoid malignancies. *Experimental and molecular pathology* **77**, 1-6
 15. Shlomchik, M. J., and Madaio, M. P. (2003) The role of antibodies and B cells in the pathogenesis of lupus nephritis. *Springer seminars in immunopathology* **24**, 363-375
 16. Shlomchik, M. J., Aucoin, A. H., Pisetsky, D. S., and Weigert, M. G. (1987) Structure and function of anti-DNA autoantibodies derived from a single autoimmune mouse. *Proc. Natl. Acad. Sci. U.S.A.* **84**, 9150-9154
 17. Shlomchik, M., Mascelli, M., Shan, H., Radic, M. Z., Pisetsky, D., Marshak-Rothstein, A., and Weigert, M. (1990) Anti-DNA antibodies from autoimmune mice arise by clonal expansion and somatic mutation. *J. Exp. Med.* **171**, 265-292
 18. van Es, J. H., Gmelig Meyling, F. H., van de Akker, W. R., Aanstoot, H., Derksen, R. H., and Logtenberg, T. (1991) Somatic mutations in the variable regions of a human IgG anti-double-stranded DNA autoantibody suggest a role for antigen in the induction of systemic lupus erythematosus. *J. Exp. Med.* **173**, 461-470
 19. Radic, M. Z., Mackle, J., Erikson, J., Mol, C., Anderson, W. F., and Weigert, M. (1993) Residues that mediate DNA binding of autoimmune antibodies. *J. Immunol.* **150**, 4966-4977
 20. Kasaian, M. T., Ikematsu, H., Balow, J. E., and Casali, P. (1994) Structure of the V_H and V_L segments of monoreactive and polyreactive IgA autoantibodies to DNA in patients with systemic lupus erythematosus. *J. Immunol.* **152**, 3137-3151
 21. William, J., Euler, C., Christensen, S., and Shlomchik, M. J. (2002) Evolution of autoantibody responses via somatic hypermutation outside of germinal centers. *Science* **297**, 2066-2070
 22. Goodnow, C. C. (2007) Multistep pathogenesis of autoimmune disease. *Cell* **130**, 25-35
 23. Casali, P., Nakamura, M., Ginsberg-Fellner, F., and Notkins, A. L. (1990) Frequency of B cells committed to the production of antibodies to insulin in newly diagnosed patients with insulin-dependent diabetes mellitus and generation of high affinity human monoclonal IgG to insulin. *Journal of immunology* **144**, 3741-3747
 24. Casali, P., and Schettino, E. W. (1996) Structure and function of natural antibodies. *Current topics in microbiology and immunology* **210**, 167-179
 25. Liu, S., Cerutti, A., Casali, P., and Crow, M. K. (2004) Ongoing immunoglobulin class switch DNA recombination in lupus B cells: analysis of switch regulatory regions. *Autoimmunity* **37**, 431-443
 26. Mevorach, D., Zhou, J. L., Song, X., and Elkon, K. B. (1998) Systemic exposure to irradiated apoptotic cells induces autoantibody production. *The Journal of experimental medicine* **188**, 387-392

27. Ehrenfeld, M., Abu-Shakra, M., Buskila, D., and Shoenfeld, Y. (2001) The dual association between lymphoma and autoimmunity. *Blood Cells Mol. Dis.* **27**, 750-756
28. Bernatsky, S., Clarke, A., and Ramsey-Goldman, R. (2002) Malignancy and systemic lupus erythematosus. *Curr. Rheumatol. Rep.* **4**, 351-358
29. Gayed, M., Bernatsky, S., Ramsey-Goldman, R., Clarke, A., and Gordon, C. (2009) Lupus and cancer. *Lupus* **18**, 479-485
30. Kiss, E., Kovacs, L., and Szodoray, P. (2010) Malignancies in systemic lupus erythematosus. *Autoimmun. Rev.* **9**, 195-199
31. Bijl, J., van Oostveen, J. W., Kreike, M., Rieger, E., van der Raaij-Helmer, L. M., Walboomers, J. M., Corte, G., Boncinelli, E., van den Brule, A. J., and Meijer, C. J. (1996) Expression of HOXC4, HOXC5, and HOXC6 in human lymphoid cell lines, leukemias, and benign and malignant lymphoid tissue. *Blood* **87**, 1737-1745
32. Bijl, J. J., van Oostveen, J. W., Walboomers, J. M., Horstman, A., van den Brule, A. J., Willemze, R., and Meijer, C. J. (1997) HOXC4, HOXC5, and HOXC6 expression in non-Hodgkin's lymphoma: preferential expression of the HOXC5 gene in primary cutaneous anaplastic T-cell and oro-gastrointestinal tract mucosa-associated B-cell lymphomas. *Blood* **90**, 4116-4125
33. Cramer, K., Nieborowska-Skorska, M., Koptyra, M., Slupianek, A., Penserga, E. T., Eaves, C. J., Aulitzky, W., and Skorski, T. (2008) BCR/ABL and other kinases from chronic myeloproliferative disorders stimulate single-strand annealing, an unfaithful DNA double-strand break repair. *Cancer research* **68**, 6884-6888